AD-A172 737 ENVIRONMENTAL STRESS SCREENING TECHNOLOGY(U) GRUMMAN AEROSPACE CORP BETHPAGE NY H QUARTIN ET AL. OCT 85 RSM-85-R-03 AFWAL-TR-85-3073 F33615-83-C-3406 1/2

UNCLASSIFIED F/G 9/5 NL

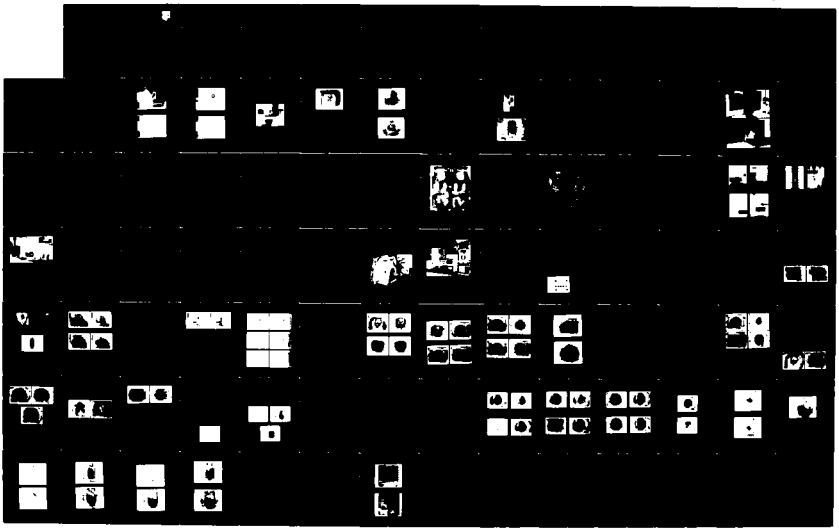

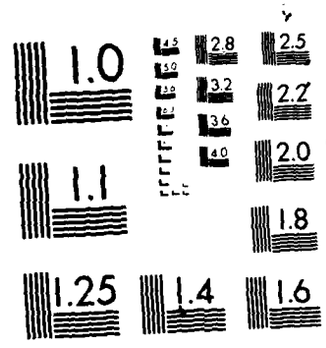

MICROCOPY RESOLUTION TEST CHART
NATIONAL BUREAU OF STANDARDS 1963-A

(12)

AD-A172 737

AFWAL-TR-85-3073

ENVIRONMENTAL STRESS SCREENING TECHNOLOGY

Herbert Quartin
Frank Kube
Joseph Popolo

Grumman Aerospace Corporation
Bethpage, NY 11714

October 1985

Final Report for Period September 1983 - March 1985

Approved for Public Release; Distribution Unlimited

DTIC
ELECTE
OCT 0 8 1986
S D
E

DTIC FILE COPY

FLIGHT DYNAMICS LABORATORY
AIR FORCE WRIGHT AERONAUTICAL LABORATORIES
AIR FORCE SYSTEMS COMMAND
WRIGHT-PATTERSON AIR FORCE BASE, OHIO 45433-6553

86 10 8 132

NOTICE

When Government drawings, specifications, or other data are used for any purpose other than in connection with a definitely related Government procurement operation, the United States Government thereby incurs no responsibility nor any obligation whatsoever; and the fact that the government may have formulated, furnished, or in any way supplied the said drawings, specifications, or other data, is not to be regarded by implication or otherwise as in any manner licensing the holder or any other person or corporation, or conveying any rights or permission to manufacture use, or sell any patented invention that may in any way be related thereto.

This report has been reviewed by the Office of Public Affairs (ASD/PA) and is releasable to the National Technical Information Service (NTIS). At NTIS, it will be available to the general public, including foreign nations.

This technical report has been reviewed and is approved for publication.

Danny L. Cooper

DANNY L. COOPER, CAPT, USAF
Mechanical Engineer
Combined Environment Test Group
Environmental Control Branch

Preston S. Hall

PRESTON S. HALL
Tech Manager
Combined Environment Test Group
Environmental Control Branch

FOR THE COMMANDER

Rudi J. Berndt

RUDI J. BERNDT
Acting Chief
Vehicle Equipment Division

"If your address has changed, if you wish to be removed from our mailing list, or if the addressee is no longer employed by your organization please notify AFWAL/FIEEA, *W-PAFB, OH 45433 to help us maintain a current mailing list".*

Copies of this report should not be returned unless return is required by security considerations, contractual obligations, or notice on a specific document.

Unclassified
SECURITY CLASSIFICATION OF THIS PAGE

REPORT DOCUMENTATION PAGE

1a REPORT SECURITY CLASSIFICATION Unclassified	1b RESTRICTIVE MARKINGS N/A
2a SECURITY CLASSIFICATION AUTHORITY N/A 2b DECLASSIFICATION / DOWNGRADING SCHEDULE	3 DISTRIBUTION / AVAILABILITY OF REPORT Approved for public release; distribution unlimited
4 PERFORMING ORGANIZATION REPORT NUMBER(S) RMS-85-R-03	5 MONITORING ORGANIZATION REPORT NUMBER(S) AFWAL-TR-85-3073
6a NAME OF PERFORMING ORGANIZATION Grumman Aerospace Corporation 6b OFFICE SYMBOL (If applicable) RM&S	7a NAME OF MONITORING ORGANIZATION Flight Dynamics Laboratory (AFWAL/FIEE) Air Force Wright Aeronautical Laboratories
6c ADDRESS (City, State, and ZIP Code) Bethpage Long Island New York 11714	7b ADDRESS (City, State, and ZIP Code) Wright-Patterson Air Force Base Ohio 45433
8a NAME OF FUNDING SPONSORING ORGANIZATION Flight Dynamics Laboratory 8b OFFICE SYMBOL (If applicable) AFWAL/FIEE	9 PROCUREMENT INSTRUMENT IDENTIFICATION NUMBER F33615-83-C-3406
8c ADDRESS (City, State, and ZIP Code) Wright-Patterson Air Force Base Ohio 45433	10 SOURCE OF FUNDING NUMBERS PROGRAM ELEMENT NO: 62201F PROJECT NO: 2402 TASK NO: 04 WORK UNIT ACCESSION NO: 47

11 TITLE (Include Security Classification)
Environmental Stress Screening Technology

12 PERSONAL AUTHOR(S)
Quartin, Herbert; Kube, Frank; Popolo, Joseph

13a TYPE OF REPORT	13b TIME COVERED	14 DATE OF REPORT (Year, Month, Day)	15 PAGE COUNT
Final	FROM Sept. 83 TO Mar. 85	1985, October	98

16 SUPPLEMENTARY NOTATION
N/A

17 COSATI CODES

FIELD	GROUP	SUB-GROUP
09	03	
14	04	

18 SUBJECT TERMS (Continue on reverse if necessary and identify by block number)
Infrared (IR), Environmental Stress Screening, Thermography, Acceptance Testing, Electronics

19 ABSTRACT (Continue on reverse if necessary and identify by block number)

The objective of this study ~~program~~ was to evaluate the feasibility of ~~utilizing~~ using infrared thermography for the detection and growth tracking of environmentally sensitive workmanship defects in printed circuit board assemblies. It was determined that the detection of defects, as manifested by power deviations as small as 15 milliwatts, is practical and feasible under static environmental conditions. ~~Further~~ Techniques for the ~~utilization~~ use of infrared thermography under dynamic environmental conditions were developed and evaluated. These techniques allowed the detection of intermittent as well as permanent failures. In all cases, the environmental stimulus was random vibration and rapid thermal cycling.

The ability of infrared thermography to detect the growth of a defect was verified and determined to equate to power changes on the order of 5 milliwatts. The experimental results were sufficiently accurate and repeatable to warrant continued investigations into the development of a failure prediction method.

20 DISTRIBUTION / AVAILABILITY OF ABSTRACT ☒ UNCLASSIFIED/UNLIMITED ☐ SAME AS RPT. ☐ DTIC USERS	21 ABSTRACT SECURITY CLASSIFICATION Unclassified
22a NAME OF RESPONSIBLE INDIVIDUAL Capt. Daniel Cooper	22b TELEPHONE (Include Area Code) 513-255-6078 22c OFFICE SYMBOL AFWAL/FIEE

DD FORM 1473, 84 MAR — 83 APR edition may be used until exhausted. All other editions are obsolete.

SECURITY CLASSIFICATION OF THIS PAGE
Unclassified

PREFACE

This research was performed by Grumman Aerospace Corporation, Reliability, Maintainability and Safety Section, Bethpage, NY, under Contract F33615-83-C-3406, for the Flight Dynamics Laboratory (AFWAL/FIEE) Air Force Wright Aeronautical Laboratories, Wright-Patterson Air Force Base, OH. David Earls (AFWAL/FIEE) was the WPAFB Project Engineer, and Captain Daniel Cooper (AFWAL/FIEE) was the technical advisor.

This effort described was accomplished from September 1983 through March 1985.

The evaluation of the feasibility of using infrared thermography for detecting and tracking workmanship defects in PCBs is a direct extension of Grumman's ongoing research. Recognizing that a significant driver to the technical efficiency and cost-effectiveness of any screening technique is the early and accurate identification of defects, infrared thermography, if feasible, has the potential for great benefit.

The authors would like to recognize the outstanding support contributed by the UTI Instruments Company, in particular, Herbert Bolton and Robert Brady.

In addition to Herbert Quartin, Frank Kube, and Joseph Popolo, the other Grumman study team members were John Connelly, Frederick Danner, Thomas Georges, Russell Ives, PhD, Robert Kosson, PhD, and Gilbert Kelley.

A-1

QUALITY INSPECTED 4

CONTENTS

Section		Page
	PREFACE	iii
	SUMMARY	xi
1	INTRODUCTION	1
2	THERMOGRAPHIC SYSTEM	7
	2.1 System Operating Modes & Features	7
	2.1.1 Normal Scanning/Freeze-Frame Mode	7
	2.1.2 Delta Therm Mode	8
	2.1.3 Magnification Mode	10
	2.1.4 Data Storage	10
3	DISCUSSION	13
	3.1 Program Approach	13
	3.2 Thermographic System Familiarization	15
	3.3 Phase I - Static Component Level Tests	17
	3.4 Phase II - Static Printed Circuit Assembly Level Tests	18
	3.5 Phase III - Dynamic Printed Circuit Assembly Level Tests	19
	3.5.1 Random Vibration	19
	3.5.2 Thermal Cycling	22
4	TEST ARTICLES & TEST SET-UP	25
	4.1 Test Articles	25
	4.1.1 Phase I Individual Components	25
	4.1.2 Phase II Populated Printed Circuit Assembly - Static Tests	25
	4.1.3 Phase III Populated Printed Circuit Assembly - Dynamic Tests	30
	4.2 Test Set-Ups	32
	4.2.1 Phase I Component-Level Tests	32
	4.2.2 Phase II Static PCB-Level Tests	35
	4.2.3 Phase III Dynamic PCB-Level Tests	39

CONTENTS (contd)

Section		Page
5	STUDY PROGRAM IMPLEMENTATION	41
	5.1 Phase I Component-Level Experiments	41
	5.1.1 System Repeatability Experiments	43
	5.1.2 Threshold of Detection Experiments	46
	5.1.3 Unit-Unit Variation Experiments	49
	5.1.4 Defect Tracking Feasibility Experiments	50
	5.2 Phase II Static PCB-Level Experiments	52
	5.2.1 Initial "Golden Board" Experiments	58
	5.2.2 Solder Joint Experiments	60
	5.2.3 PCB Trace Defect Experiments	62
	5.3 Phase III - PCB Dynamic Environmental Tests	63
	5.3.1 Random Vibration Experiments	64
	5.3.2 Rapid Thermal Cycling Experiments	80
6	CONCLUSIONS	87
7	RECOMMENDATIONS	89
	REFERENCES	90
	APPENDIX A	91
	APPENDIX B	97

ILLUSTRATIONS

Figure		Page
1	Typical Thermal Signature	5
2	Typical Delta Mode, "No Failure"	5
3	Typical Delta Mode, "Complete Failure"	6
4	Typical Delta Mode, "Partial Failure"	6
5	CCT-9000 Thermongraphic System	7
6	Typical Normal Scan/Freeze Mode Display	8
7	Typical Delta Mode Display (No Failure)	9
8	Typical Delta Mode Display (Failure)	9
9	Typical Software Magnification Mode Display	11
10	Study Flow	14
11	Thermal Shroud	16
12	Random Vibration Spectrum	20
13	Rapid Thermal Cycle Chamber Profile	21
14	Populated Printed Circuit Assembly (Component Side View-Enlarged)	26
15	Populated Printed Circuit Assembly (Wiring Side View Enlarged)	28
16	Typical Printed Circuit Assembly Schematic	29
17	No Solder Joint (10x)	31
18	Poor Solder Joint (10x)	31
19	External Lead Wire Damage (10x) At Component	31
20	External Lead Wire Damage (10x) At PCB	31
21	Internal Wire Bond Defector (5x)	32
22	PCB Trace Damage (10x)	32
23	Component Test Holding Fixtures and Test Equipment	33
24	Component Test Set-Up No. 1 Schematic	33
25	Component Test Set-Up No. 2 Schematic	34
26	PCB Test Set-Up Wiring Diagram	36
27	Switch Assembly Schematic	37
28	Monitor Assembly Schematic	38
29	Test Article Mounted On Shaker Head	39
30	Random Vibration Test Set-Up	40
31	Carbon Composition Resistors - 100 ohm	42
32	Typical Resistor Temperature Stabilization Periods	43

ILLUSTRATIONS (contd)

Figure		Page
33	Cool-Down Curve for Resistor Dissipating Approximately 1W.	44
34	Threshold of Detectability	46
35	Heat Spread vs Detectability	47
36	Software Magnified Thermal Image of Resistor Network	47
37	Unmagnified Delta Runs of a Resistor Network at Reduced Power Levels (-0.05 W).	48
38	Unmagnified Delta Runs of Resistor Network at Reduced Power Levels (0.025 W).	48
39	Positional Variations Affect Thermal Signature	50
40	Defect Growth Tracking in Delta Mode	51
41	Reference and Delta Image Comparisons.	53
42	PCB Level Repeatability Experiments	53
43	PCB Level Tracking Experiments - Defect Analogs (Sheet 1 of 3) . .	54
43	PCB Level Tracking Experiments - Defect Analogs (Sheet 2 of 3) . .	55
43	PCB Level Tracking Experiments - Defect Analogs (Sheet 3 of 3) . .	56
44	PCB Level Golden Board Experiments - Ambiguities.	59
45	Solder Joint Experiment - PC Trace Cut and Bridged with Bus Wire (Sheet 1 of 2)	60
45	Solder Joint Experiment - PC Trace Cut and Bridged with Bus Wire (Sheet 2 of 2)	61
46	PCB Level Solder Joint Experiments (Clip Resistant)	62
47	PCB Level Circuit Trace Experiments.	63
48	Vibration Set-Up (Outside Shroud) Verification, Delta Image - No Failure	64
49	Vibration Delta Thermograph Showing "Cool Down"	65
50	Static Delta Thermograph Verifying No Failure	65
51	Vibration Delta Thermograph Showing "Cool Down" - Repeat	65
52	PCB Temperature/Time History	67
53	Delta Image Comparison - PCB #5 vs PCB #5 (Base Runs)	69
54	Delta Image Comparison - PCB #2 vs PCB #5	69
55	Delta Image Comparison - PCB #3 vs PCB #5	70
56	Delta Image Comparison - PCB #4 vs PCB #5	70

ILLUSTRATIONS (contd)

Figure		Page
57	Delta Image Comparison - PCB #5 vs PCB #5	71
58	Delta Image Comparison - PCB #6 vs PCB #5	71
59	Delta Image Comparison - PCB #6 vs PCB #5 (Check Run Following Weekend Shutdown)	72
60	Delta Image Comparison - PCB #1 vs PCB #5	73
61	Delta Image - PCB #1 vs PCB #5 - Static	74
62	Delta Image - PCB #1 vs PCB #5	75
63	Delta Image - PCB #1 vs PCB #5	76
64	Delta Image - PCB #1 vs PCB #5	77
65	Delta Image - PCD #1 vs PCB #5 (New Static Reference)	78
66	Temperature Cycling Test Resistor Board - Component Side View	81
67	Temperature Cycling Test Resistor Board - Wiring Side View	81
68	Typical Chamber Cycle	84
69	Scan Head Assembly	92
70	Display Monitor	92
71	Central Processing Unit	93
72	Keyboard Entry System	94
73	Disc Storage Unit	94
74	Front Surface Mirror	95
75	Close-Up Lens Assembly	95

TABLES

Table		Page
1	PCB vs Golden Board Reference Data	68
A-1	Thermographic System Specifications	96

SUMMARY

This study program was initiated to evaluate the feasibility of utilizing Infrared (IR) thermography for detecting and growth tracking workmanship defects. The scope of this study was limited to electronic Printed Circuit Board (PCB) assemblies and to those workmanship defects which have historically proven to be environmentally sensitive. Should the IR technique prove feasible, a very powerful tool would be available to significantly upgrade the quality level of production electronic equipment.

This program utilized simulated defects (failure analogs) to establish thresholds of detectability under laboratory standard (static) conditions. It then explored the effect that dynamic environmental conditions had on these thresholds, using both the failure analogs and actual defects. The primary means of observing the defects was through the use of the difference imaging (delta) mode feature of the thermographic system. This mode permitted direct visual display of only the difference between two thermal images, that difference being due to a deviation in power experienced by the circuit as a direct result of the defect.

The program was conducted in three phases. Phase I examined typical electronic components powered both singularly and in selected groupings. It was accomplished under laboratory ambient conditions and provided insight into the constituents of an IR thermal signature as well as system repeatability data. PCB assemblies were fabricated for Phase II tests and were populated with typical circuits using previously examined components. Tests under static conditions were again conducted which provided baseline circuit data and afforded the opportunity to further examine signature constituents. The test results allowed the definition of assembly-to-assembly comparison variables and the investigation of the feasibility of using a single reference "golden board" for production board comparisons. Phase III explored the effects of random vibration and rapid thermal cycling on the detection of the specific failure analogs. Upon completion of the failure analog experiments, actual examples of these workmanship defects were incorporated on selected boards to provide verification of the established level of detection.

Phases I and II provided data relative to both the threshold of detection and the threshold of the "trackability" of the growth of a defect.

Phase III showed that intermittent failures could be observed during dynamic environmental testing.

1 - INTRODUCTION

This final report presents the results and conclusions derived from a study program conducted for the Flight Dynamics Laboratory, Air Force Wright Aeronautical Laboratories. The program objective was to evaluate the feasibility of using infrared thermography for the detection and growth tracking of workmanship defects in electronic printed circuit board assemblies. The program was accomplished in three phases, each building upon the previous, and each representing a substantial increase in complexity. Although the study was sufficiently structured to maintain its general character and direction, enough flexibility was included in its design to allow modification as experimental results and their related analyses dictated.

Section 2 identifies the thermographic system and defines its operating modes and features. Section 3 follows with a detailed discussion of the program approach and principal observations. This discussion starts with an overview of the experimental methods utilized and progresses to comprehensive explanations of individual tasks associated with each of the three program phases. Section 4 fully defines the test articles and test set-ups used in conducting each of the three phases. The laboratory experiments and samples of the acquired data are presented in Section 5. As with the previous sections, this segment is also divided into three phases. Conclusions and Recommendations address the overall program objectives and are presented in Sections 6 and 7, respectively.

Brief descriptions of each of the thermographic system components, with respective photographs, are contained in Appendix A. In addition, the salient features of the thermographic system are included in tabular form. A method for transient thermal analysis of a PCB is presented in Appendix B.

Continuing advances in development and qualification testing have increased the potential for providing a basically sound and inherently reliable design. However, as this potential has increased, so have the complexity and density of packaging of the equipment being designed. This advanced technology amplifies the persistent problem of detecting and correcting latent manufacturing defects. Equipment malfunction, after several hours of operation, is often caused by something as simple as an unsoldered wire. If such a malfunction occurs on aircraft-installed equipment, inordinately high repair costs are involved. The fact that the equipment was fully

qualified, and initially demonstrated a mean-time-between-failure orders of magnitude above a given requirement is almost meaningless when such a malfunction, in production equipment, results in mission failure or loss of life.

The ability to detect these workmanship-related defects through even the most intense visual inspection and bench checkout has become a thing of the past, partially due to increased complexity. Therefore, acceptance testing of production equipment under environmental conditions which precipitate failure of these defects has become a necessity (Ref 1 and 2). A principal driver of the effectiveness of Environmental Stress Screening (ESS) is the ability to rapidly and accurately detect the existence of a defect, whether permanent or intermittent. This detection capability was a major program thrust.

The stated program objectives were to evaluate the feasibility of utilizing IR thermography as a tool for early and accurate detection of PCB assembly defects. If the initial feasibility study proved positive, this technique's ability to accurately assess the growth of a defect from a localized disturbance to a functional failure was to be evaluated. As an illustrative example, one can examine the natural progression of a defective solder joint from an acceptable condition to a functional failure. The mechanics of failure is fatigue, driven by the environmental stimuli of ESS testing. The growth of this fatigue-driven fracture would not be detectable by conventional methods (of functional monitoring) until complete separation occurred. If thermographic detection and growth tracking of a fatigue-driven fracture proved feasible, it would enable the detection of imminent failures far earlier than possible by performance monitoring. It could also provide a database for subsequent fracture mechanics studies that could lead to the development of accelerated testing techniques.

As a result of the knowledge and experience gained during our diverse investigations into ESS effectiveness in disclosing latent workmanship defects (Ref 1 and 2), the importance of detecting both short-term intermittent anomalies and permanent failures was fully appreciated. Furthermore, since intermittent anomalies occur only during the application of environmental stimuli, they would go undetected if thermographic examinations were restricted to benign periods. Although neither the specified study requirements nor our response proposed to evaluate the feasibility of thermographic examination during dynamic periods of random vibration and rapid thermal cycling, it became apparent that restricting the thermographic examinations to static periods would severly limit the usefulness of this technique. Note that a procedure to facilitate thermographic examinations during periods of

random vibration and rapid thermal cycling must be developed. This capability can provide significant benefits in terms of equipment quality and potential cost savings.

Another technical benchmark in the progression of the study program was the conception and refinement of the "golden board" approach to the thermographic monitoring of a quantity of PCB assemblies. Simply stated, one PCB would be visually and electrically examined in minute detail to verify its suitability as a standard. Then a powered thermal image would be obtained and designated as the reference image for evaluating a common set of assemblies. One must recognize that the successful utilization of the "golden board" approach necessitated the development of methods to either normalize or cancel generic variables that would otherwise cause incorrect interpretation of an ambiguous display. These methods must, at present, rely upon discrete manipulations of the thermographic system as well as the visual acuity and experience of the observer. Preliminary investigations clearly indicated that substantial benefit in this area and other areas could be derived from the use of an external multi-programmable computer through the existing IEEE-488 interface. Although the indications were all positive, the computer effort was not pursued since it was judged to be substantial and clearly beyond the scope of this study.

During the environmental stress screening segment of the program (Phase III), selected examples of environmentally sensitive workmanship defects were incorporated in the test article (PCB). These workmanship defects were:

- No solder connections
- Poor solder connections
- Component external lead wire damage
- Component internal wire bond defect
- PCB trace damage.

Each of these workmanship defect examples is further defined in the Section 4, Test Articles.

The thermographic system utilized in this study is a subjective device which depends upon the presentation of a color image as its principal data readout. Although digital thermal readout at a specific point is available, this "individual point" mode of operation is not compatible with the program objectives. Therefore, the bulk of data accumulated during the experimental program and referred to in this report was acquired through detailed examination of either a specific infrared image or by comparing a series of images.

Throughout this report, individual photographs and sequences of photographs are presented in conjunction with specific portions of text. They are provided to substantiate and illustrate the stated observation. A simple example of this is presented in Figures 1 through 4. This sequence starts with a powered thermal signature of a single component and progresses through the thermal images associated with a "no failure", "complete failure" and "partial failure." This is representative of the form and nature of almost all the acquired data. In practice, these pictures were examined individually, and compared to data gathered under both similar conditions and conditions representative of controlled differences. These examinations yielded a catalog of repeatable thermographic signatures for a variety of thermal conditions.

It is acknowledged that the analysis of visual (photographic) data is subjective in nature. During this study we attempted to limit the error effect of inherent subjectivity by providing repeated observations of reference versus delta therm scenarios and ensuring that the derived conclusions are repeatable.

The thermographic image presented by this system is a 256-level color display. Each of these discrete colors represents a specific temperature (or range) and is thus a principal method of data interpretation. This continuous tone color display was photographed in color and is reproduced here in black and white. It should be understood that the included photographs are half-tone reproductions which do not represent continuous-tone images. Due to this severe reduction in resolution, some of the very subtle points, which were clearly detectable in the actual thermal presentation and referred to in the text, may not be discernible in the photographs reproduced herein.

During many of the more complex experiments associated with environmental stress screening, color video recordings were made of the dynamic segments. In some instances these video recordings were produced in conjunction with an extensive sequence of still photographs. In the thermal cycling experiments, the video recordings represent the full extent of visual data acquisition. Copies of representative video recordings have been supplied to the Funding/Sponsoring Organization.

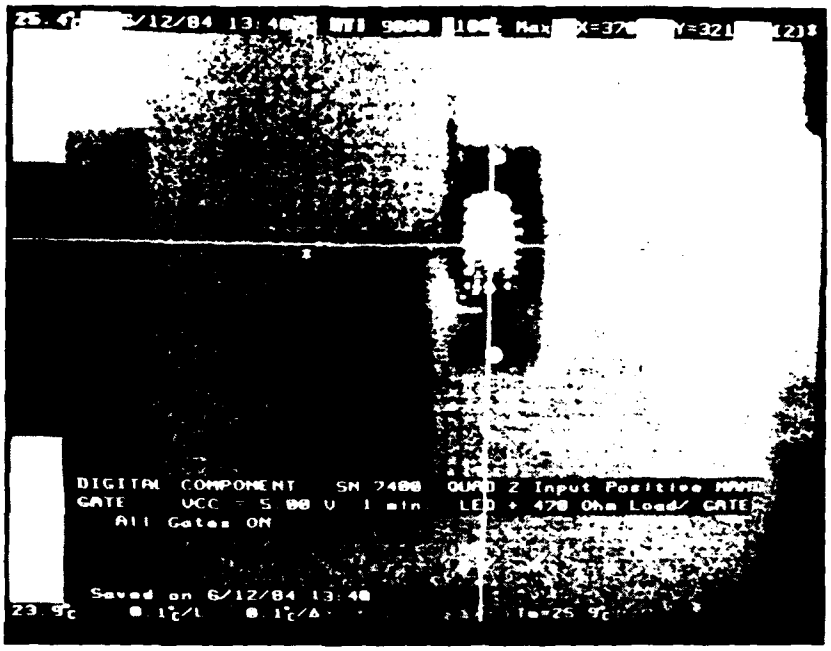

Figure 1 Typical thermal signature

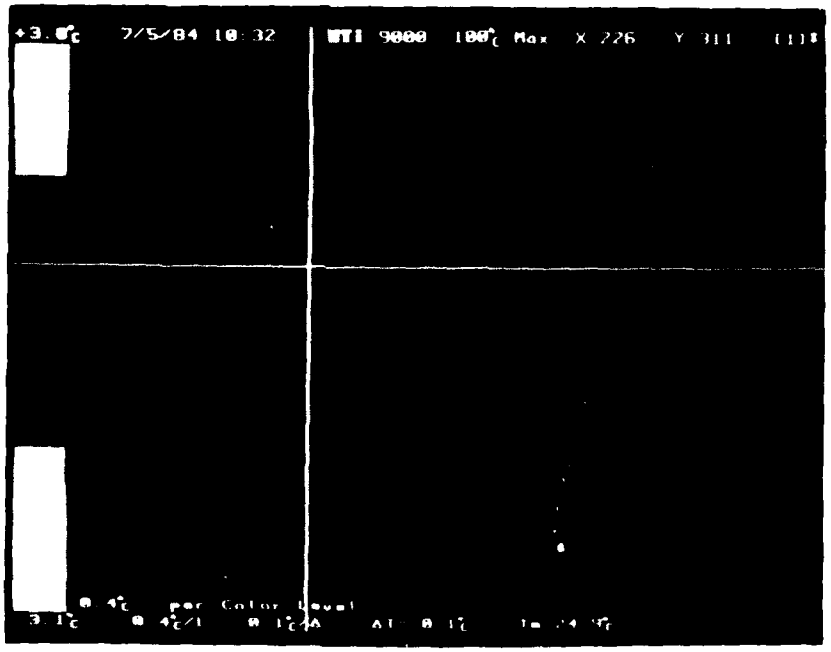

Figure 2 Typical delta mode, "no failure"

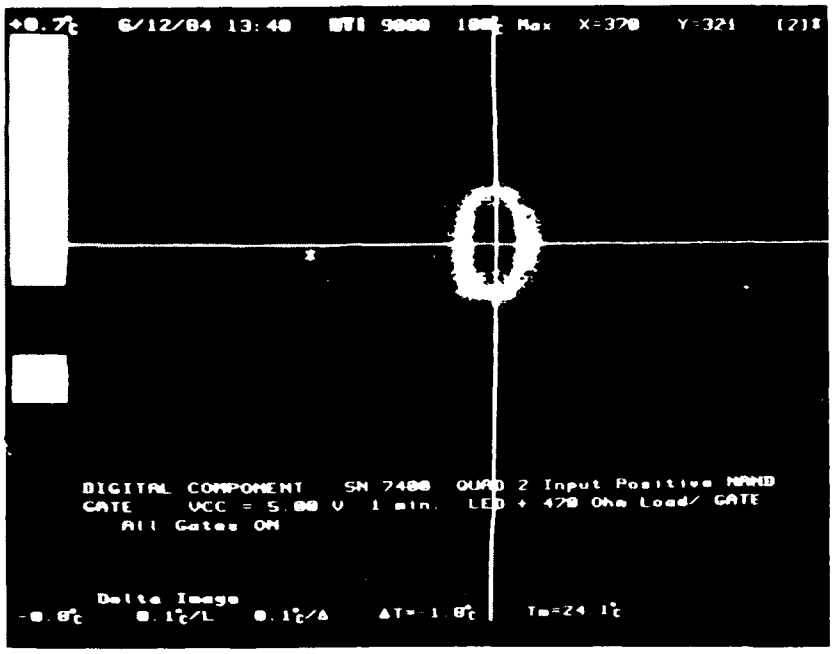

Figure 3 Typical delta mode, "complete failure"

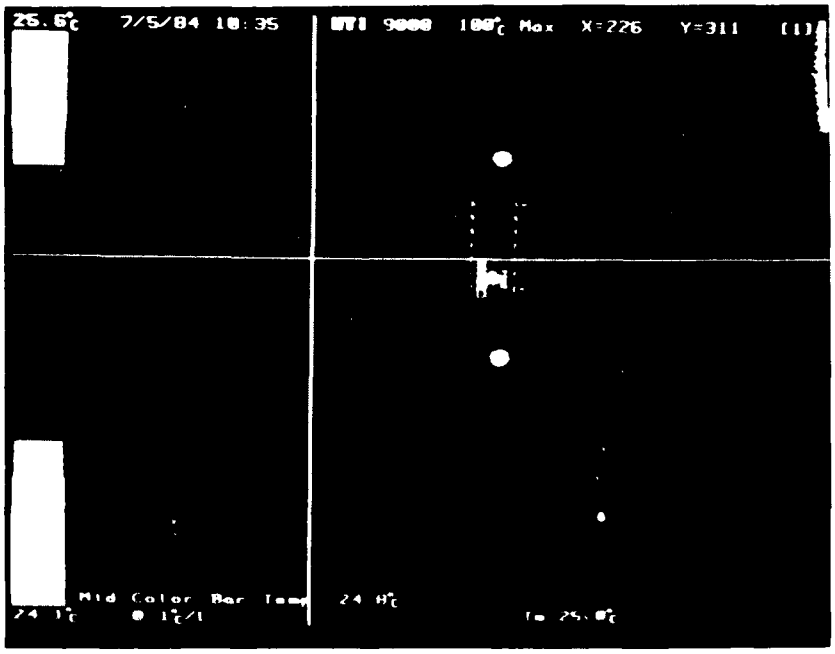

Figure 4 Typical delta mode, "partial failure"

2 - THERMOGRAPHIC SYSTEM

The thermographic equipment used in this program was the CCT-9000 system, manufactured by the UTI Instrument Company. Comparisons of this system with other available systems showed it to have features which made it especially suited to accomplish the study objectives. The overall system is shown in Figure 5 and a system definition is presented in Appendix A.

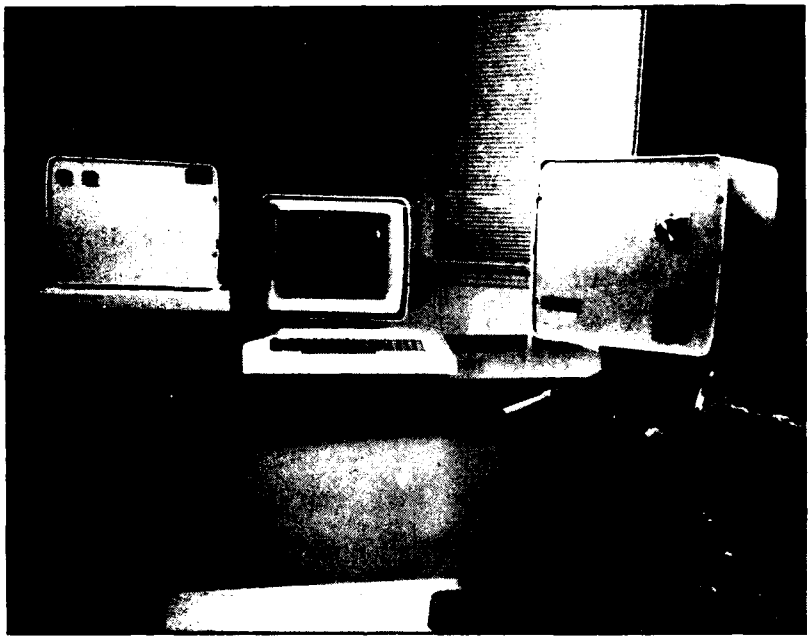

Figure 5 CCT-9000 thermographic system

2.1 SYSTEM OPERATING MODES & FEATURES

2.1.1 Normal Scanning/Freeze-Frame Mode

The normal scanning mode (Figure 6) produces a thermal signature of any heat-producing object within the scanner's field of view (FOV). The resulting visual image is displayed in up to 256 color levels or a 64-level "gray scale." A 16-level color gradience reference can be selected for identifying approximate temperatures across the displayed image. The temperature value assigned to the midpoint of this reference is selectable within the range in use.

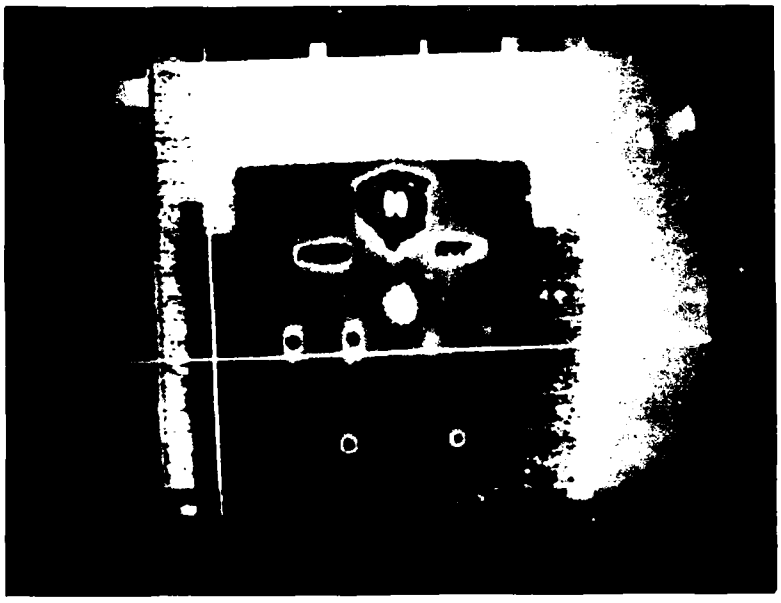

Figure 6 Typical normal scan/freeze frame mode display

A digital readout of the temperature at any point in the display is available by positioning a movable cross-hair which can be programmed for eight discrete points. A digital readout of the X and Y coordinates of the cross-hair position is also provided. The readout can be made to indicate the temperature at the cross-hair in either degrees C, F, or K. This temperature can also be corrected for reflectance and emissivity parameters.

The scanning of the object in the FOV can be interrupted to capture and display the thermal signature associated with a discrete period of time. This thermal signature can then be examined in detail, with all of the functions available in the normal scan mode, e.g., temperature readout and magnification. This signature may be used as a reference for subsequent comparisons to define the operational status of the test article.

2.1.2 Delta Therm Mode

The delta therm mode provides a "difference" viewing capability. It presents a display representing only the thermal differences between the FOV actively being scanned and reference data previously stored in the system memory. If there is no difference between the two, the displayed image has a homogenous mid-range color (Figure 7). Differences are displayed as a color (or black and white) image which is continuously updated. This image represents variations either above or below the mid-range, which are presented in increments as low as ±0.1°C (Figure 8). A color bar reference is available, as well as a digital readout of both the absolute value and the differential (delta T) value of temperature represented by the pixel under the cross-hairs.

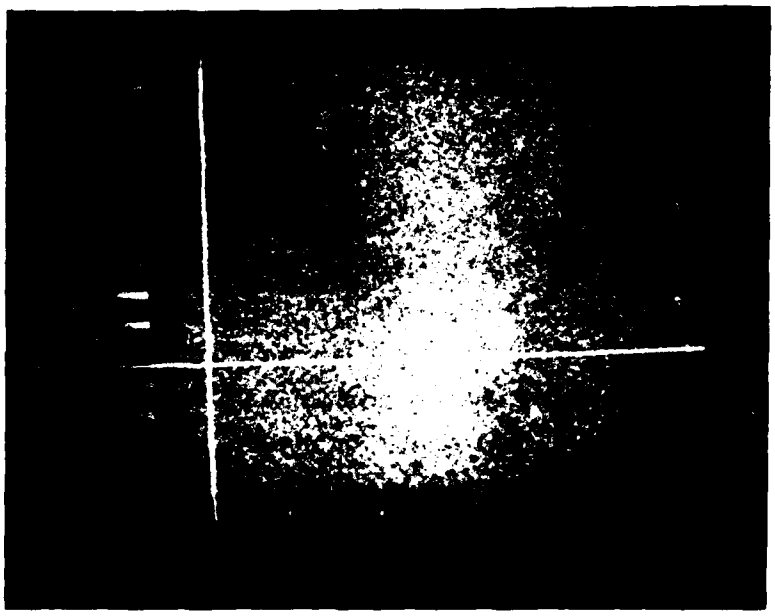

Figure 7 Typical delta mode display (no failure)

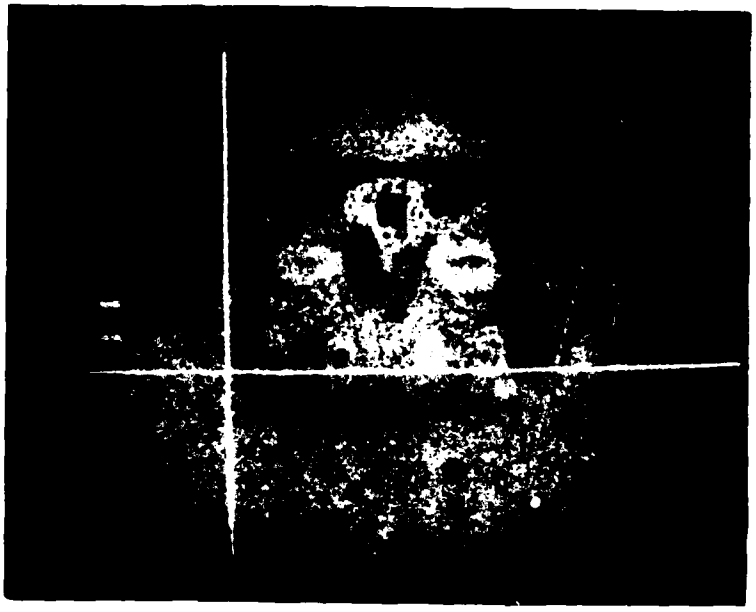

Figure 8 Typical delta mode display (failure)

With the system in the delta therm mode, the thermal signature comprising the reference data as it was at the time of storage, may be recalled and viewed at any time. In addition, the image representing these reference data, along with any changes that have taken place, is also available.

During delta therm operation, a variable "dead band" may be activated which causes the differences within the selected range above and below the mid-range to be blanked out, i.e., only differences greater than this band will be displayed. This feature enables the setting of minimum display threshold levels.

An offset feature is available in the delta therm mode. This feature permits correcting for ambient temperature changes which have occurred between the time of storing the reference data and delta therm operation. It should be noted that this feature only corrects the visual display.

2.1.3 Magnification Mode

To effect a maximum of 32X magnification, 2X optical and 16X software magnification are available either separately or in combination. The attachment of an external lens system provides an additional magnification of 2.5X. The magnification feature is available in any of the operating modes. Figure 9 shows a normal component thermal signature and a 16X software magnification of the same image.

2.1.4 Data Storage

The basic system provides for temporary storage of the image data required for the freeze frame and delta therm modes of operation. This storage system is volatile and reference data is lost upon system shut-down.

Permanent storage of reference image data is accomplished through interfacing with an eight inch floppy disk drive unit. This unit is capable of recording one complete thermal image along with descriptive text, permitting recall of the data at any time.

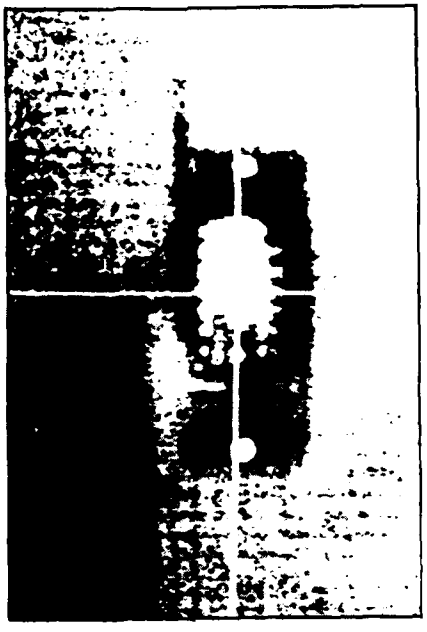

(UNMAGNIFIED VIEW)

(MAGNIFIED VIEW)

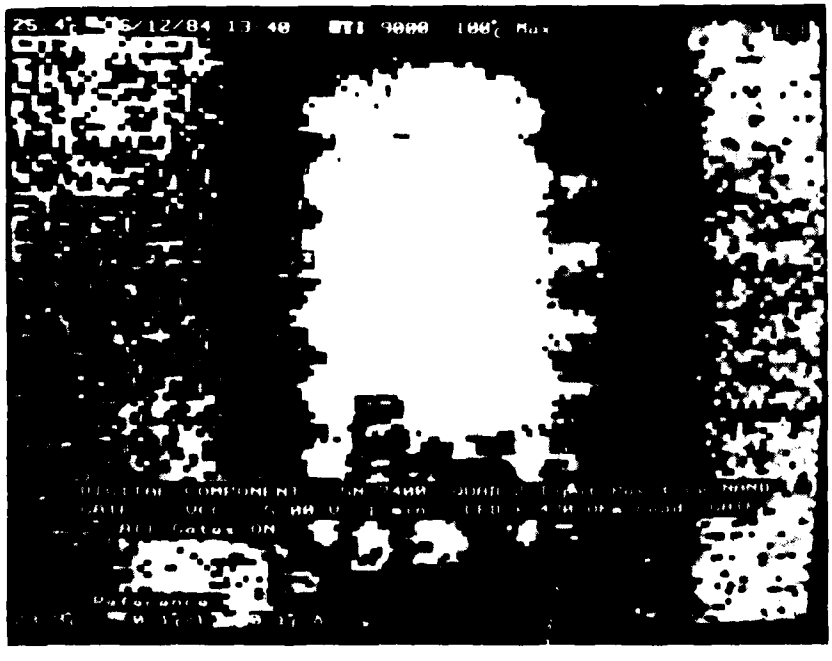

Figure 9 Typical software magnification mode display

3 - DISCUSSION

This section presents a detailed discussion of the methods and procedures utilized in designing and conducting the study. Starting with an overview of the experimental methods, it progresses to explain the intended purpose of each of the major investigative sequences. The postulated versus actual results are discussed and, as appropriate, program modifications including rationale are specified. This section emphasizes the logic associated with each investigative sequence, its expected contribution to the program objectives, and the interrelationship between tasks.

3.1 PROGRAM APPROACH

The program utilized the building block approach described in Figure 10, where each part provided the necessary foundation for the subsequent part. This method afforded numerous advantages, including an orderly increase in complexity, a reasonable degree of confidence in the acquired database, a high level of program visibility, and the option to return to any specific point in the program when necessary.

The study was designed as an iterative exercise utilizing both laboratory experimental methods and analytical techniques. Starting with single elements, each thermal signature was manipulated and analyzed until the full range of parameters affecting the signature was identified. Having thus bounded the drivers, subsequent experiments and analyses were directed toward acquiring sufficient data to weight each parameter individually and in significant combinations. In addition, methods of normalizing principal variables were continuously investigated.

The design of the laboratory program was in part based upon the ability to repeat the specific experiment accurately, and since workmanship defects are inherently unrepeatable, an analog approach to the insertion of workmanship defects was used. The implementation consisted of a system whereby the applied power to any one component or set of components could be accurately and repeatably varied to represent any failure condition, from an open circuit to a full short. In addition to enabling the exac and repeatable variation of power, the system provided for the application of any specific desired duty cycle. Through this system of analogs, it became practical to fully evaluate the feasibility of utilizing thermography for the early detection of defects and also the ability to accurately track the growth of a

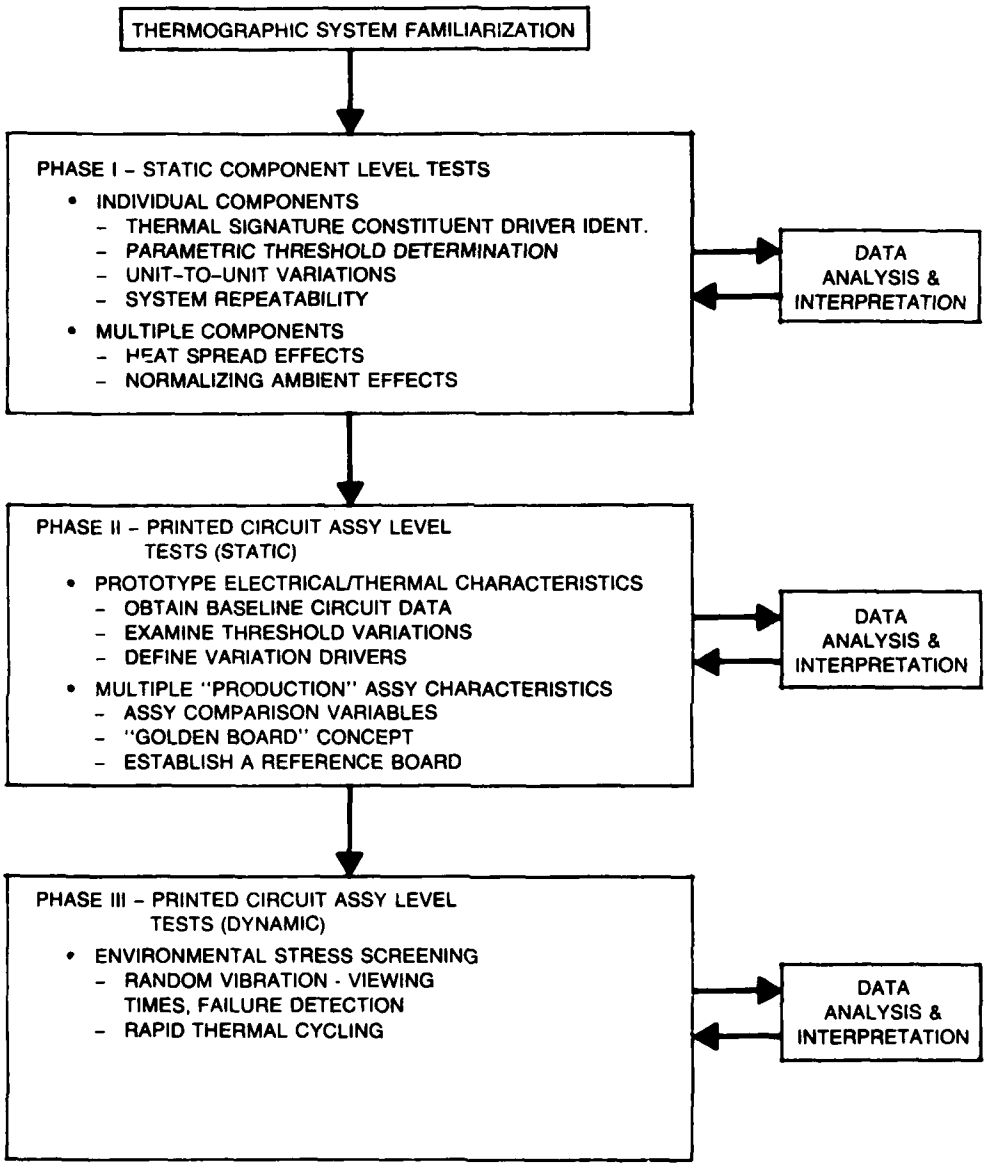

Figure 10 Study flow.

defect. These analogs of defects were used exclusively in Phases I and II. Defect analogs were also used during the initial portion of Phase III. The latter experiments of Phase III were accomplished using actual examples of typical workmanship defects.

3.2 THERMOGRAPHIC SYSTEM FAMILIARIZATION

The UTI CCT-9000 Thermographic System was received at Grumman, Bethpage, at the end of October 1983. Upon completion of the receiving cycle, the system was set up in the Component Evaluation/Failure Analysis Laboratory in Plant 14 and a period of system familiarization followed. During this period, a variety of simple experiments using single or multiple resistors was conducted to aid in understanding the details of system operation and system limitations. Resistors were chosen because they were typical of any heat-producing device and were easily manipulated. This familiarization process afforded the opportunity to become conversant with the multiple operating modes of the system and also to begin selection of the modes most beneficial to achieving program objectives.

Since the objective of this study was to investigate the thermographic system's ability to recognize very small changes in thermal signature, it was concluded that the differencing or delta mode of operation was best suited to the task. The maximum system sensitivity settings and the color mode of operation were selected for the same reasons. As the work progressed and experience grew, it was noted that variations in the sensitivity settings (degrees/color level and dead band) would, at times, aid in the correct interpretation of an especially difficult or confusing thermal image.

The thermographic system, as utilized for this study, is a subjective device essentially dependent upon the visual acuity and perception of the operator (observer) for its accuracy. In addition, the high sensitivity setting (0.1 C per color level) coupled with the inherent thermodynamic instability of extremely low mass items (microcircuits) made it obvious that accurate identification and control of the ambient temperature and effective shielding from extraneous heat reflections were mandatory for satisfactory resolution.

Given the above, an investigation was initiated to establish the most practical method of stabilizing the test article ambient temperature and providing effective shielding. Although a conditioned air driven chamber was considered for this purpose, the established temperature tolerance of ±2.0 C (MIL-STD-810) for all such equipment precluded its use. Recognizing that any active chamber would provide some cyclic thermal environment which would be unacceptable, a passive thermal shroud (Figure 11) was designed and constructed. In use, the scanning head

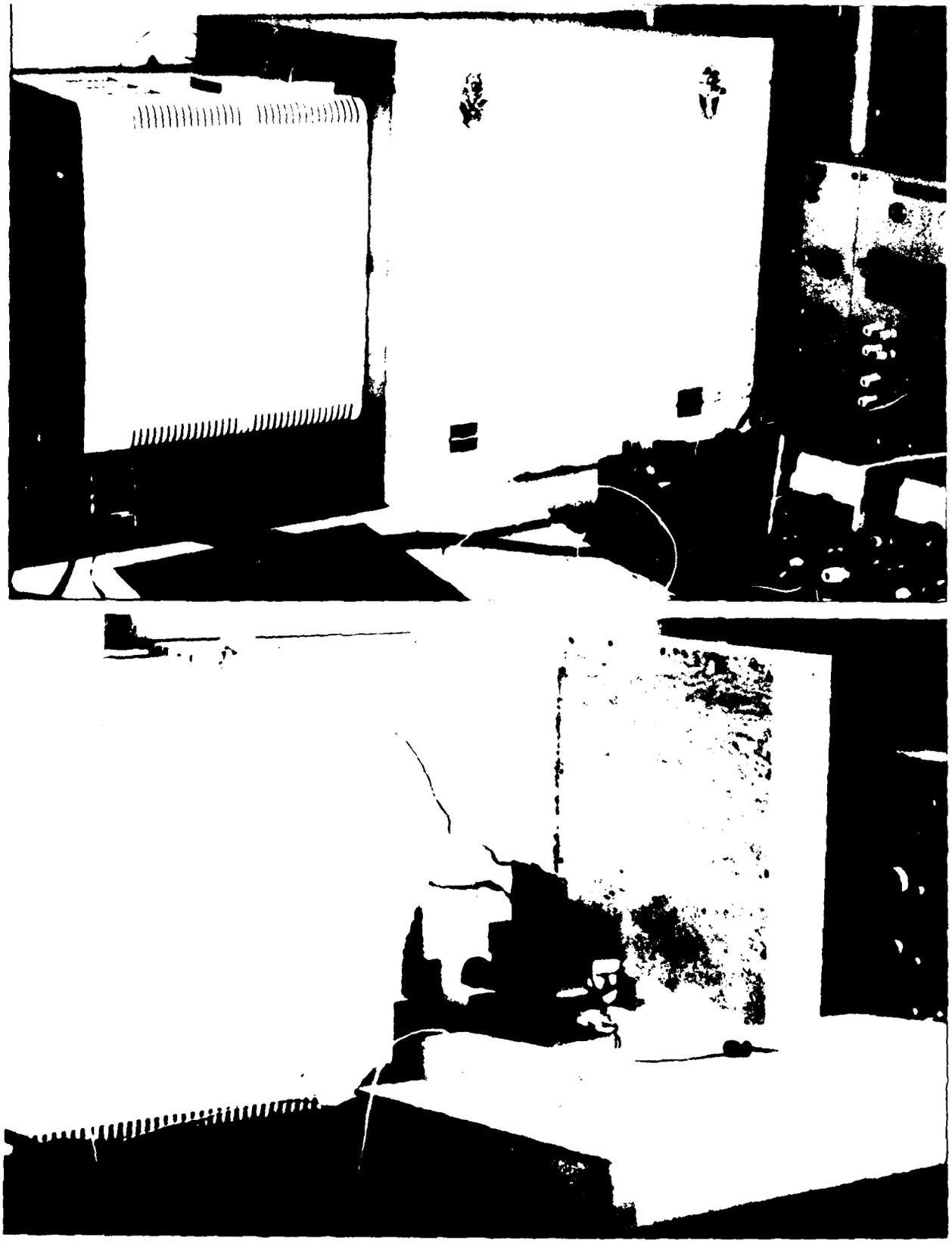

Figure 11 Thermal shroud

assembly was coupled to the shroud, which housed the test article in its fixture. A low volume circulation fan and ventilation ports were provided for improved thermal stability. During the investigation, optimum ambient temperature measurement points were selected. These points, which were continuously measured thermographically, were evaluated and modified as required throughout the study.

Upon completion of these early experiments, a reasonably broad base of entry-level data and experience was available to provide a foundation for the subsequent tasks. This included:

- Initial sensitivity settings
- Initial mid-color settings
- Optimum temperature range setting
- Optimum image size
- Optimum system operating mode
- Requirement for a thermally stable environment
- Requirement for a fixed positional relationship between the imager and the test article
- Basic thermal signature characteristics.

3.3 PHASE I - STATIC COMPONENT LEVEL TESTS

The thermal signature of an article is affected by a host of constituents, including input power, duty cycle, ambient temperature, material, total thermal mass, power dissipation and physical mounting configuration. Since the study's purpose was to evaluate the feasibility of using this thermal signature as a tool for the early detection of workmanship defects and measurement of their growth, it was mandatory that each constituent's contribution be identified and quantified to the extent possible. This task was accomplished during the initial period of the program and further refined throughout the subsequent phases. Using individual components, it was possible to construct a series of semi-idealized experiments in order to provide a broad database for each component. The evaluation of this data provided the foundation for the necessary understanding of the relationship between a thermal signature and its individual constituents.

One can postulate an idealized scenario utilizing a single component and a set of closely controlled thermal signature constituents. If the only variable is input power, it can be shown that the temperature of the component varies with input power, rising as power is increased and falling as power is decreased. It can be shown further that this relationship between input power and component temperature

is repeatable, and therefore the change in thermal signature reflects not only a change in component temperature but also a change in input power. Continuing with the idealized example, the same scenario holds true for all of the other constituents of a thermal signature, given that each is varied individually.

Having established the above, it became necessary to investigate the effects of changes in each constituent upon the others and upon the thermal signature. Each was varied, as in a real-world situation, and the resulting change was recorded. Upon task completion, a broad database was available for a variety of components. This work continued in stages, each building upon the previous, until a sufficiently broad and repeatable database was established to assure reliable identification of those thermal signature constituents which must be treated as variables (input power, duty cycle) and those which must be kept constant (all others). In addition, specific information was acquired for a broad range of component types. These data included unit-to-unit variations in power dissipation, variations in emissivity, and temperature/time histories for powered components.

3.4 PHASE II - STATIC PRINTED CIRCUIT ASSEMBLY LEVEL TESTS

Subsequent to the completion of the effort outlined above, the building block approach was continued with the introduction of a typical production printed circuit assembly. The laboratory program was conducted under standard ambient conditions and evaluated the thermal signature differences associated with analogs of a host of typical manufacturing defects in various stages, progressing to catastrophic failure. The experimental program was designed as a parametric study of the effect of the thermal signature constituents, both individually and in combination. Throughout this set of experiments, analyses were conducted which again enabled an iterative system of modification and redirection to be employed.

Recognizing that the method of utilization of the thermographic system (for this study) is subjective, subsequent experiments were designed as parametric exercises whose purpose was to define the minimum visually detectable thermal signature change in a "production" PCB assembly. This minimum level defines the Threshold Of Detection (TOD). To this end, a set of six test articles (Subsection 4.1.2) was constructed and subjected to ambient testing, utilizing the analog system to insert manufacturing defect representations. Again, through an iterative sequence of laboratory experiments and data analyses, bounds of detection for analogs of typical defects in host devices were developed. In addition to variations in power dissipation levels, the effect of component geometry, positional differences, case material, emissivity, and heat spread, among others, were qualitatively investigated.

Utilizing the acquired database, the investigation continued into the determination of the additive effects of ambient temperature variations and the ability of the thermographic system to compensate for these effects in the presented visual image. These experiments enabled the definition of those parameters associated with designating a PCB as a suitable standard (reference) for the "golden board" technique.

3.5 PHASE III - DYNAMIC PRINTED CIRCUIT ASSEMBLY LEVEL TESTS

Upon completion of the Phase II static ambient tasks, the same test articles were examined under dynamic conditions of random vibration (Figure 12) and thermal cycling (Figure 13), still using the failure analog approach. One of the typical production boards of Phase II was designated as the reference board.

3.5.1 Random Vibration

It must be understood that the ability to isolate defects relies on the change of one constituent element of the thermal signature at a time. Defects could be masked by concurrent changes in signature drivers. It was determined that the application of random vibration caused an increase in air circulation resulting in additional cooling across the test article. This cooling effect, caused by the vibratory motion, presented an ambiguity in the resultant thermal signature. For the random vibration portion, this situation necessitated a redirection of the previously established approach.

The results of continuing random vibration experiments indicated that static delta imaging at discrete increments of time, as originally planned in Ref 3, would disclose permanent defects; however, short-term intermittent occurrences would not be detectable. Additional experiments led to the realization that the occurrence of short-term intermittents is detectable via continuous delta imaging during the application of random vibration. The approach was re-ordered to concentrate on the development of a practical means of providing valid reference for continuous delta images throughout the entire vibration exposure. After many trials, a reference consisting of ten minute power-on plus five minutes power-on under random vibration was considered to be optimum. Cooldown due to vibration was repeatable and allowed the operator to detect short-term intermittent anomalies as they occurred.

Having completed the tasks associated with the analog portion of Phase III, vibration, the acquired database was reviewed and evaluated to verify that it was appropriate to progress to those experiments that utilized environmentally sensitive workmanship defects. Five of the six production-configured PCBs were reworked to incorporate actual examples of workmanship defects as noted in Section 5, Study

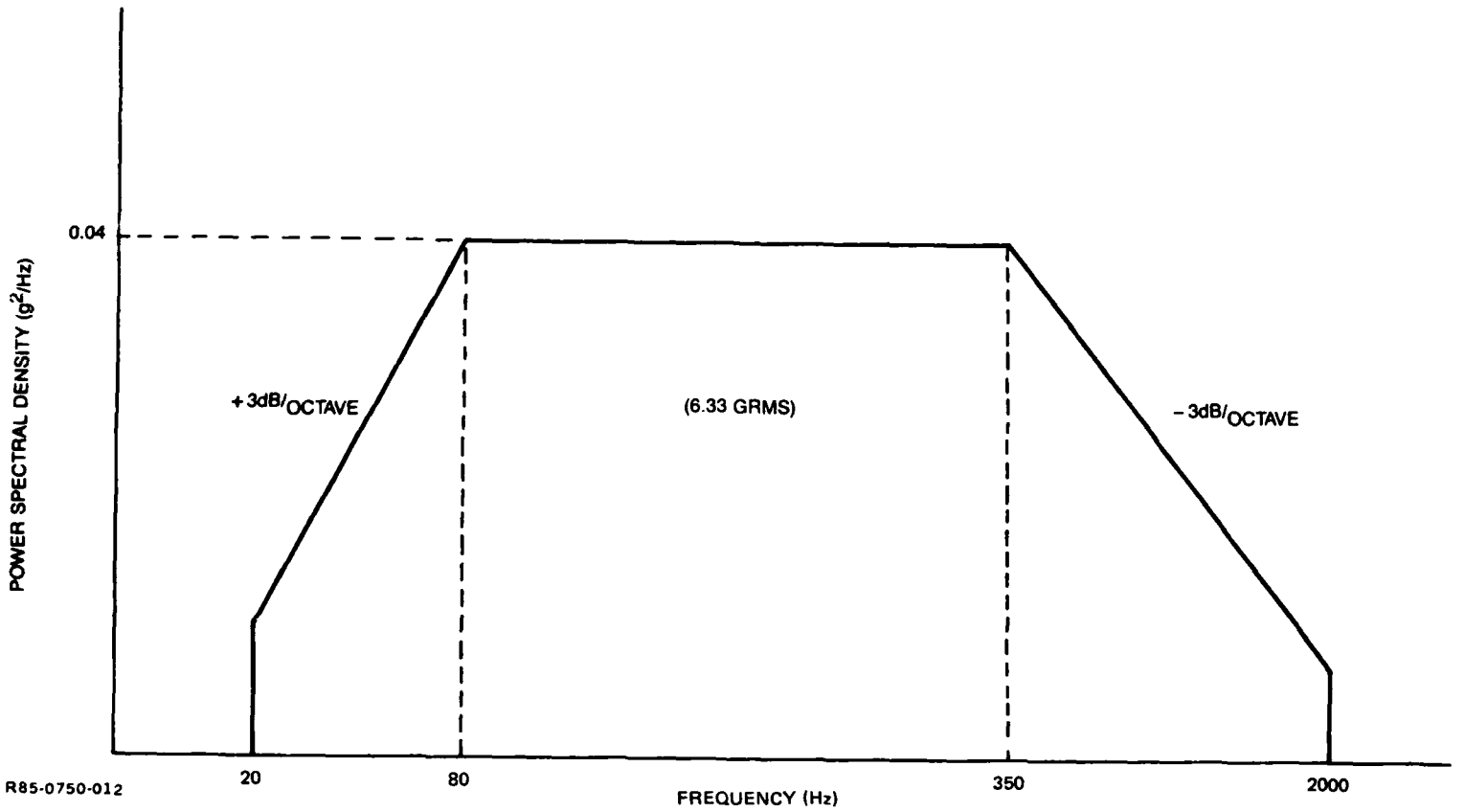

Figure 12 Random vibration spectrum

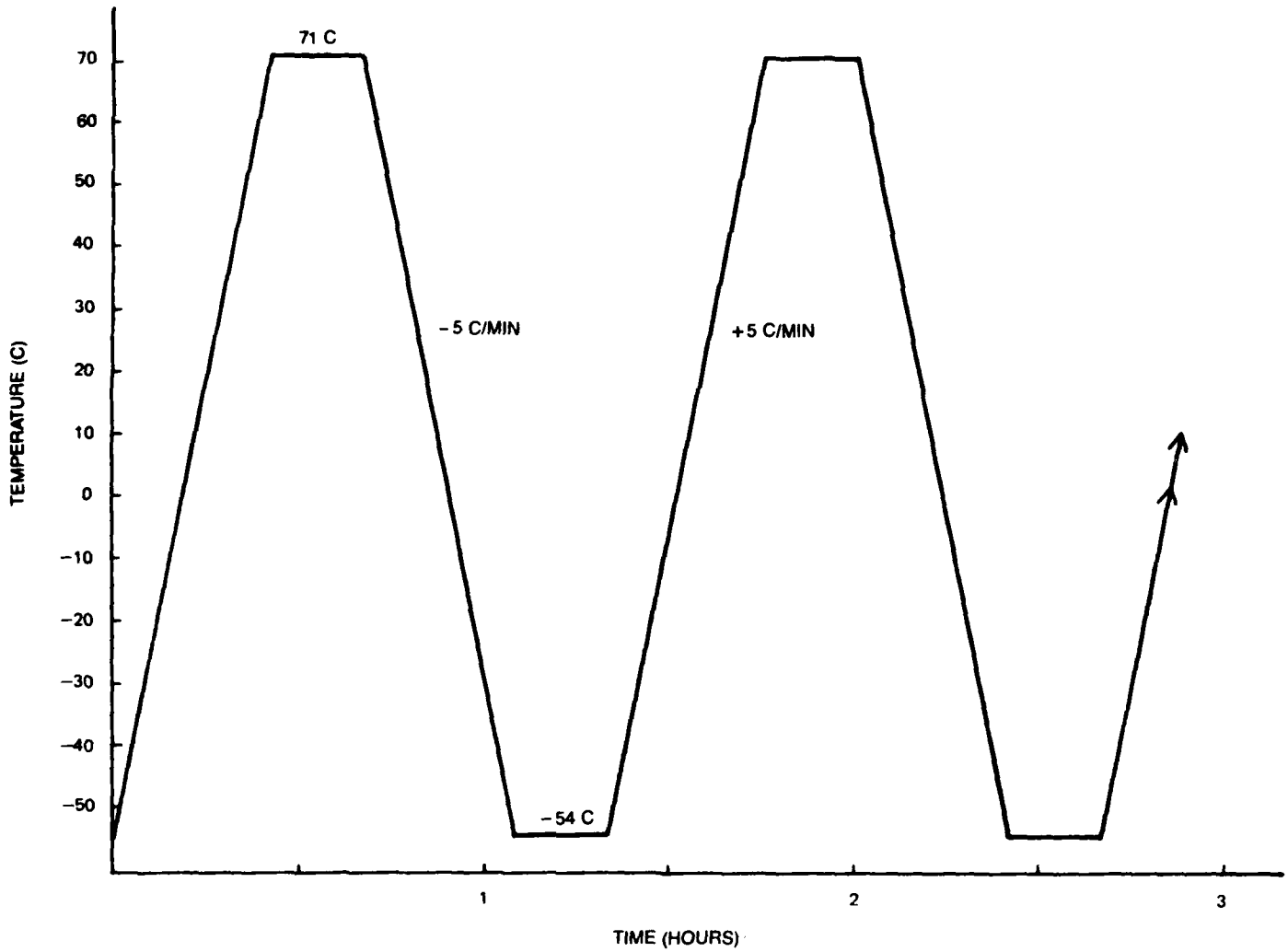

Figure 13 Rapid thermal cycle chamber profile

Program Implementation. The defect types were selected on the basis of historical data relating to frequency of occurrence and sensitivity to either random vibration or thermal cycling, or both. The sixth board was retained unmodified as a "golden board" and provided the thermographic reference for the other five boards.

Using the "golden board", both static and dynamic powered references were recorded for use in the subsequent random vibration exposure. Each of the other five boards was, in turn, powered and thermographically examined against the appropriate reference, both statically and during exposure to random vibration. Each random vibration exposure lasted five minutes with continuous thermographic examination. Static examinations preceded and followed each vibratory exposure. It should be noted that the specifics of this experiment were identical to those outlined for the experiment using analogs and the results paralleled those obtained using analogs.

It is of interest that the "golden board" experienced a failure which was unplanned and completely unexpected. The details of the failure and the subsequent troubleshooting procedures are given in Subsection 5.3.1, Study Program Implementation. It must be emphasized that this event consumed much active laboratory time, and while it ultimately enhanced our confidence in the thermographic techniques, it did decrease in our confidence in our test specimens since they contained large numbers of components.

3.5.2 Thermal Cycling

Upon completion of the random vibration tasks, the program's concentration was directed toward thermal cycling. The planned approach was to perform a thermographic examination at the start, at each ten hour period, and at the conclusion of the 50 hour thermal cycling exposure. In addition, each of these examinations would be performed at room ambient with the test article powered and installed in the thermal chamber. It was acknowledged that this approach would detect only permanent failures; however, it was considered a valid starting point, and therefore its implementation was attempted. Although the initial thermograph presented no problem, subsequent examinations indicated that this approach was impractical.

The difficulties associated with returning and holding the thermal chamber at the reference ambient temperature with the door open introduced inaccuracies in the data. The concept of removing the board from the chamber and performing the periodic delta therm examinations on the bench was dismissed due to the necessity of providing fixtures for repeating the boards position to the required accuracy.

The investigation was redesigned to utilize an IR transmissible window in the chamber door and to eliminate the chassis cover, as defined in the test plan (Ref 3). This setup facilitated thermographic monitoring of the test article at any discrete point in the thermal cycle without the need to perform any operation that would disturb the thermodynamic integrity of the system. This enabled the use of repeated "local" reference runs, each followed closely by a delta therm. At points in the thermal cycle where the rate of change of the ambient temperature is "slow" (less than 6.0 C per minute) and the chamber temperature is above 0.0 C (lower limit of thermographic equipment), this technique provided meaningful data. The feasibility of this revised approach was verified through the use of analogs and actual defects inserted into a resistor board using both the Tenny and Statham Thermal Chambers.

A concentrated effort was then directed toward developing a practical technique applicable to periods of rapid temperature change. This would have provided visibility into intermittents during the conditions in which they are most likely to occur. However, this could not be done using purely visual techniques. Whether computer augmentation could provide a solution was considered beyond the scope of this study.

Subsequent to this work, both the resistor board and the prototype PCB were run in the Tenny Thermal Chamber in order to produce a video tape that would demonstrate the ability to see failures (analog) as they occurred.

4 - TEST ARTICLES & TEST SET-UP

4.1 TEST ARTICLES

4.1.1 Phase I Individual Components

The test articles used in Phase I consisted of components typical of those found on present-day PCB assemblies. They were mounted individually and in selected multiple groupings. The mounting techniques ranged from simple suspension in free air via a bus wire to attachment to a vector board or PCB materials. These components included discrete resistors, resistor network packages, transistors, and Integrated Circuits (ICs).

The discrete resistors were of carbon composition, metal film, and wirewound types. Standard resistance values between 10 ohms and 10 K ohms with a ±5% tolerance and power ratings between 0.1 W and 2.0 W were used.

The resistor networks (Sprague P/N 916C501X2SR) contained eight separate 500 ohm resistors within a 16-pin, Dual-In-Line (DIP) plastic package. Each resistor had a ±5% tolerance and the total allowable package power was 3.5 W.

The ICs used included digital logic, timing, and interface circuits. The digital ICs were quadruple 2-input NAND gates. The SN7400s in plastic packages and the SN5400s in ceramic packages were standard Transistor-Transistor Logic (TTL) types having typical power dissipations of approximately 10 mW per gate. The SN74LS00 devices were low-power Schottky types which dissipate only approximately 2.0 mW per gate. Each of these devices performs the same logic functions and is contained in 14-pin DIPs. The timing circuit was the NE555 type in an 8-pin plastic DIP. Hermetically sealed, ceramic-metal, 18-pin DIP interface circuits (Sprague UDS2980 series) were used. They contained eight independent source drivers capable of operating at a total package power of approximately 1.6 W.

4.1.2 Phase II Populated Printed Circuit Assembly - Static Tests

Figure 14 is an enlarged view of the test article representing a typical PCB assembly. It shows the component side and gives the location of the 34 individual circuit elements along with their schematic reference designators.

The assembly consists of a single-sided, epoxy-copper-clad having overall dimensions of approximately 4-1/2 x 5-3/8 x 1/16 in. One prototype board and six fully populated "production" boards were fabricated. All of the components were

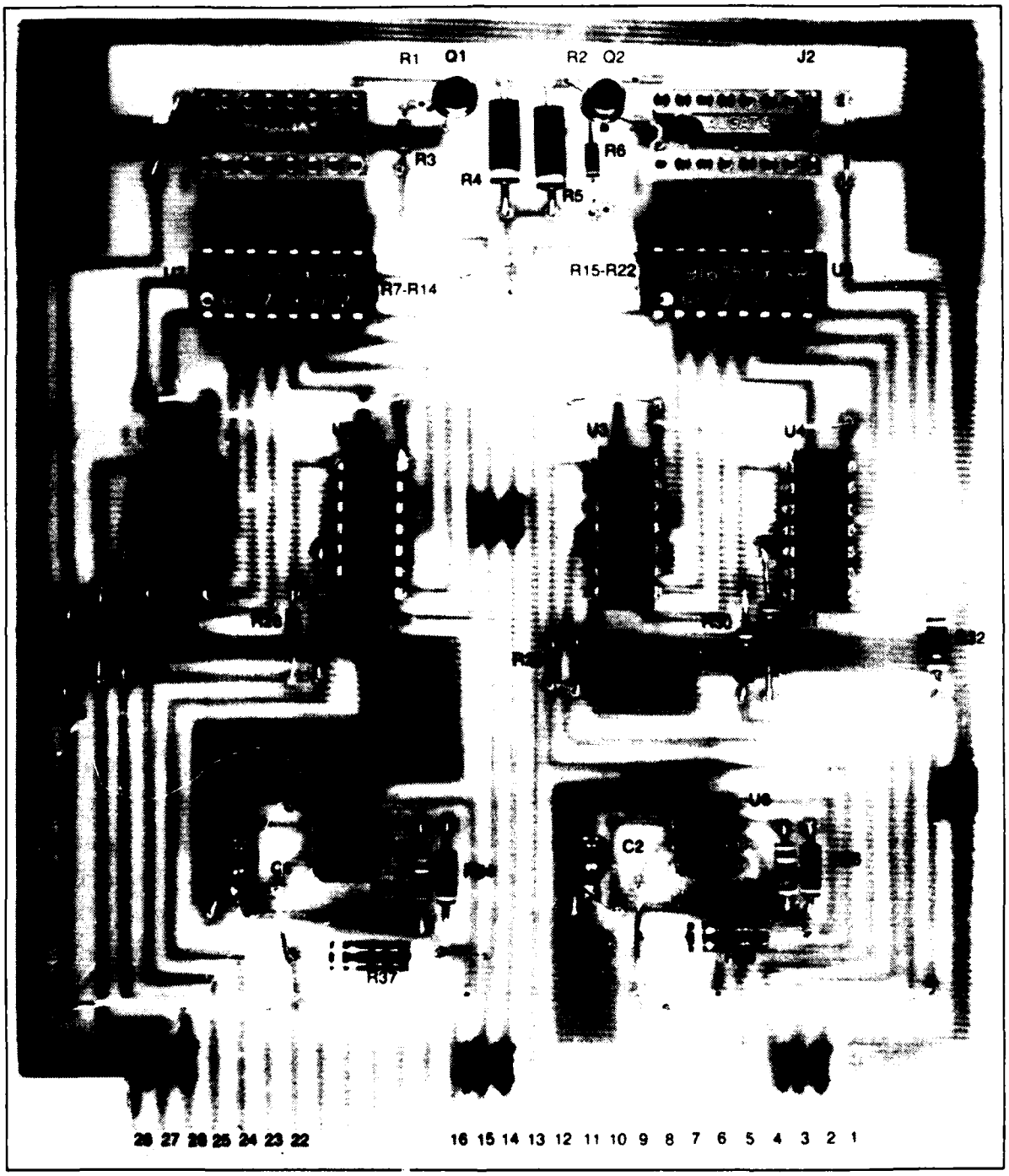

Figure 14 Populated printed circuit assembly (component side view--enlarged).

hand soldered and comprised 202 connections per assembly. The solder joints were inspected visually using a bench light magnifier.

The wiring (circuit trace - solder connection) side of the assembly is shown in Figure 15. The location of the major components is shown, and the first of each IC package is identified along with the edge connector pin-out.

An overall schematic diagram of the PCB is shown in Figure 16. It describes two each of three basic circuit types:

- NPN Transistor circuit (Q1 & Q2)
- Astable Multivibrator (U5 & U6)
- Digital Logic NAND Gate
  - Normal TTL (U1 & U2)
  - Low Power Schottky TTL (U3 & U4).

Connector P1 (printed circuit trace "fingers") provided for connection of the assembly to a power supply and to input control circuits. Connectors J1 and J2 are 16-pin Dual-In-Line, DIP sockets which provide interconnection to a monitoring circuit.

- Transistor Circuits (Q1 & Q2) - Both transistors are 2N2222A Silicon NPN devices in metal TO-18 size cans. The circuit is a common emitter (e) configuration typical of a relay or lamp driver. Collector (c) current (Ic) is from P1-14 through load resistors R4/R5. The base (b) current is supplied through P1-15/13 limited by resistors R3/R6. External bias voltages applied to the base permit operation of the transistors from cut-off through saturation.

  R1/R2 provide connection, via connectors J1-9/J2-16, to Light Emitting Diodes (LEDs) which indicate the operating status (ON-OFF) of the two circuits.

  Power dissipation of the circuit components in the full ON condition (base supply and Vcc = 5 Vdc) are typically:

  R1/R2 = 19 mW

  R3/R6 = 36 mW

  R4/R5 = 250 mW

- Astable Multivibrator Circuits (U5 & U6) - Both circuits are SN555 Integrated Circuits (ICs) in an 8-pin DIP. The circuit configuration used is that of a free-running astable multivibrator. The component values shown resulted in a period of approximately 300 msec with a duty cycle of 25%. The output pulse period and high/low times are determined by the value of

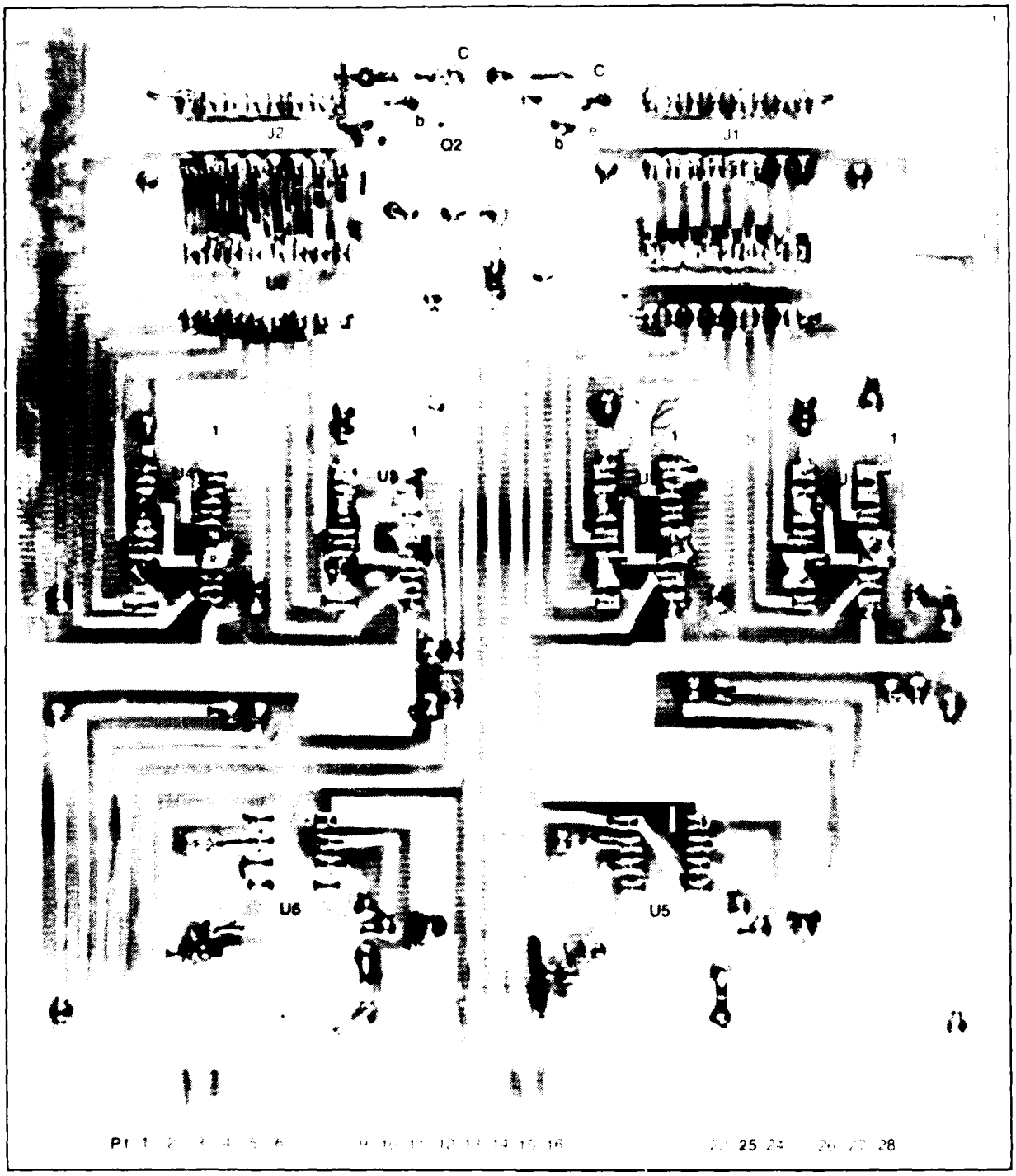

Figure 15 Populated printed circuit assembly

(wiring side view enlarged)

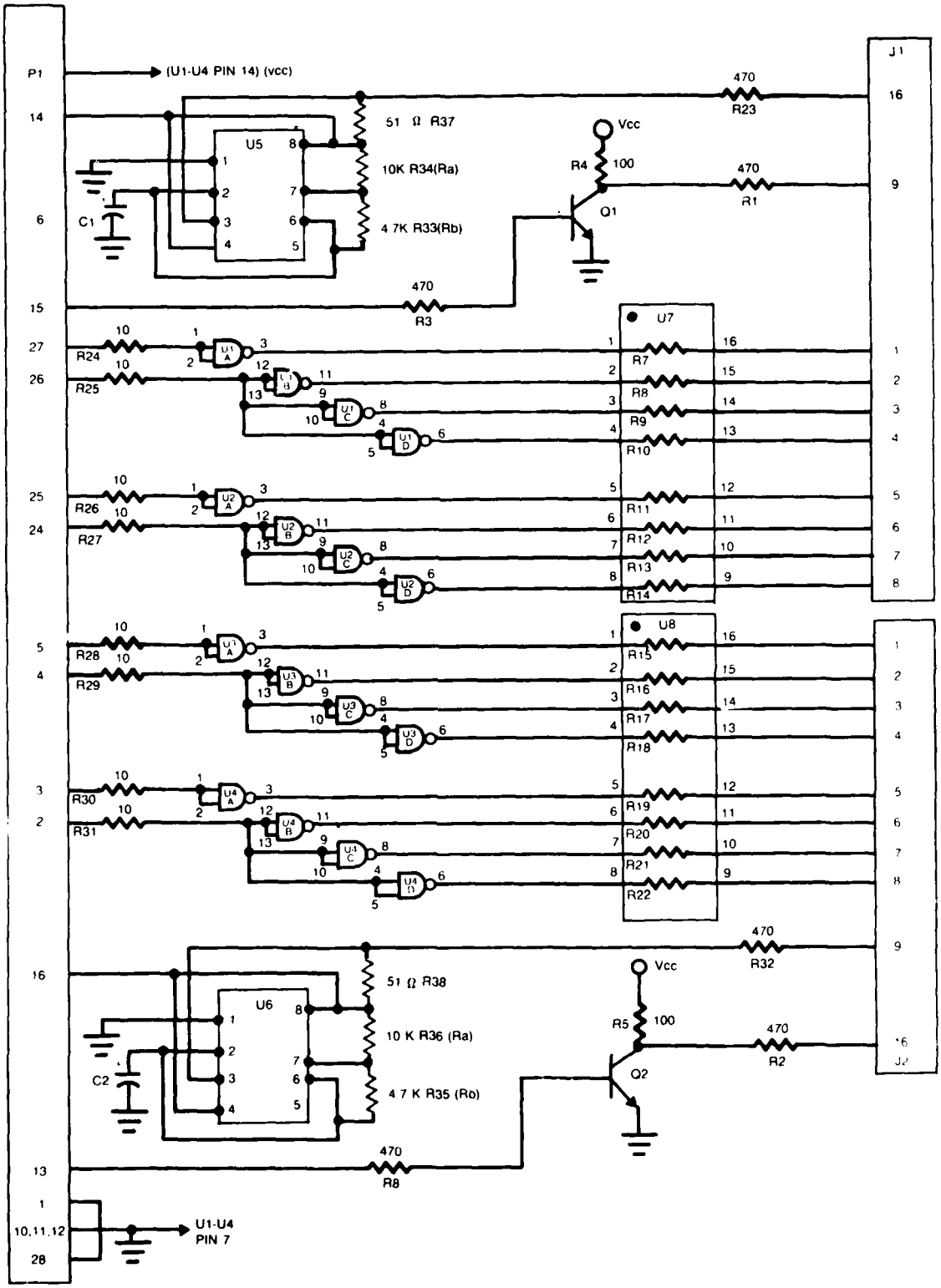

Figure 16 Typical printed circuit assembly schematic

capacitor C1 and Ra, Rb. The output high time is determined by the formula 0.685 (Ra + Rb) C1 and is calculated to be 221 msec. An output low time of 71 msec is derived from 0.686 (Ra) C. A Vcc of 5.0 Vdc is applied to IC pin 8 through P1-6/16. The reset pin 4 is not used and is tied to pin 8. Output pin 3 is connected through R37/R38 to Vcc resulting in a current sink load of approximately 100 mA. Resistors R23/R32 provide connection to the monitor circuit LEDs via J1-9/16

- Digital Logic Circuit (ICs U1 - U4) - All four of the circuits are logically identical and differ only in power dissipation characteristics. Only the operation of U1 will be detailed.

  Both of the inputs (pins 1 and 2) of Gate A are connected together and brought to J1-27 through R24. The output (pin 3) of this gate is connected to J1-1 through R7 (1/8 of Resistor Network U7). Application of a logic 1 (high 2 Vdc) to J1-27 causes the output to go low and illuminate an LED on the monitoring circuit. Connecting the inputs to ground (0.8 Vdc) causes the output to go high and the LED to be off.

  All of the inputs to Gates B, C, and D are connected together and through R25 to J1-26. The output pins (6, 8 and 11) of these gates are connected through separate resistors (R8, 9, 10 of U7) to one LED on the monitor circuit which now indicates that three gates are either on or off.

  Each of the four ICs may, therefore, be independently set to either of the following states:

  - Four Gates ON
  - Three Gates ON
  - One Gate ON
  - Four Gates OFF.

4.1.3 Phase III Populated Printed Circuit Assembly - Dynamic Tests

The test articles for this phase were the same PCBs used in Phase II with actual workmanship defects incorporated. The defects were:

- No solder connections (Figure 17)
- Poor solder connections (Figure 18)
- Component external lead wire damage (Figure 19 and 20)
- Component internal wire bond defect (Figure 21)
- PCB trace damage (Figure 22).

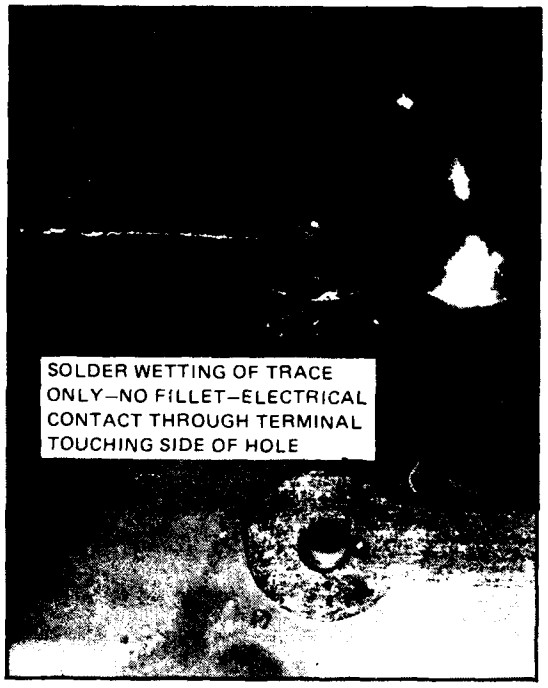

Figure 17 No solder joint (10X)

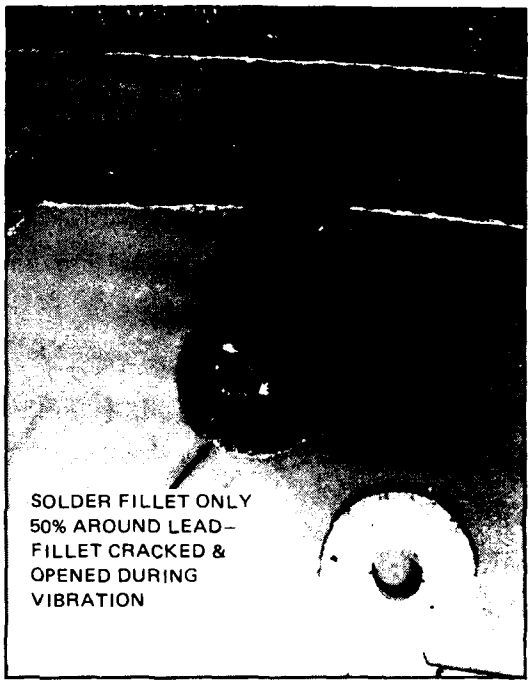

Figure 18 Poor solder joint (10X)

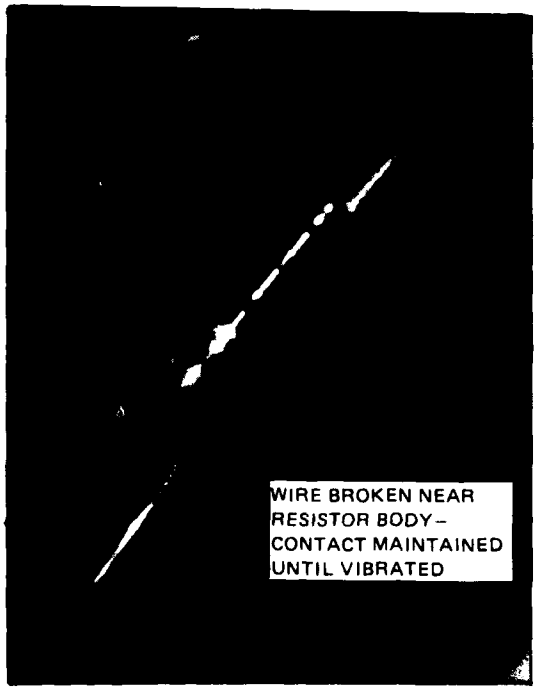

Figure 19 External lead wire damage (10X) component

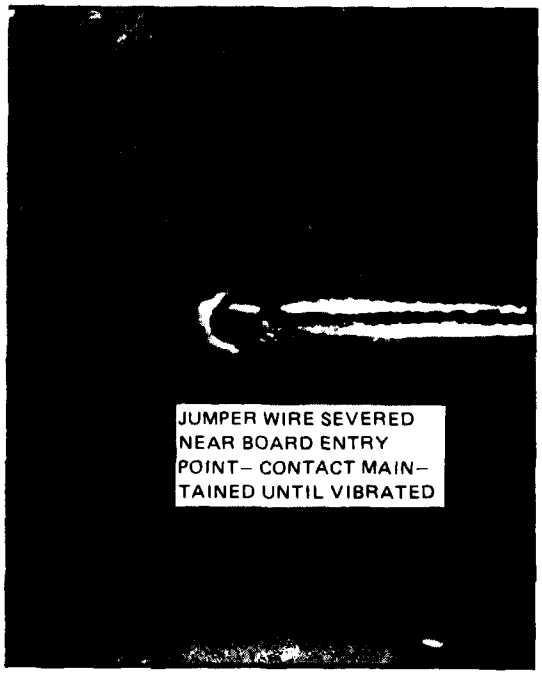

Figure 20 External lead wire damage (10X) PCB

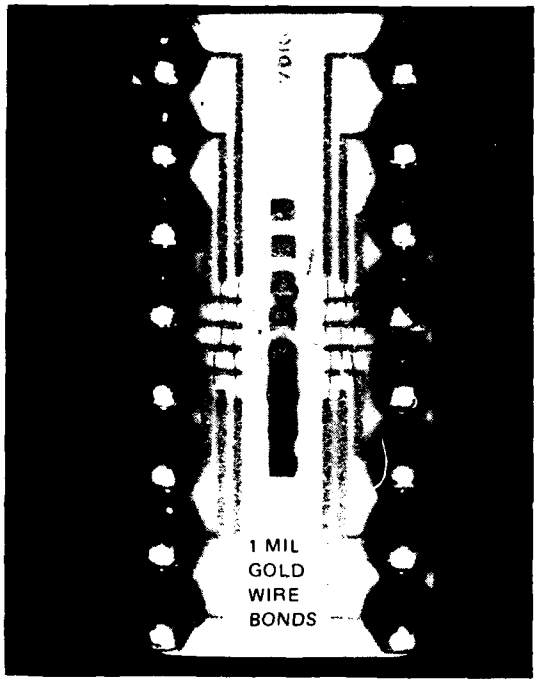

Figure 21 Internal wire bond defects (5X)

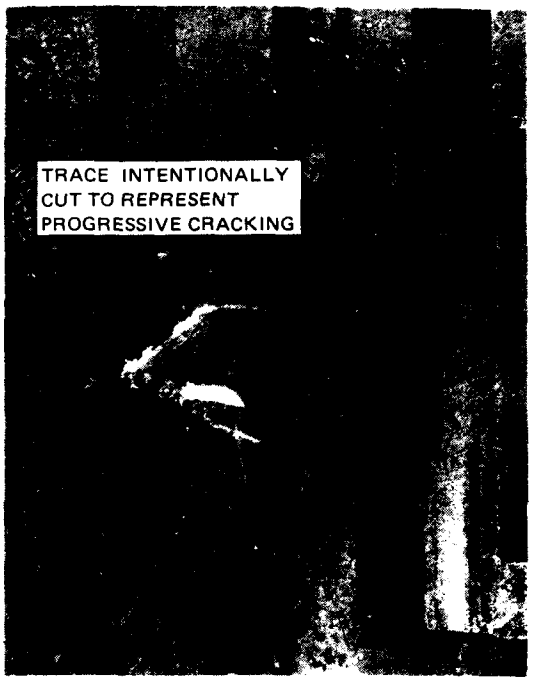

Figure 22 PCB trace damage (10X)

4.2 TEST SET-UPS

4.2.1 Phase 1 Component-Level Tests

Figure 23 shows the various holding fixtures and test equipment used to perform component-level tests. They permitted the electrical characterization of the component and the viewing of their thermal signatures under variable operating conditions.

Test set-up schematic No. 1 (Figure 24) allowed any one, or all, of 16 remotely located points to be connected to an external variable power source. Loads connected between these points and a common ground could then be powered independently or in combination. This permitted the direct comparison of the thermal signatures of components of the same or different types. Toggle switches S1 through S16 allowed the setting of the 16 positions to a variable voltage level or to ground. Switches S17 through S33 permitted the remote position to be connected directly to the voltage source or selectively, via rotary switch S34, through an external current meter to determine individual power levels. Power dissipation of the connected loads could be changed simultaneously with the variable supply or individually by insertion or external series resistors.

Figure 25 shows the schematic of the test setup which permitted either or both of two ICs, of up to 16 pins each, to be powered under various input/output terminal conditions. The devices could be tested directly at the switch assembly

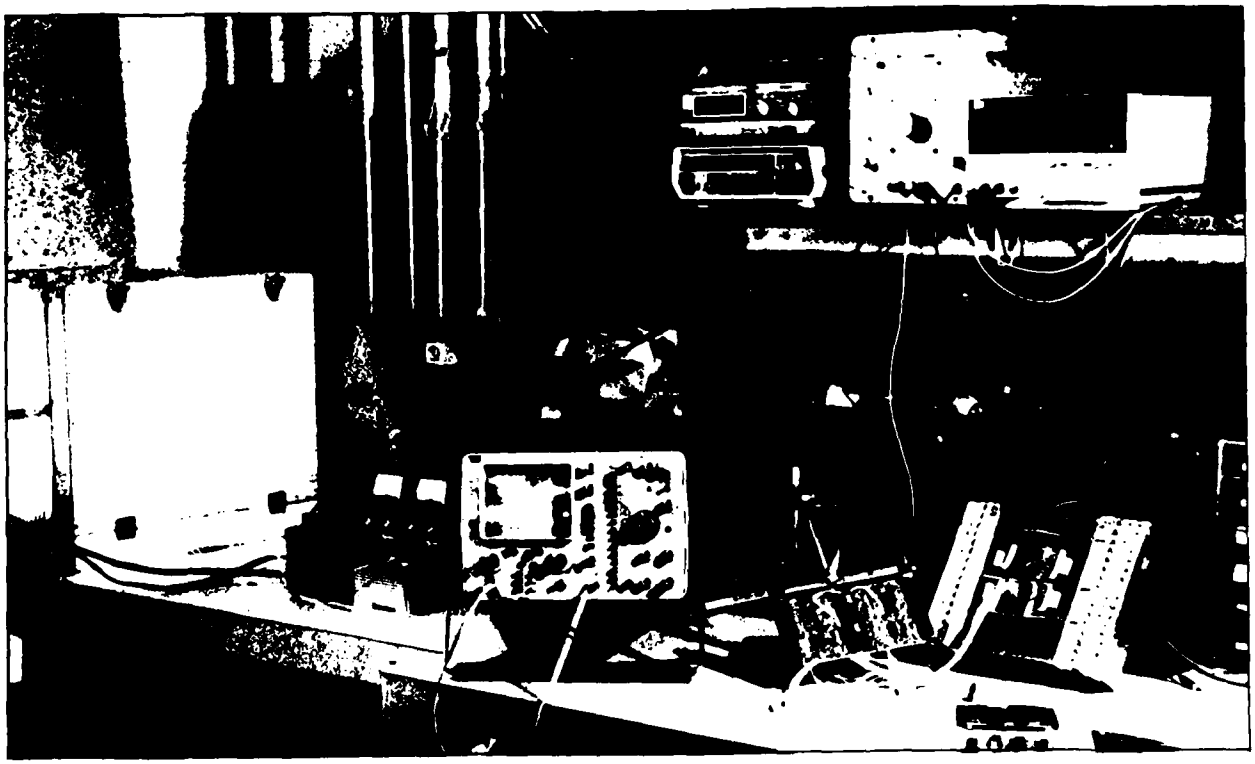

Figure 23 Component test holding fixtures and test equipment

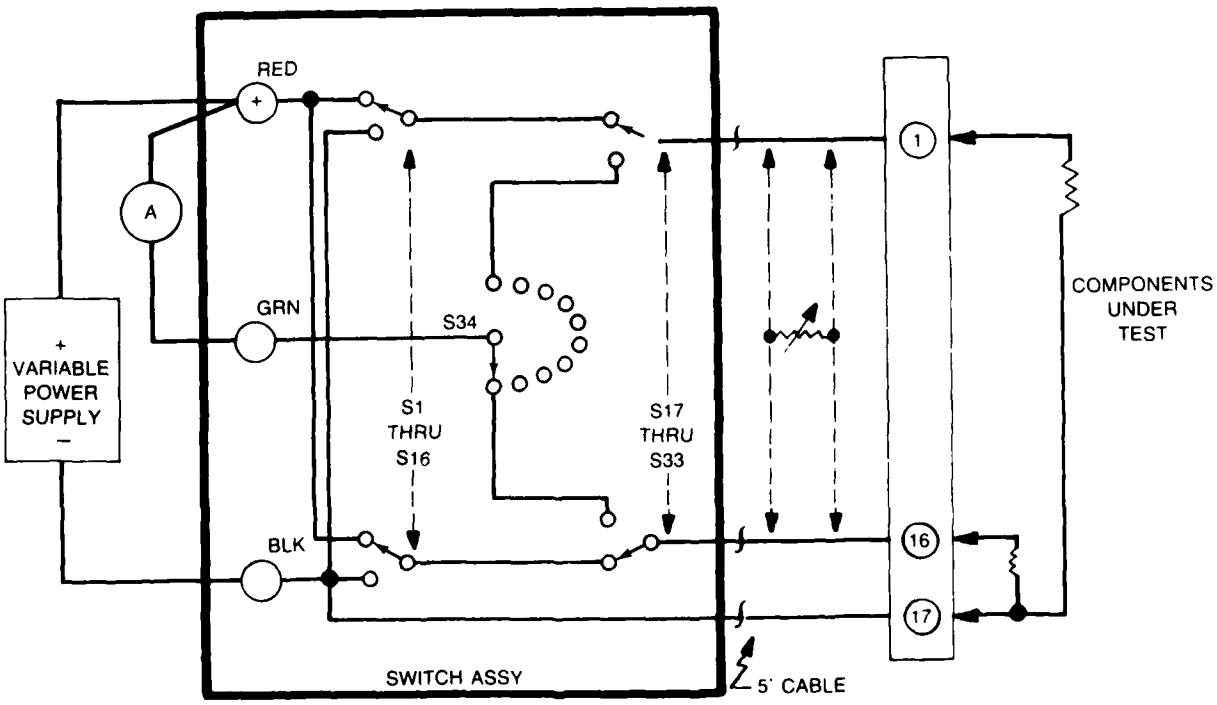

Figure 24 Component test set-up no. 1 schematic

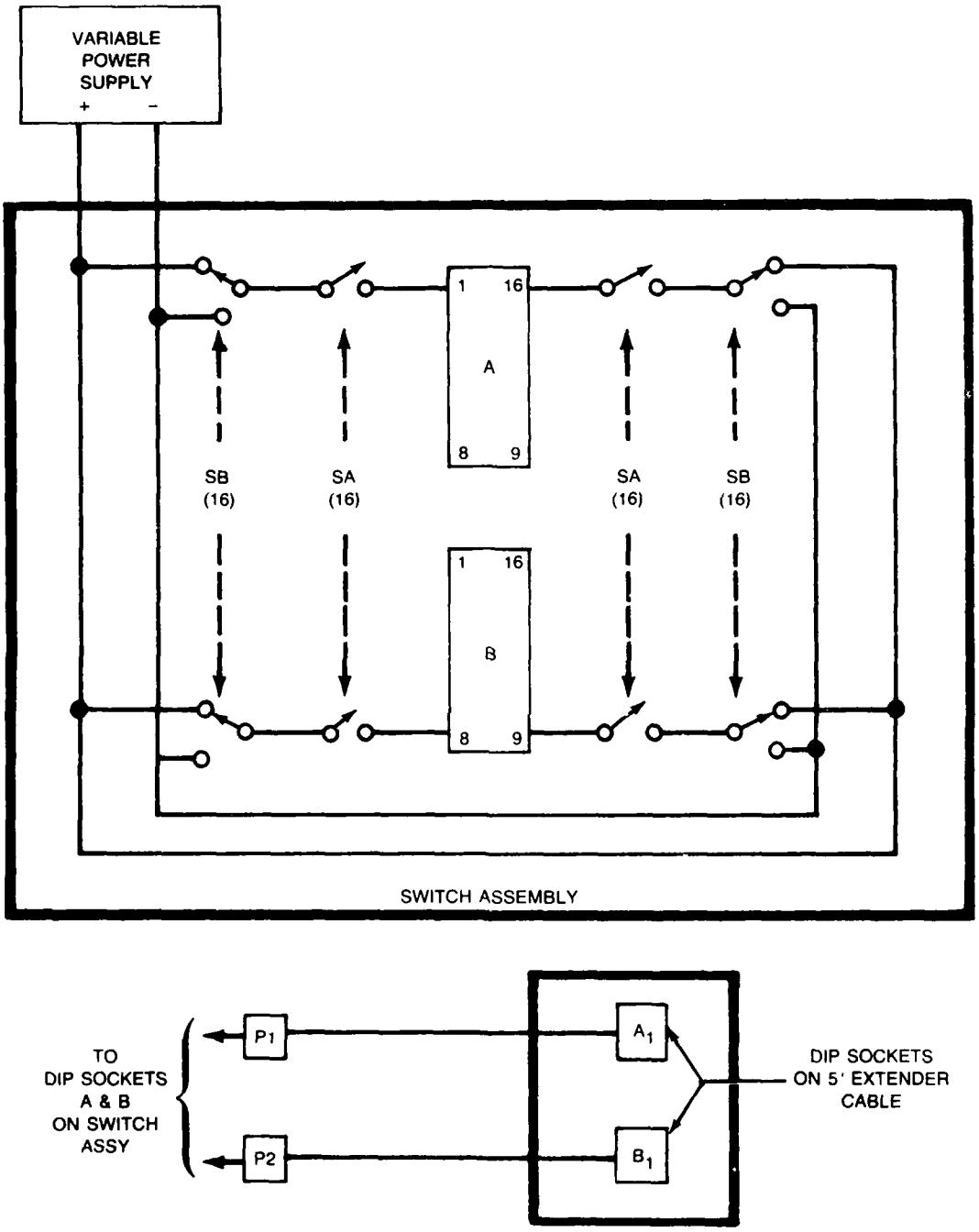

Figure 25 Component test set-up no. 2 schematic

(test sockets A/B) or at remotely located test sockets A1/1. These sockets were zero-insertion-force types allowing quick changing of the test articles. The toggle switches identified as SA allowed the test socket terminal to be connected, via the switches designated SB, to either of two buses. Placing the SA switches in an open position permitted the insertion of a current meter or the connection of output loads.

4.2.2 Phase II Static PCB-Level Tests

Figure 26 shows the electrical interconnections used to perform the static PCB-level tests. Each of the test articles was mounted in a holding fixture within the field of view of the thermal imager. The holding fixture contained an edge-type connector which permitted any of the test articles to be connected to the switching assembly via a five foot cable. Augat connectors on the test articles allowed connection to a remote monitoring assembly.

The switching assembly shown schematically in Figure 27 provided the means of inserting various failure analogs into the test articles. Toggle switches S1 through S12 allowed the individual circuits of the PCB to be set to a given operating status which then represented a normally functioning PCB. Deviations from this normal condition were then accomplished by resetting these switches to simulate complete or partial failure of a given circuit. Switches S1 and S2 caused the transistor circuits to be turned fully on or off. Partial turn-off of these circuits was accomplished through insertion of external series resistances connected to TPI and TP2 with S13/S14 opened. The on-off condition of gate A of integrated circuit U1 was controlled by S3 while gates B, C and D of this device were simultaneously controlled by S4. The device could therefore be set to any of four conditions, i.e., one gate on and three off; one off and three on; four on; four off. ICs U3 through U4 could be set to the same conditions through manipulation of switches S5 through S10. Switches S11 and S10 controlled the functions of U5 and U6.

Figure 28 shows the monitoring circuit schematic diagram. Twelve LEDs provided a visual indication of the operating status of the circuits on the PCB. They were connected between +5 Vdc and the individual circuits by two six foot ribbon type cables via J1 and J2. LEDs 1 and 7 were illuminated when transistor circuits Q1 and Q2 were turned on. The pulsed operation of timing circuits U5 and U6 was indicated by the flashing of LEDs 2 and 8. The status of the A gate of each of the integrated circuits U1 through U4 was indicated by LEDs 3, 5, 9, and 11, while that of gates B, C, and D was shown by LEDs 4, 6, 11 and 12.

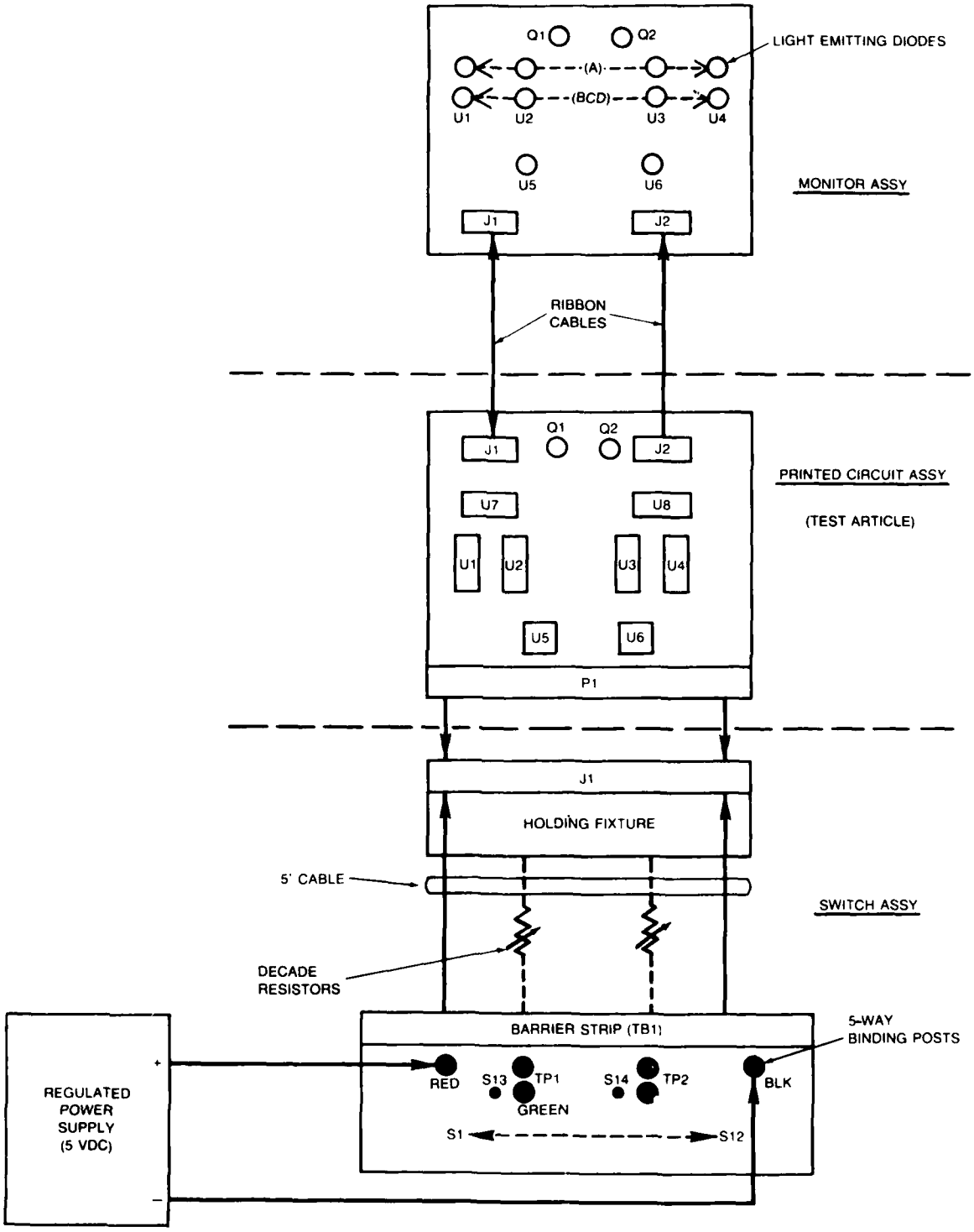

Figure 26 PCB test set-up wiring diagram

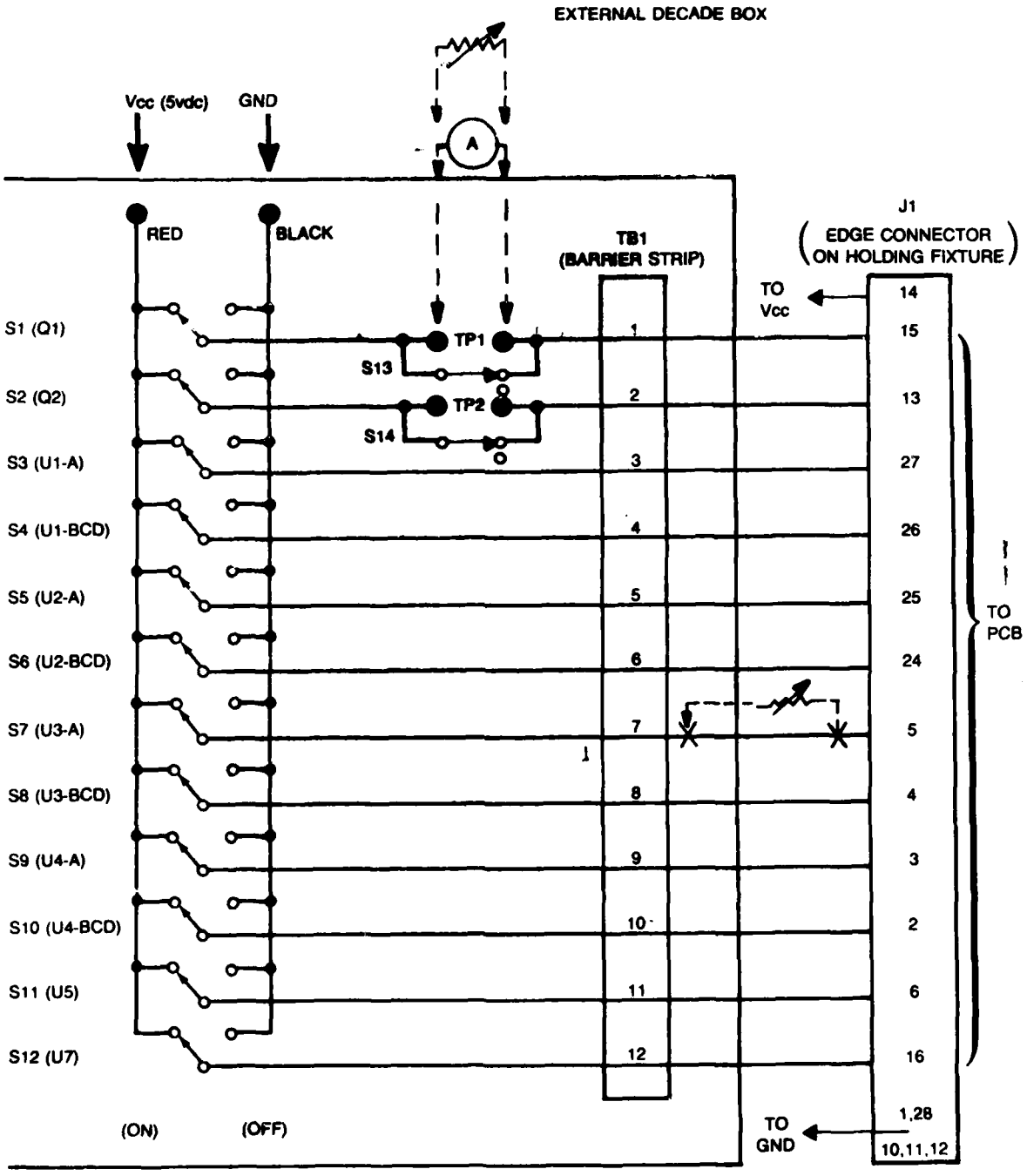

Figure 27 Switch assembly schematic

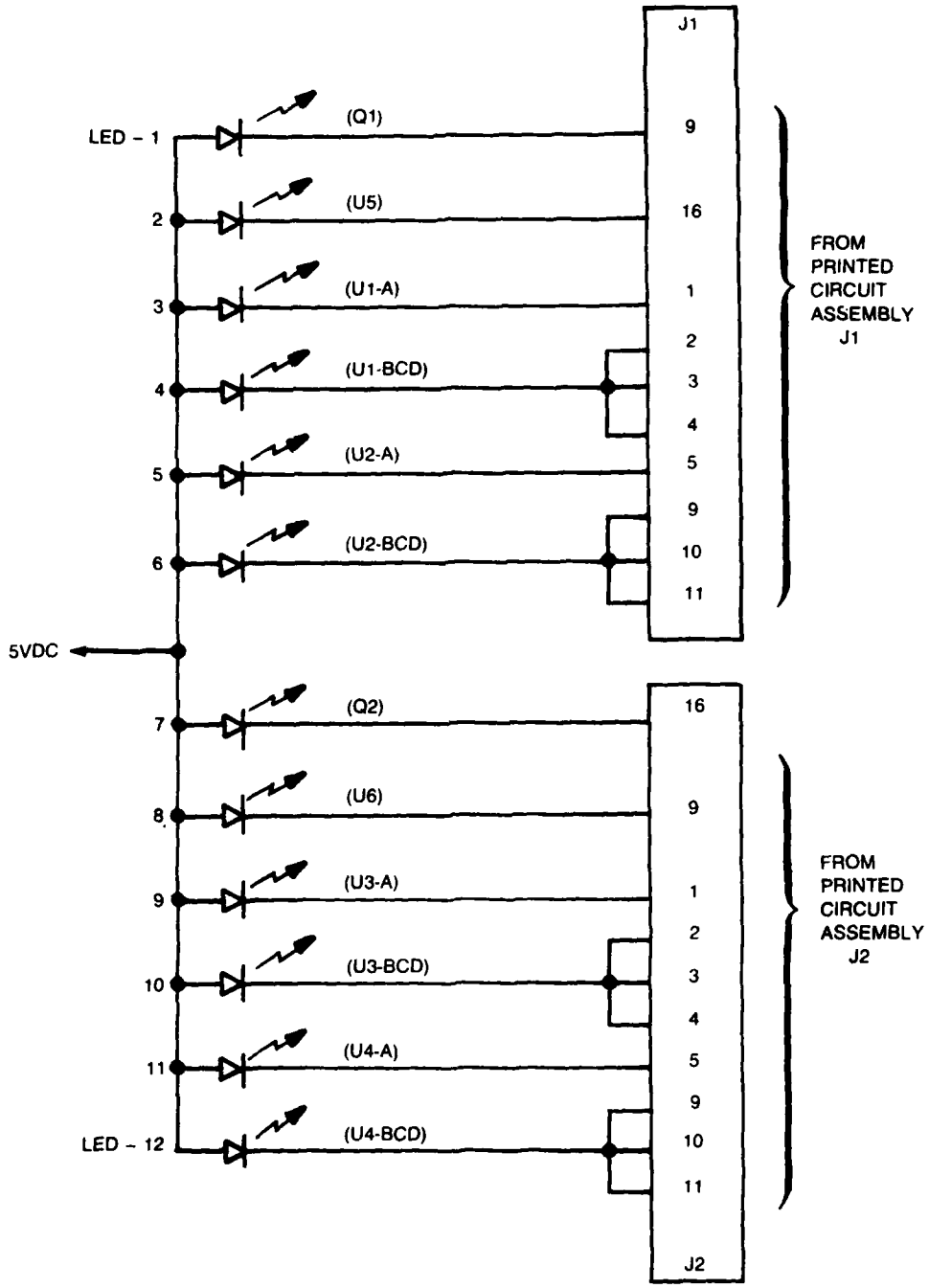

Figure 28 Monitor assembly schematic

4.2.3 Phase III Dynamic PCB-Level Tests

The electrical test fixtures described above also were used during environmental tests of the PCBs.

Figures 29 and 30 depict one of the test articles as mounted on the shaker head and viewed by the thermal imager via the front surface mirror.

The random vibration spectrum was supplied by an audio tape played back on a Sony EL7 tape deck (Ref 4). Power amplification was provided by a Model 2250 MB amplifier and applied to a PM50 vibration exciter.

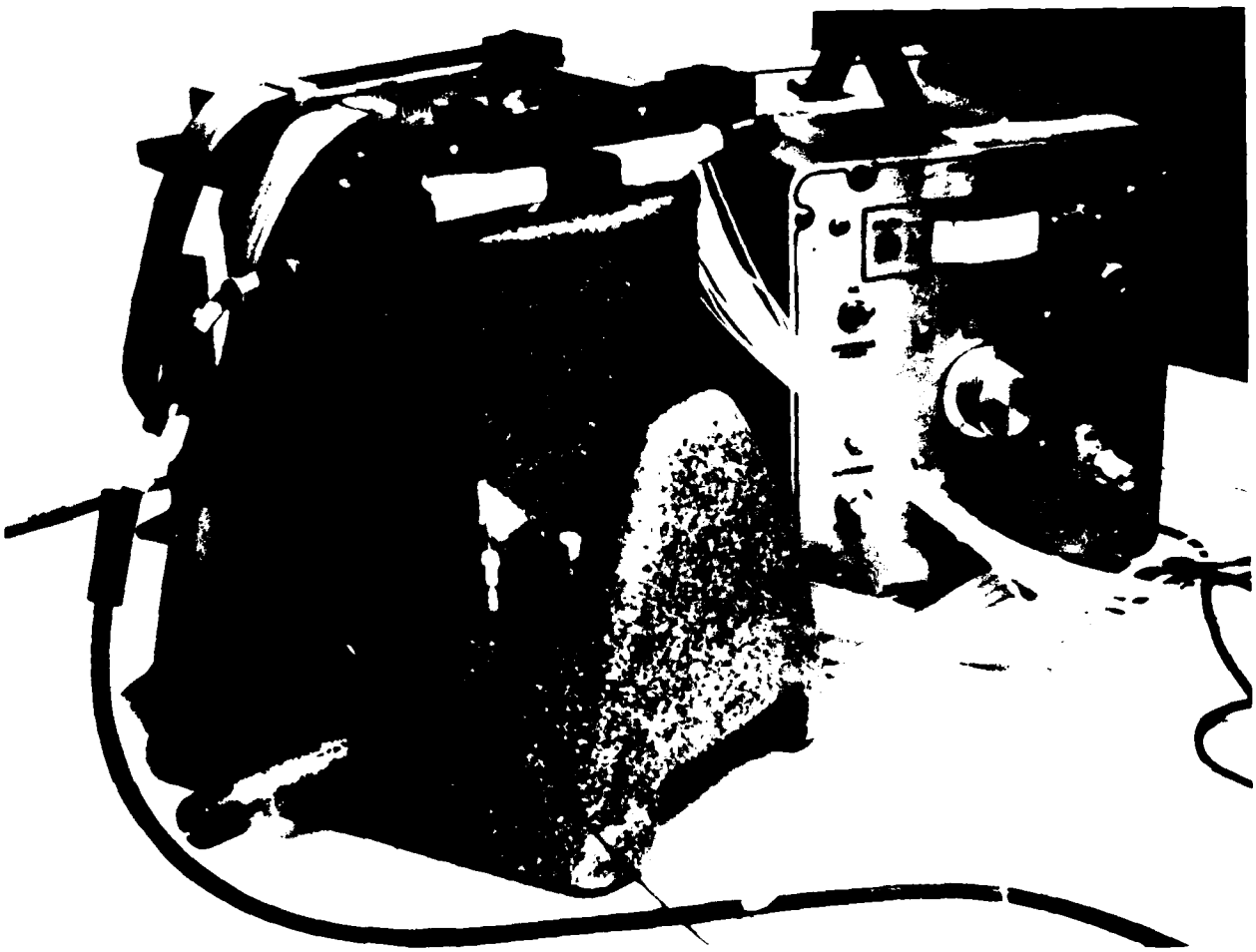

Figure 29 Test article mounted on shaker head

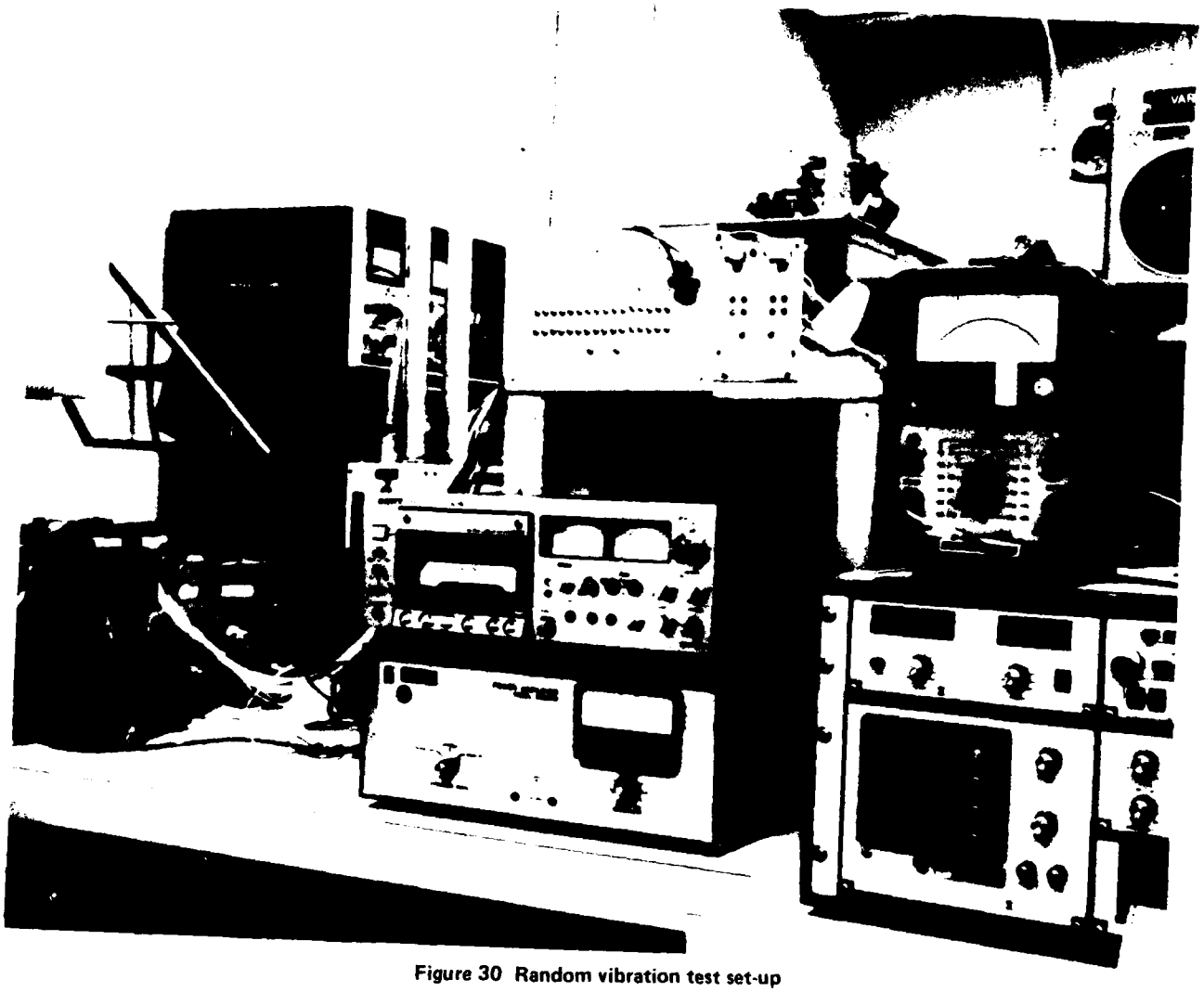

Figure 30 Random vibration test set-up

5 - STUDY PROGRAM IMPLEMENTATION

5.1 PHASE I COMPONENT-LEVEL EXPERIMENTS

The Phase I experiments were conducted on individual and then multiple groupings of typical components. They were accomplished under the ideal conditions of a standard laboratory environment, with all but one of the thermal constituents held constant. The tests were designed so that the effects of the principal parameters of concern (ambient temperature, unit-unit power differences, case material, emissivity and heat spread) could be determined and effective means of normalizing any variations established. These tests were accomplished in order to establish the system's Threshold Of Detectability (TOD), its repeatability and to explore the feasibility of defect growth tracking.

Approximately 300 resistors were randomly selected from stock. They included those resistance values and power ratings expected to be used in subsequent fabrication of printed circuit assemblies. The bulk of these were carbon composition types with a 5.0% tolerance, which represents a worst-case condition. Additional components including resistor network packages, transistors, and integrated circuits were also examined. All of the components were first inspected visually with the aid of a magnifier for evidence of existing or potential flaws.

Electrical characterizations were then accomplished relative to specification parameters, to provide verification of the component's operational status and information about unit-unit differences, thereby establishing a basis for interpreting subsequent thermal images. Resistance measurements of approximately 300 resistors showed what appeared to be a normal distribution within the 5.0% tolerance limit. Operation of any given resistance value at the minimum acceptable power derating of 50% would produce a maximum power deviation of ±50 mW for a 2.0 W size and ±3.1 mW for an 1/8 W size. The worst-case power differential between any two resistors of the same resistance value and physical size would therefore be 100 mW. Power measurements of typical integrated circuits having different manufacturing date codes showed a "high" to "low" power dissipation range of 20 mW, while the devices with the same date code only exhibited a 2.0 mW range.

Thermographic image examinations were then made under existing laboratory ambient conditions and at a given input voltage applied for a specific time period.

The purpose of these examinations was to establish thermal signature characteristics, assess the system's threshold of detectability and provide time temperature information so that repetitive experiments could be designed to permit comparisons. These tests were made with the individual components mounted in the Field Of View (FOV) of the imager and connected to a variable voltage supply. They were mounted by various means (suspended in free air via bus wire supports, on vector boards or on PCB material) in order to define the surrounding area effects.

The signature of components having different sizes, geometric shapes or materials of construction were (not unexpectedly) found to have recognizable differences. This is illustrated by Figure 31, which depicts the thermal image of a number of 100 Ohm carbon composition resistors operating at the same applied voltage for the same period of time, therefore dissipating the same power but having different physical sizes. The "footprint" of the larger sizes (R7-R9) is clearly different from those of the smaller ones (R1-R6). The observed differences are primarily attributable to their different masses and the corresponding effect on the IR radiation. These differences were considered beneficial since the intended utilization of the system would entail delta mode comparisons of the same item when an assembly was compared against itself (e.g., prior to and after environmental exposure) or like items from assembly to assembly, if it proved feasible to compare a number of production boards against a standard. The substitution of, for example, a 0.5 W resistor for a 1.0 W size in a production run could therefore be expected to be readily detectable.

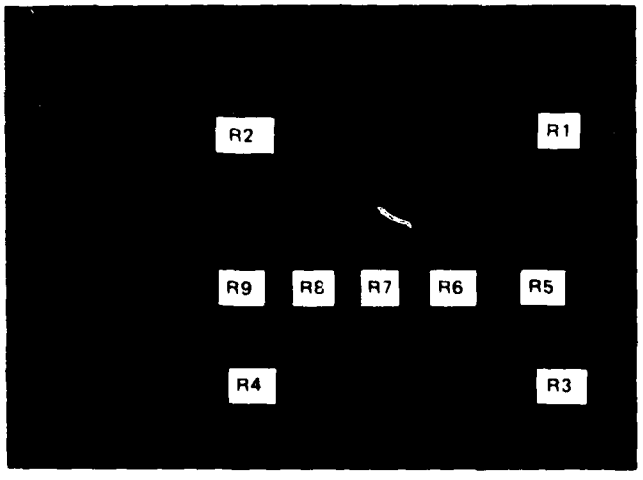

R1,2,3,4&6 = ¼ W SIZE
R5 = ⅛ W SIZE
R8 = 1 W SIZE
R9 = 2 W SIZE
R7 = ½ W SIZE

Figure 31 Carbon composition resistors - 100 ohm

5.1.1 System Repeatability Experiments

A number of delta runs using a resistor operating at approximately 50 mW for 30 seconds were then made, which produced complete cancellation suggesting good system repeatability. Additional delta runs with components operating at power levels greater than 250 mW yielded apparent non-repeatability. The ambient temperature during these runs had been monitored and observed to remain stable. Measurements of the actual applied voltage and current showed the power dissipation of the test article to remain constant. It should be noted that the short periods of power application were being utilized in order to preclude the possible effects of heat spread and that the maximum system sensitivity setting was considered to be necessary for the earliest detection of defects.

Since two of the three primary thermal signature constituents were known to be constant, it was decided to more fully assess the effects of the short power-on or "exposure" time and the mechanics of its repeatability.

Temperature measurements of components operating at various power levels were made, utilizing the system's digital readout. These measurements yielded temperature-time histories, typically represented by Figure 32. Since repetitive

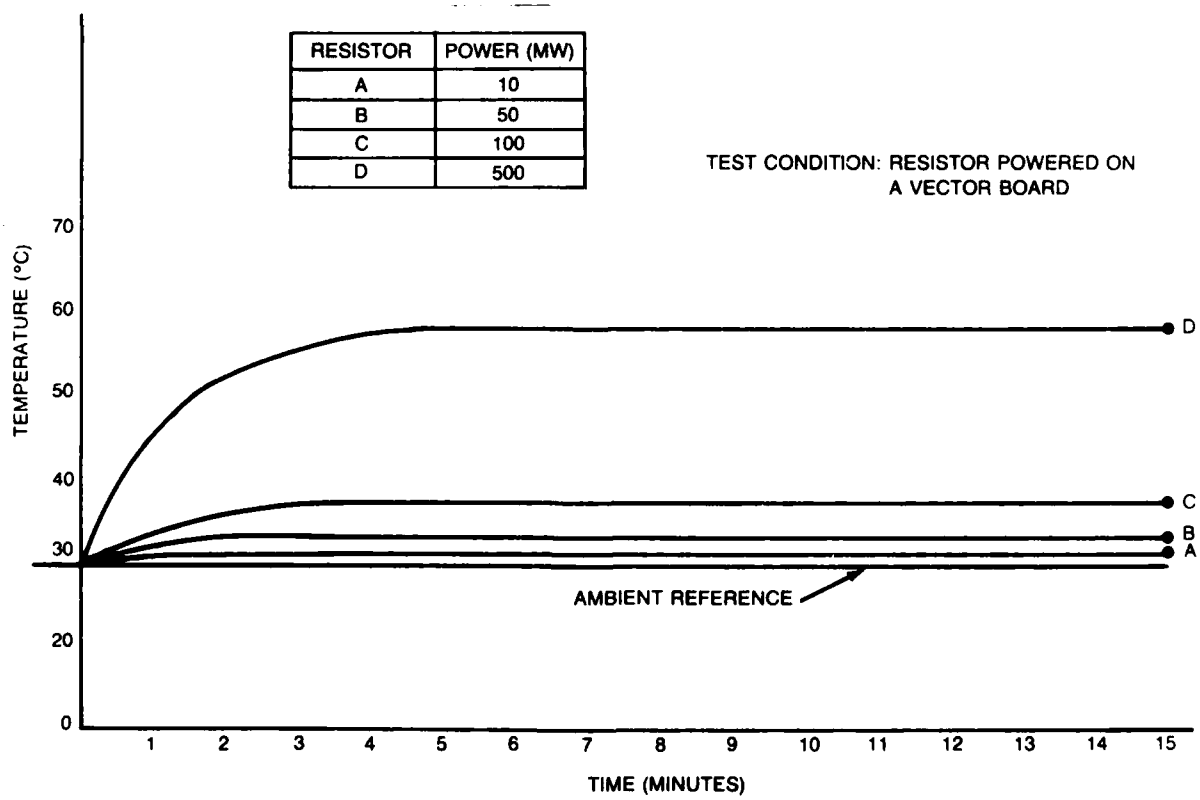

Figure 32 Typical resistor temperature stabilization periods

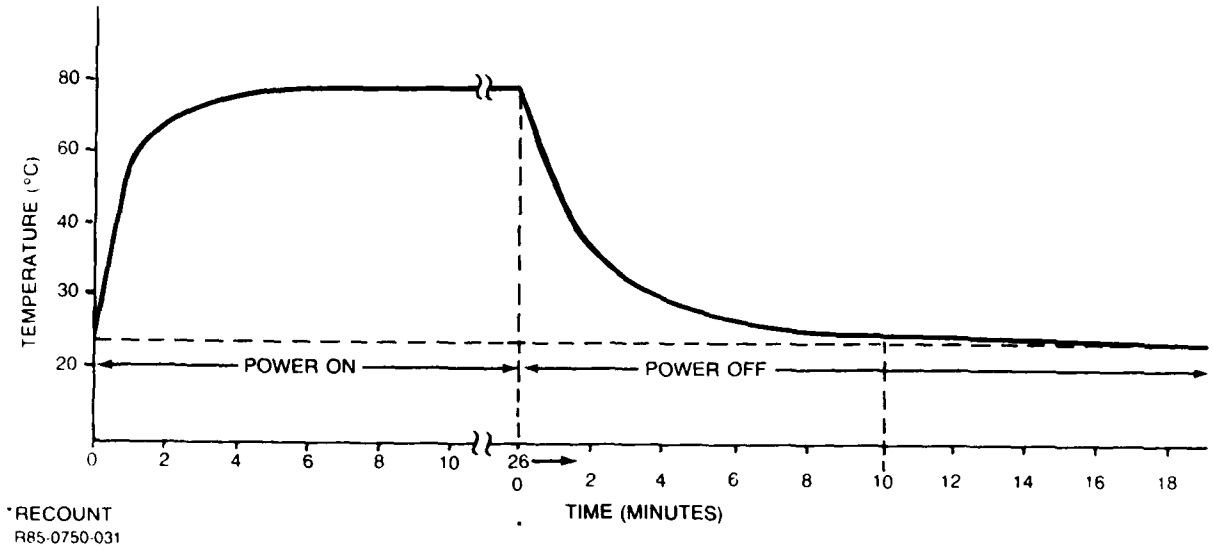

Figure 33 Cool-down curve for resistor dissipating approximately 1W

experiments on the same test article were to be made, data were obtained relative to the time required for a component dissipating approximately 1.0 W to cool down to its starting temperature (Figure 33). The 1.0 W level was considered to be typical of the highest single-component dissipation on a PCB. Examination of these curves shows a high rate of temperature rise (especially for the higher power components) during the initial period of time following turn-on. The data also shows that a period of at least ten minutes is required for the high-power device to return to its original starting temperature.

The mechanics of establishing a reference image and then making delta runs were reviewed in order to more fully define the variables affecting repeatability.

The "reference run" was made by placing the Test Article (TA) in a fixed position within the FOV with the imager operating in the normal scan mode. Power was then automatically applied to the TA at the beginning of a selected time interval and removed at the end of this interval. During this interval, the system continuously updated the data comprising the thermal image with a complete image (top to bottom of the FOV), displayed every 1.5 seconds. This updating was stopped by manually initiating the freeze-frame mode (scan hold) at the end of the time interval. The resulting image constituted the "Reference Image". Subsequent initiation of the delta mode caused the data constituting this image to be stored in the system memory, and scanning of the FOV to be re-initiated with the instantaneous difference between the FOV and the stored image displayed. A delta run consisted of a repeat of the same power-on versus time conditions which resulted in a complete algebraic subtraction and cancellation of the visual display if none of the conditions had changed.

Several factors affecting the accuracy of a given delta run were identified:

- The power-on or "exposure" time was controlled by a photographic enlarger timer. The maximum difference between repetitive runs of a given time interval was found to be 0.25 seconds when checked against a stopwatch
- The reaction time between visually identifying the end of the run (zero time) and manually initiating the freeze frame mode was identified as 0.25 seconds (human factors data)
- The system design caused the scan in progress at the time of initiating freeze frame to be completed before data updating was halted. There could therefore be up to 1.5 seconds difference in data updating between the reference and delta images depending upon where the initiation took place in each case
- Assuming a worst case condition of the additive influence of all three of the above factors a total difference of two seconds between reference image and delta images could occur.

Coupling this information with the temperature-time data, one can readily see that the high rate of temperature change (typically 30.0 C/minute = 0.5 C/second) occurring during the initial heating period of the higher dissipating components could result in temperature differences of up to ±1.0 C. These differences would be immediately apparent at the chosen 0.1 C/CL sensitivity. The use of an exposure time of for example, ten minutes, would appear to obviate the error since there would be virtually no temperature change over the timing error period. However, this approach would require all comparisons to be made for the ten minute period and was considered to be a decided disadvantage for the production card screening scenario for which this technique is intended.

Examination of the knee of the curve of a 1.0 W resistor showed the rate of rise at three minutes to be on the order of 10 C/minute = 0.016 C/second. This three minute time period was considered to be a viable tradeoff since, the maximum temperature differences between runs could be expected to be ±0.032 C or less and probably not be visually identifiable.

Reference and delta runs for three minutes of power-on time were then accomplished and did produce more repeatable results. However, some runs did result in ambiguities that were greater than the expected maximum. It was then realized that the initiation of freeze frame was accomplished coincidently with removal of power from the TA. The cool-down data for the high power component (Figure 33) shows the initial period after turn-off to also have a very high rate of change, which would still greatly influence the final thermal signature regardless of the power-on time.

It was concluded that the procedure should be revised to cause data updating to be discontinued prior to power shut-down and thereby permit the error to be influenced only by the low rate of rise at three minutes. Subsequent runs in which updating was stopped two seconds prior to turn-off resulted in sufficient repeatability for continuing with experiments to define the threshold of detectability and the effects of unit-unit variations.

5.1.2 Threshold of Detection Experiments

Reference images of various components operating at known power levels were then made and subsequently compared with operation for the same time period but at specific reductions in the measured power levels. Figure 34a shows the delta image resulting from a power reduction of approximately 25 mW in a TTL integrated circuit, while Figure 34b depicts the image resulting from a 15 mW reduction. This degree of non-cancellation was typical of the other components examined and was considered to be the minimum threshold of detectability practicable, with all other thermal signature constituents held constant.

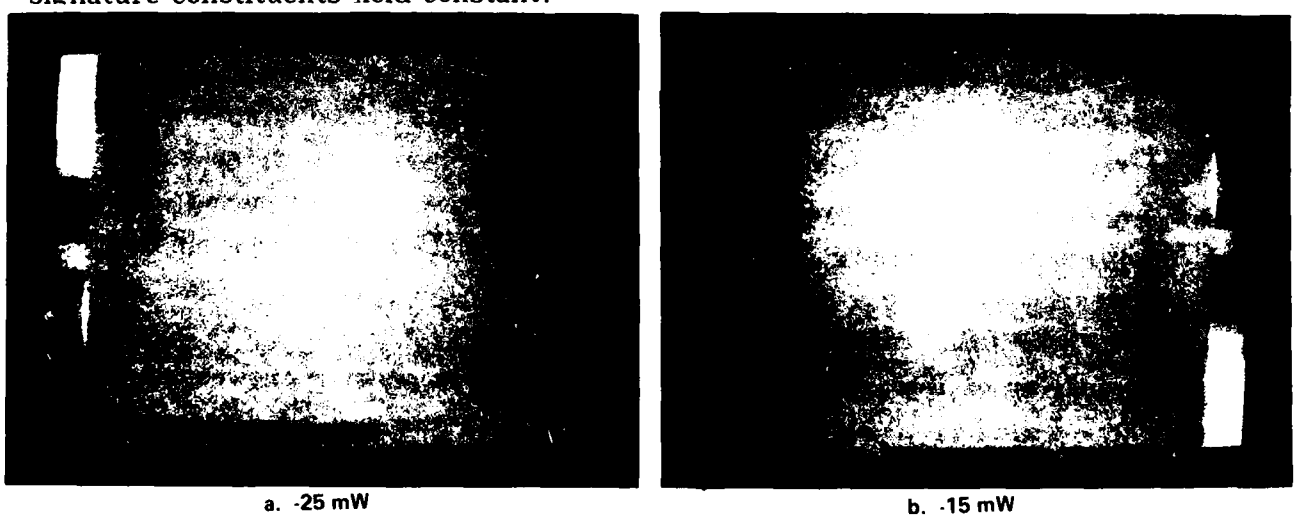

a. -25 mW b. -15 mW

Figure 34 Threshold of detectability

The ability to detect small power changes in a component which is in close proximity to a higher power dissipating device was explored. It was determined that heat spread would probably not be a significant factor for medium density PCBs. Figure 35a is the reference image of a typical experiment which evaluated the heat spread from two resistors (locations 2 and 3), operating at approximately 0.25 W each extending to one (at location 1) operating at 0.036 W. Figure 35b shows the delta image obtained when the power dissipation of the smaller one was reduced by approximately 20 mW while the operation of the other two remained the same. This change is readily discernible within the heat spread of the other resistors.

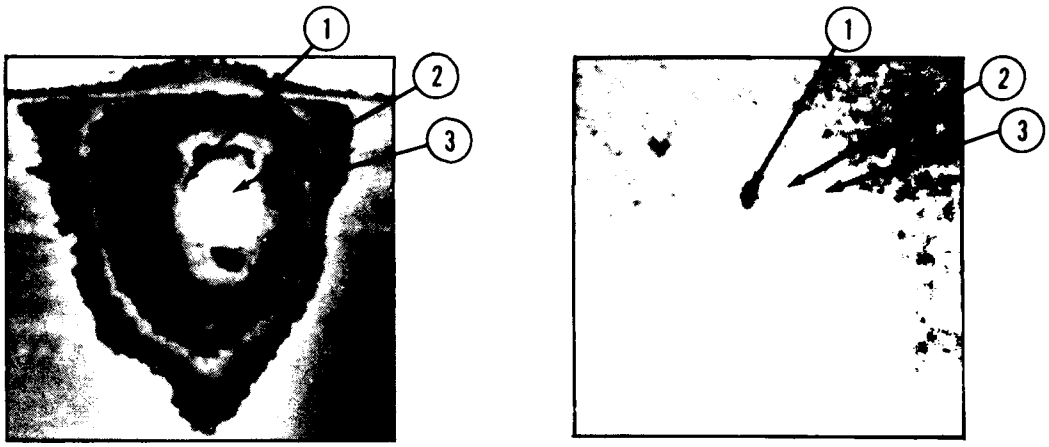

a. Reference image of typical experiment

b. Delta image-resistor 1 reduced ≈ 20 mW

Figure 35 Heat spread vs detectability

However, the effects of heat spread within a device such as a resistor network were found to be significant. Figure 36 shows a software-magnified thermal image of a resistor network having eight individual 500 Ohm resistors on a common substrate. The total package power dissipation was 0.400 W (8.0 x 0.05 W).

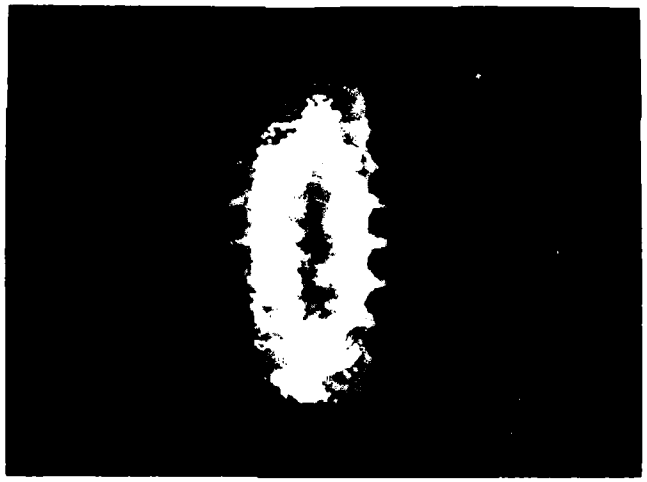

Figure 36 Software magnified thermal image of resistor network

Figures 37 and 38 depict unmagnified delta runs of the resistor network at reduced power levels. Figure 37a is the result of completely turning off one resistor located at the end of the package (all others left on), while Figure 37b shows the result of turning off one in the center of the package. Both conditions represent a decrease of 0.05 W in total package dissipation, but the end resistor is much more apparent. This was considered to be due to the heat spread from adjacent resistor elements.

The reduced ability to detect a change in the central area of the package was even more apparent when the resistor power was only partially decreased (approximately -0.025 W) and is shown in Figures 38a and 38b.

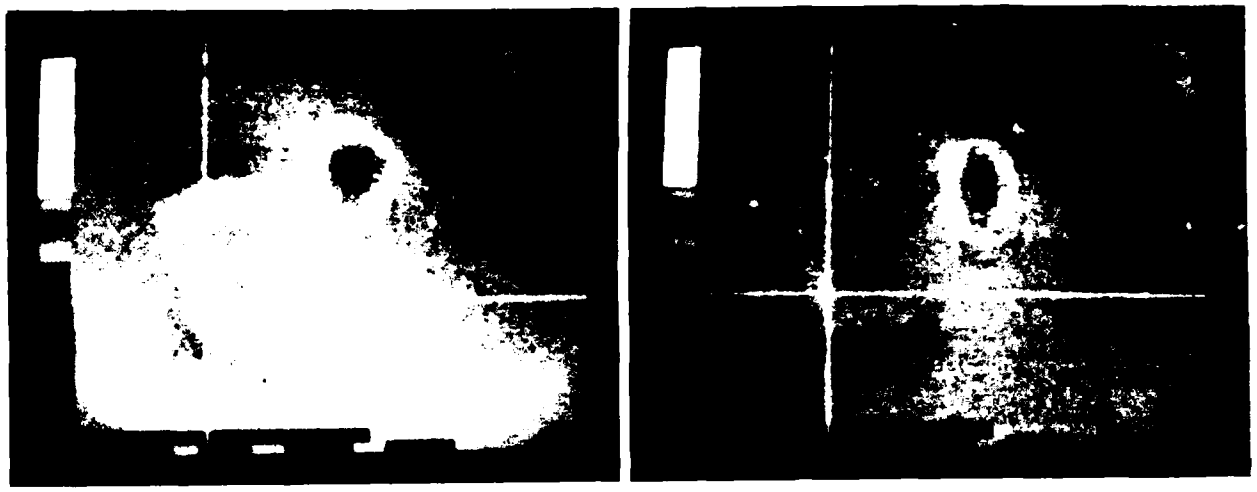

a. End resistor turned off, others power on

b. Center resistor turned off, others power on

Figure 37 Unmagnified delta runs of a resistor network at reduced power levels (-0.05W)

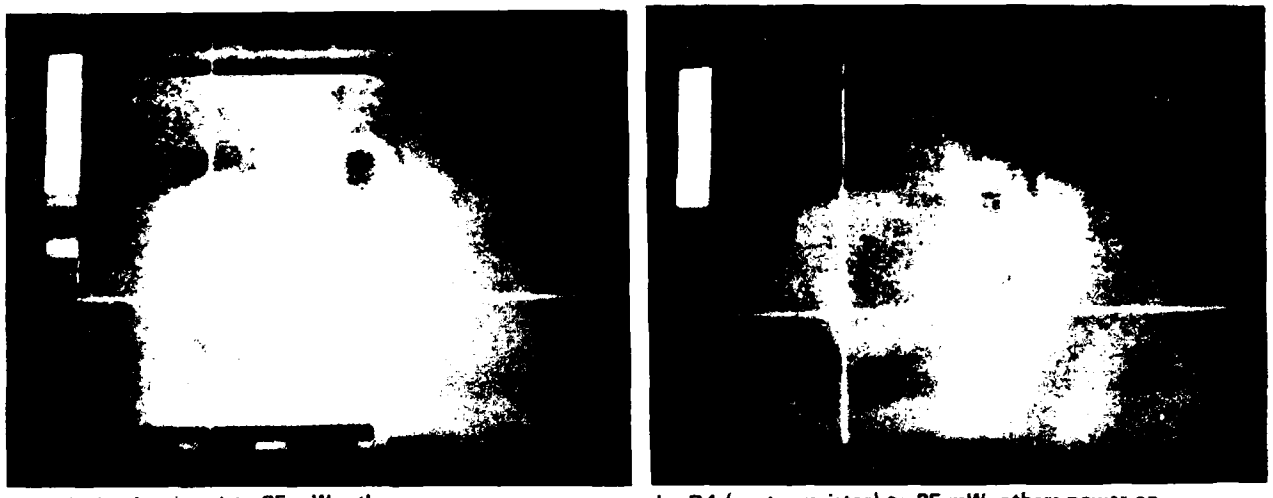

a. R1 (end resistor) ≈ -25 mW, others power on

b. R4 (center resistor) ≈ -25 mW, others power on

Figure 38 Unmagnified delta runs of resistor network at reduced power levels (-0.25W)

5.1.3 Unit-Unit Variation Experiments

The effect of unit-unit variations on the ability to accurately interpret delta images was then investigated. The experiments were conducted to provide baseline data relative to the intended system application of making comparisons of production PCBs against a standard reference.

Delta mode comparisons of a number of components of a given type referenced to a standard of that type were made (this would normally be the case with any given location on a PCB when making the assembly-assembly comparisons).

The experiments were again accomplished under idealized conditions with the input voltage, exposure time and ambient temperature held constant.

Since the comparisons would be of like items ostensibly having the same physical sizes, geometries, emissivities, and materials, it was expected that power differences would constitute the primary observed differences.

The actual power dissipation of each component under a given input condition was known from previous electrical characterizations and could be verified at any time by electrical measurements.

The utilization of an item having a power dissipation at the high or low end of the range observed for that component type, and its comparison to one at the opposite extreme of the range produced visually identifiable differences (where the spread was J15 mW). This implies that items having power differences within device specification requirements might be misconstrued as representing defectives (because of the low TOD available). It should be noted that this is not necessarily a drawback since it would cull out possible defectives. Additional fine tuning of the equipment such as the utilization of lower sensitivity settings or use of the dead band function could be developed to minimize this ambiguity.

Items determined to have identical power dissipations (and theoretically no defect) were, however, also observed to yield thermal signature differences. Differences in the actual surface condition (and therefore their emissivity characteristics) were first considered to be a factor. Intentional alteration of the surface conditions, e.g., application of black and/or white paint dabs, did not appear to significantly affect the visual results. Therefore the emissivity differences between like items was not considered to be a major driver.

The test fixture holding the components was in a fixed position relative to the FOV of the imager. However, it was determined that a sufficient amount of motion of the Test Article (TA) within the zero insertion force socket or the bend point of resistor leads could introduce a positional error between the standard and subsequently compared items. Figure 39 shows two different samples of a resistor

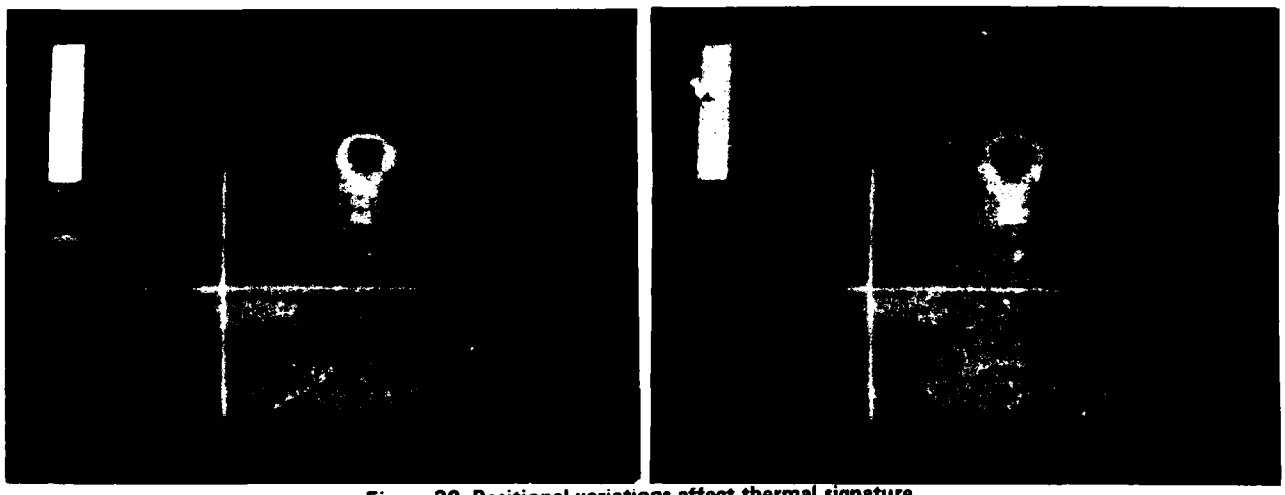

Figure 39 Positional variations affect thermal signature

network package, both with one resistor at the top end of the package turned off (reference image had it on). Electrical measurements showed less than a 0.3 mW difference and therefore no signature difference should be visually detectable. It was considered that this problem would not be as great when comparing PCB's since the individual component locations for a given position on a board are rather precisely fixed through photographic processes. The overall position of the board itself within an electrical connector is variable but it was considered that a means of repetitive location could be established and that overall mispositioning could be readily identified.

5.1.4 Defect Tracking Feasibility Experiments

The concept of tracking the growth of a "defect" was explored by varying the power applied to a resistor in known increments while keeping the period of application the same. The results are shown by the photographic sequence of Figure 40. It should be noted that the photographs tend to emphasize some of the conditions existing on the actual CRT display and to de-emphasize others. It should also be noted that the power to only one resistor (R3) of five mounted on a vector board was controlled. A reference image was made with power applied to all of the resistors for a given time period. Figure 40a shows the virtually complete cancellation obtained when a delta run was made under the same conditions Figure 40b depicts the delta image obtained when the power to R3 was reduced first by approximately 10% and subsequently through 100%. Figures 40c through 40f show the results of further incremental reductions in power, as noted. These power reductions (25 mW through 250 mW) were considered analagous to a defect such as a poor solder joint, first introducing a small resistance in series with the component and progressing toward a full failure represented by an open circuit. Additional defect growth tracking experiments were conducted in Phase II.

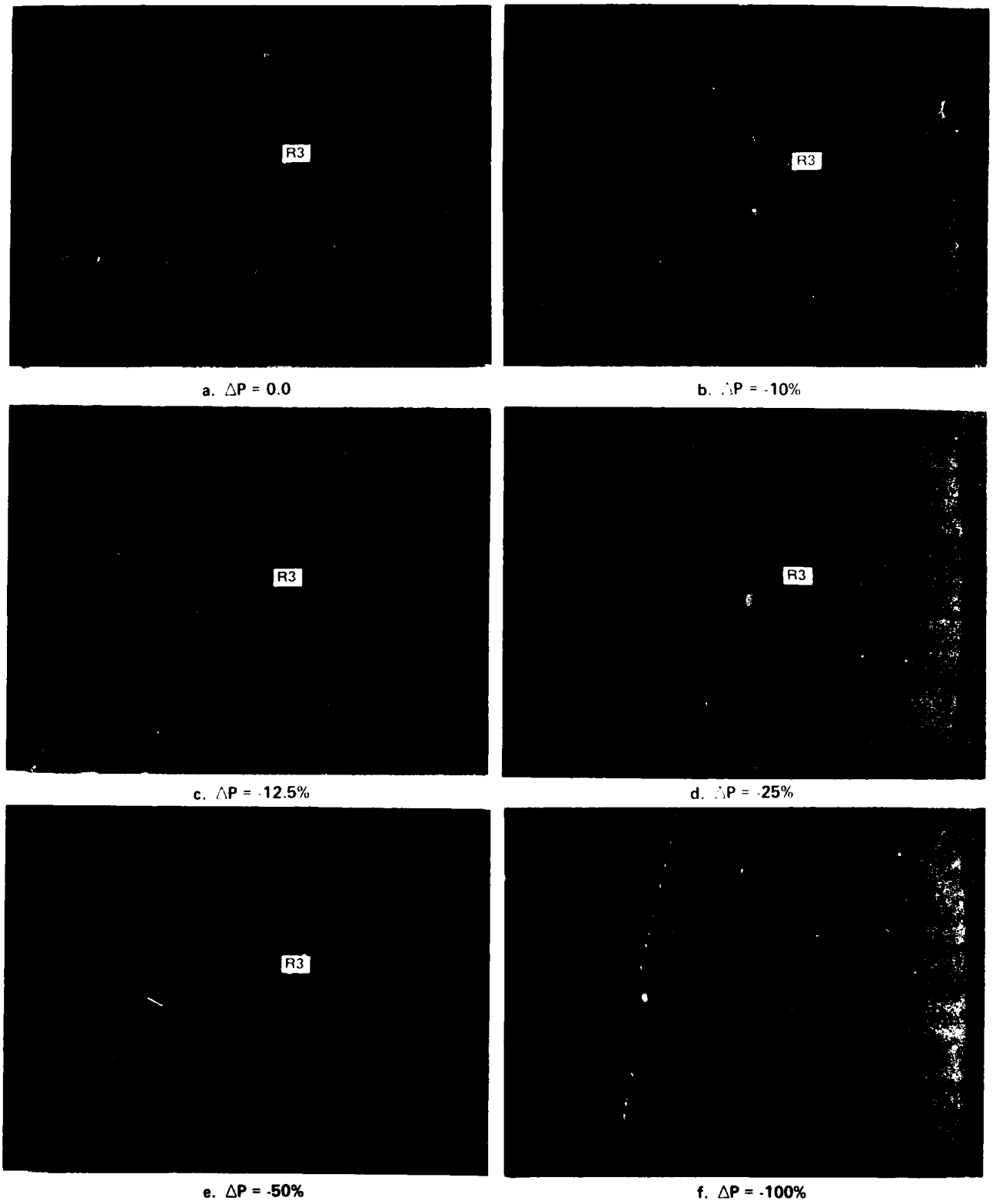

a. $\Delta P = 0.0$

b. $\Delta P = -10\%$

c. $\Delta P = -12.5\%$

d. $\Delta P = -25\%$

e. $\Delta P = -50\%$

f. $\Delta P = -100\%$

Figure 40 Defect growth tracking in delta mode

5.2 PHASE II STATIC PCB-LEVEL EXPERIMENTS

The experiments of Phase II were conducted under standard laboratory environmental conditions. A total of seven (one prototype and six "production" test articles) were fabricated. The assemblies were populated with typical circuits made up of the components examined in Phase I.

The operational suitability of the selected circuits and their compatibility with the external insertion of "failure analogs" was confirmed through electrical/thermographic tests conducted on the prototype.

Electrical characterization of the six identically configured "production" test articles was accomplished in order to verify their functional status and to define any unit-unit power differences that existed. All of the circuits were determined to be fully operational. The highest power components were the load resistors for the two transistor circuits. These resistors dissipated approximately 250 mW each and exhibited a maximum difference of 12 mW. A maximum power variation of less than 3.0 mW was found to exist between any of the other resistors on the boards. The TTL integrated circuits had an average power dissipation of 60 mW (with all four gates turned on) and exhibited a 22 mW high-to-low spread. The low-power Schottky devices showed an average dissipation of 16 mW with only a 3.0 mW spread.

A thermographic comparison utilizing the delta mode of operation was then made of each PCB referenced against itself in a fixed operating condition. The purpose of these comparisons was to establish repeatability at the PCB level for a "no-failure" condition. Figures 41 and 42 show the typical results obtained with one of the PCBS. Figure 41a depicts the three minute "reference image" with the circuits operating in the configuration identified by the labeling information. The high power areas and the resultant heat spread can be seen in the upper central portions of the assembly. It should be noted that the appearance of the display is dependent upon the range, mid-color and sensitivity settings selected. The mid-color was selected (usually at or near the ambient temperature) for the most meaningful display in terms of locating components during subsequent delta mode operations. The crosshairs (lower right) were positioned at a point on the holding fixture that was considered to represent the ambient temperature. The actual temperature and the differential from the reference image appear at the bottom of the display.

Figure 41b presents the unpowered delta image of the same assembly after power had been removed for a period of ten minutes (note that the reference image circuit operating condition information is retained in this and subsequent photographs). All of the components that had previously been operating at power levels equal to or greater than approximately 15 mW can now be seen to be displayed as being cooler.

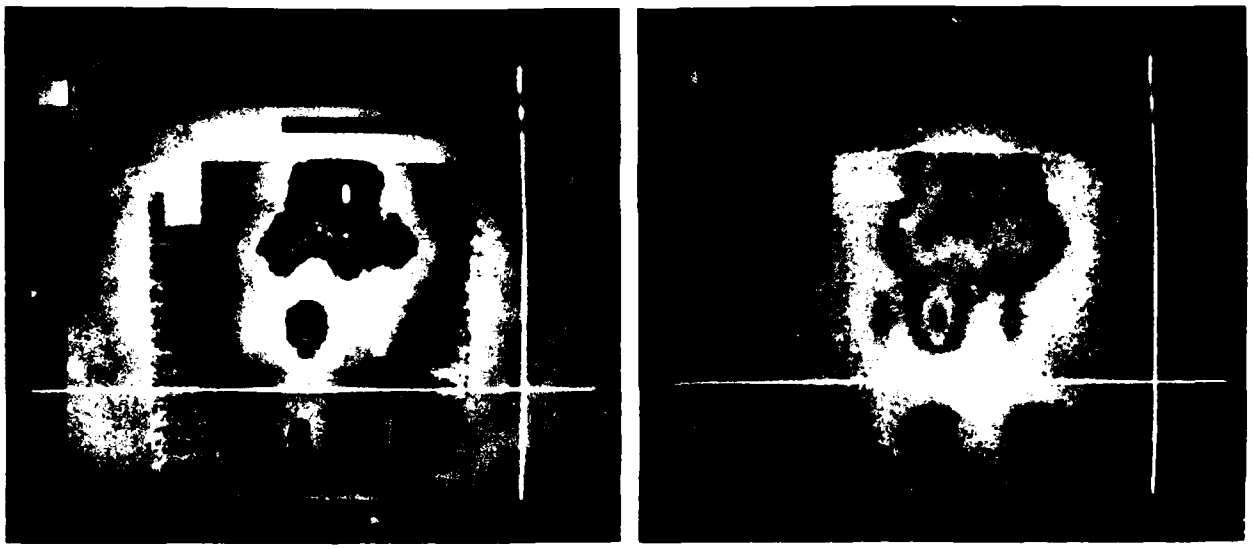

a. Reference image - power on for 3 min.

b. Delta image - power off for 10 min.

Figure 41 Reference and delta image comparisons

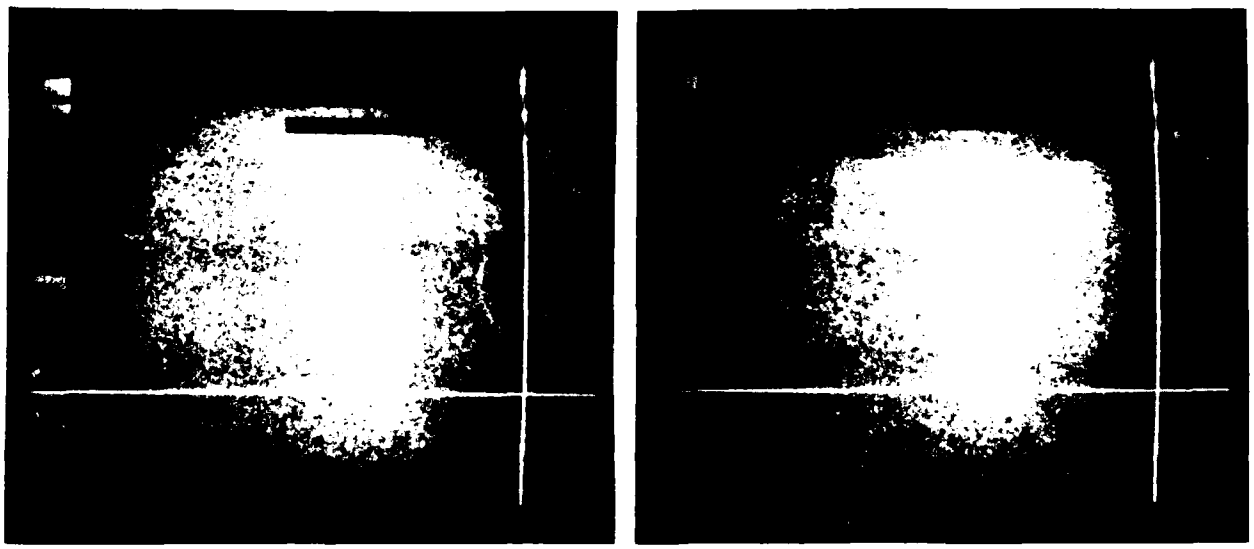

a. Delta image - 3 min. power on (no failure)

b. Delta image - 3 min. power on (no failure repeat)

Figure 42 PCB level repeatability experiments

Figure 42a shows the complete image cancellation obtained when power was again applied for three minutes with the circuits operating as they were in the reference run (no failure). A repetition of the same condition (after a ten minute cool down) is shown in Figure 42b. Experiments with the other assemblies yielded the same results, confirming repeatability of the visual interpretation of a No Failure condition at the PCB level using the power on and cool down criteria established in Phase I tests.

Still comparing a particular assembly against itself, various failure analogs were introduced in order to determine if the Phase I observations relative to TOD, heat spread effects and defect growth feasibility were applicable at the PCB level. A typical experimental sequence is shown in Figure 43.

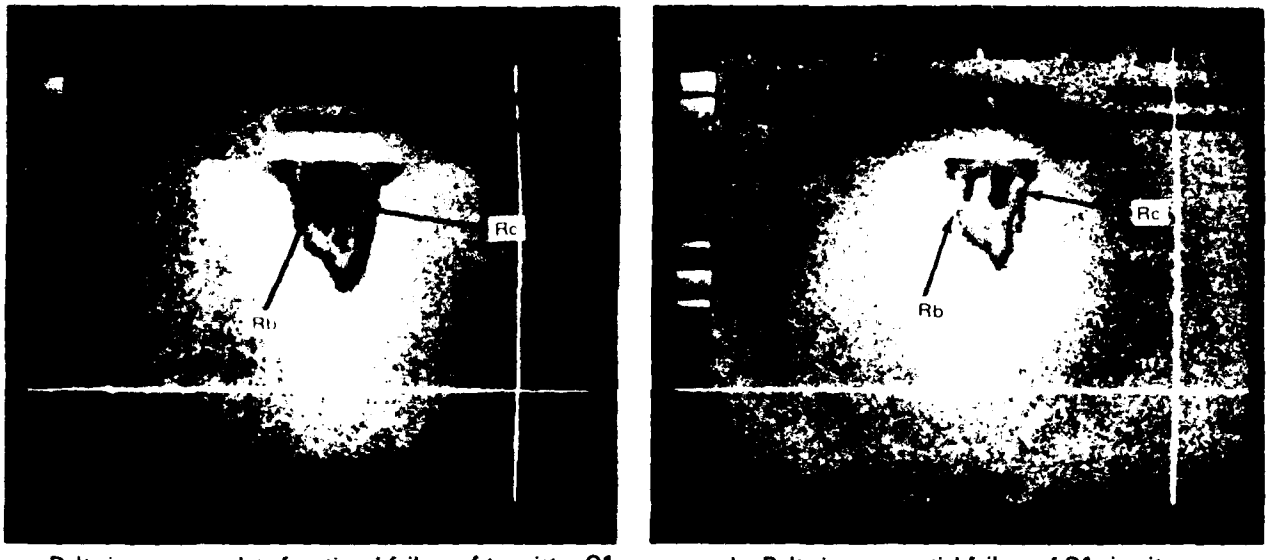

a. Delta image - complete functional failure of transistor Q1 circuit
Rb = base limiting resistor
Rc = collector load resistor

b. Delta image - partial failure of Q1 circuit
Rb = -34 mW

c. Delta image
Rb ≅ -32 mW
Rc not visible

d. Delta image
Rb ≅ - 27 mW

Figure 43 PCB level tracing experiments - defect analogs (sheet 1 of 3)

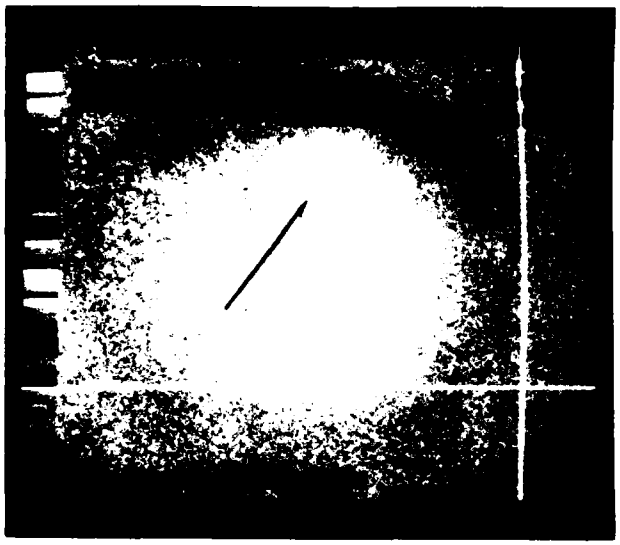

e. Delta image
Rb ≅ -15 mW

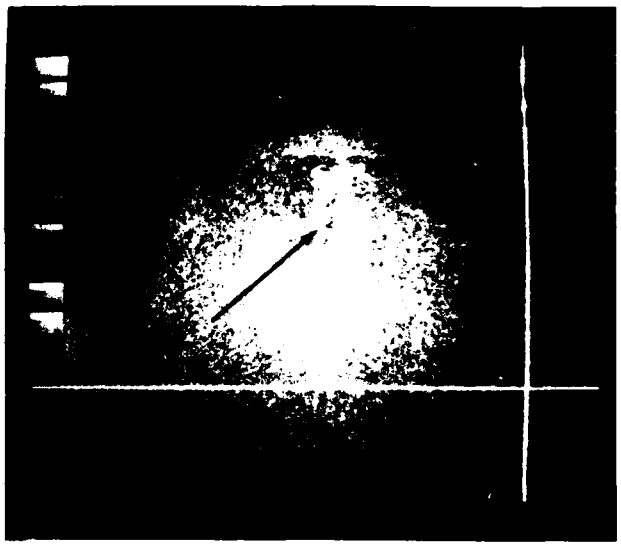

f. Delta image
Rb ≅ -15 mW @ 0.2 C dead band

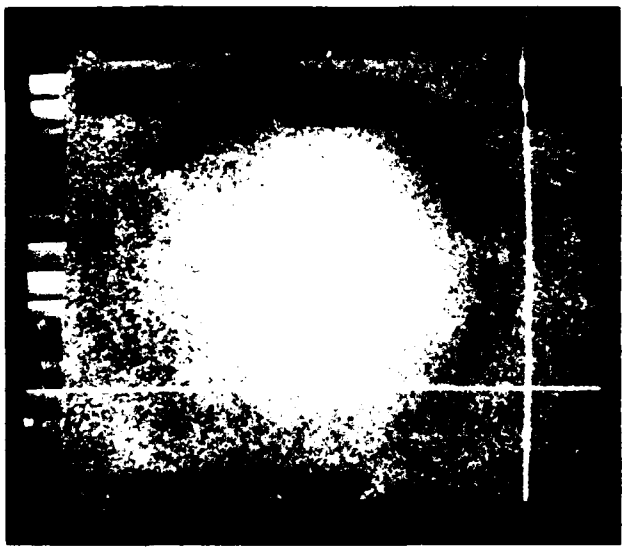

g. Delta image
Rb ≅ -15 mW repeat (no dead band)

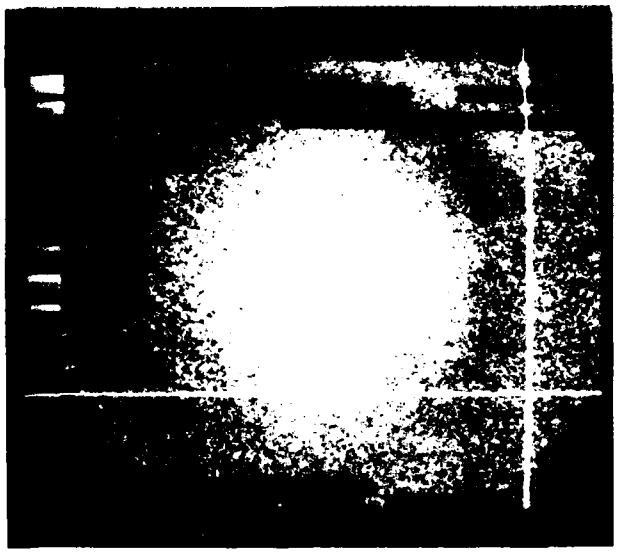

h. Delta image
Rb = -10 mW

Figure 43 PCB level tracking experiments - defect analogs (sheet 2 of 3)

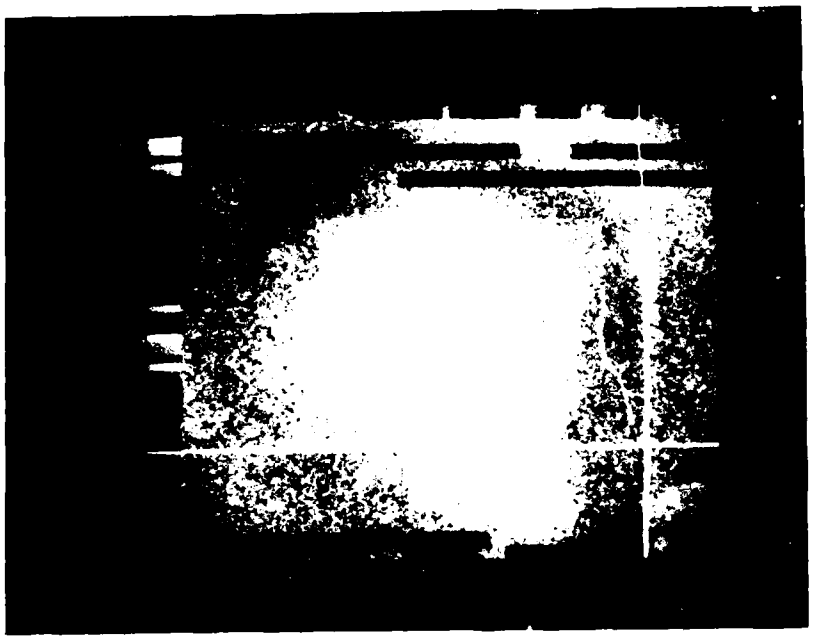

i. No fail

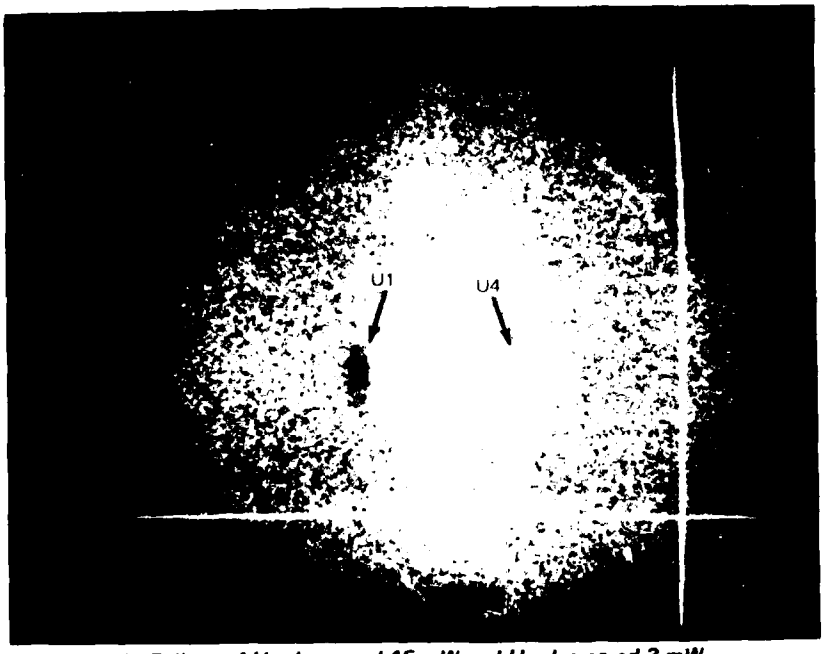

j. Failure of U_1 decreased 15 mW and U_4 decreased 3 mW

Figure 43 PCB level tracking experiments - defect analogs (sheet 3 of 3)

The simulation of an open circuit, e.g., broken wire or open solder joint, occurring within the line supplying base current to transistor Q1 resulted in the delta image of Figure 43a. It represents a complete functional failure of the circuit due to the transistor being turned off. A 36 mW reduction in power dissipation of the base-limiting resistor, and 250 mW reduction in the collector resistor (because no current is flowing in either) results in a major thermal difference being displayed. The complete functional failure of this circuit was also identified by extinguishing an indicator LED on the monitoring panel. Figure 43b shows a lesser thermal difference resulting from a relatively large decrease in the base drive current simulated by the insertion of a high series resistance in the base line of Q1. This simulates a condition which might be encountered just prior to a complete opening. It resulted in a relatively large reduction in power dissipated by both resistors but did not produce a monitor circuit indication of failure.

Figures 43c through 43e show the delta images obtained when the base drive was incrementally reduced by lesser amounts by inserting lower series resistances. These reductions in drive represented earlier stages of a bad joint which also did not produce an indication of malfunction on the electrical monitoring panel. The effects of these reductions on the conduction of the transistor, and therefore the impact on the power dissipation and thermal differences of the load and base resistors, became less to the point where Rc was not visually discernible (Figure 43e). The difference in dissipation of Rb, however, was definitely discernible at a 15 mW level (Figure 43e). The fact that delta mode differences were discernible prior to an electrical (Go-No-Go) identification of a functional failure lent credence to the system's ability to detect a defect in its early stages and track its growth to a complete functional failure. Figure 43f shows the effect of viewing the same image (Figure 43e) with a 0.2 C dead band introduced. This was sometimes found to enhance the detection, but at times confounded interpretations. A repetition of the experiment shown in Figure 43e is verified in Figure 43g. Power differences of less than 15 mW were virtually undiscernible by direct visual examination of the display under normal room lighting condition. Sometimes photographs of apparent full cancellations provided a slight indication of those small differences (Figure 43h). Figure 43i again confirms the system's repeatability by showing complete cancellation of a no-fail condition. Simulation of failures in another area on the board is shown in Figure 43j. It shows complete cancellation of the now normally-operating transistor circuits, and the definite detection of the failure of one of the four gates within integrated circuit U1, representing a power decrease of approximately 15 mW. A simultaneous failure of one gate of the low power Schottky device (a power

decrease of only 3.0 mW) was not discernible. This fact implies a system limitation, since either of these devices can be used to perform the same function, and that which could represent a complete functional failure is detectable only within one of them.

It should be noted that the experimental sequence described represents an idealized condition in which all but one of the thermal signature constituents were held constant. The delta comparisons were made of an assembly against itself in a fixed location, which obviates the effects of unit-unit power or component positional differences. The ambient temperature was also closely monitored and was held to within +0.3 C from that existing at the time of making the reference image.

The need to hold the ambient to such a close tolerance stems from the need to keep the Threshold of Detection (TOD) as low as possible. The only way to do this visually is to keep the ambient temperature essentially constant from reference run to delta-therm run. Appendix B contains an analysis which can offer an alternate computer-assisted approach to allowing the ambient to assume a constant different than that of the reference run. The analysis offers a pixel-by-pixel account of thermal variations for a well-defined "golden board" configuration. The analysis assumes that the scanning mode of the equipment can be modified for keying from an addressable clock. This would eliminate the ±1.5 second scanning time uncertainty referred to in Section 4, Test Articles and Setup, Phase I. The authors are convinced that this area would offer great benefit if studied further.

5.2.1 Initial "Golden Board" Experiments

Upon completion of the above experiments, the feasibility of establishing one reference board ("golden board"), against which all others (typically of a production lot) would be measured, was evaluated. One of the six test articles was randomly selected and a reference image made with the circuits operating as before. Subsequent to storing the reference image, the system was placed in the delta therm mode, and each of the five remaining PCBs was compared to this reference under the same operating conditions (no failure). The purpose of these experiments was to provide baseline data relative to the visual ambiguities that might be introduced by assembly-assembly positional displacements and component power differences.

Figure 44 shows some of the ambiguities (incomplete cancellations) observed. They were determined to be primarily due to the slight mispositioning of the PCB within the test fixture and its socket. However, some of the differences could be attributed to the unit-unit differences that occurred if, for example, the reference image had been made with the board containing the TTL device at the high end of the power dissipation spread.

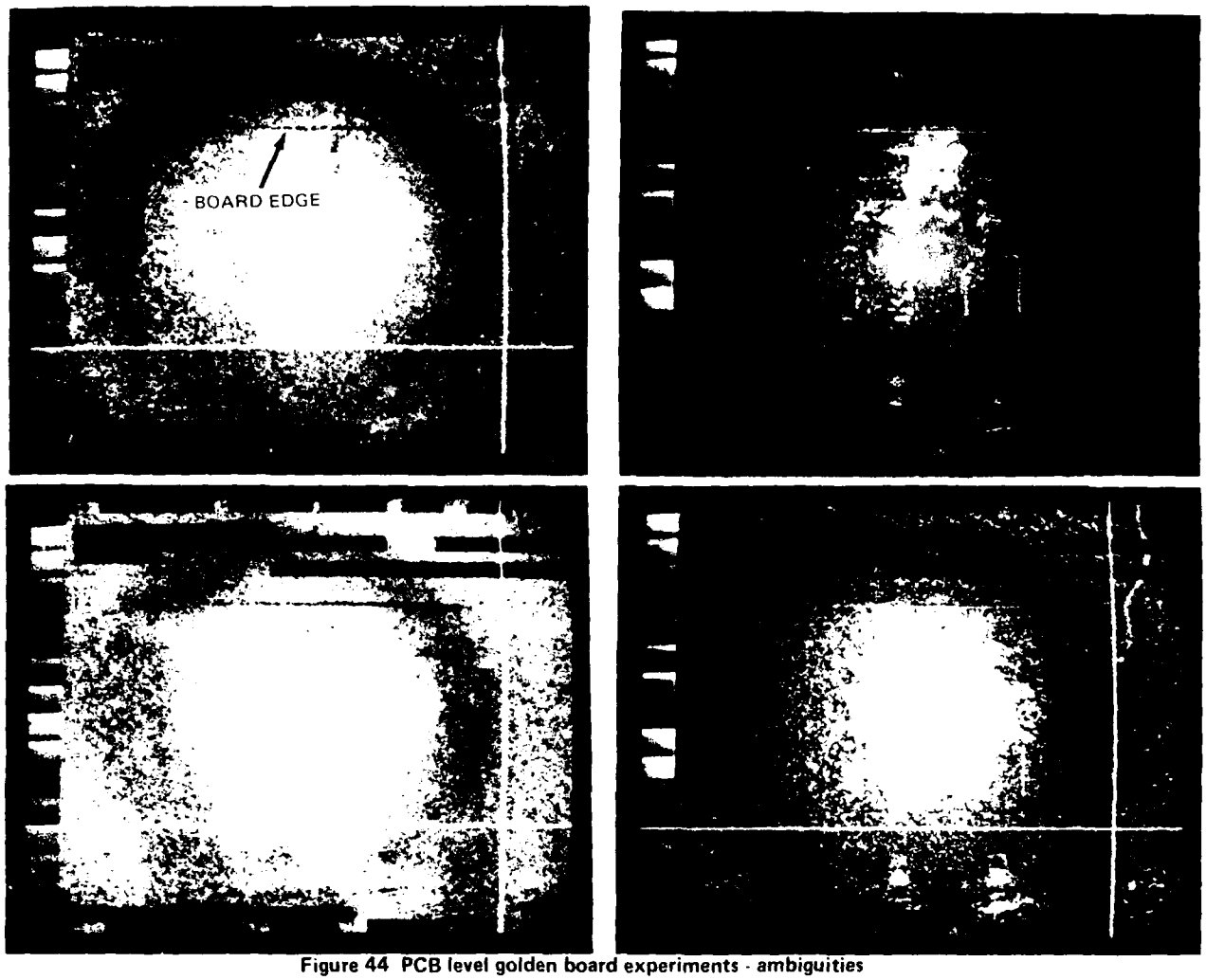

Figure 44 PCB level golden board experiments - ambiguities

The ambiguities were primarily in the areas of high power dissipation devices since slight differences in positioning produced a large differential along heat edges, i.e., the borders of components at a much higher temperature than the background (board material). The board-to-board positions of components such as integrated circuits were found to be rather precisely fixed because of the short leads and the photographically fixed location of the board connections. Components with longer leads, such as resistors, are subject to much more board-to-board variations.

Various means of positioning of the boards relative to the "golden board" were tried. "Bench marks" of high emissivity material were placed on the board such that the board under test could be manipulated to produce cancellations at these bench marks. This method did not prove useful since the physical placement of the bench marks is critical. The photographic location of these "bench marks", or the provision for mechanical placement such as alignment holes which would mate with fixture pins, are considered viable means for positioning and could be provided for

new PCB lots. The problem of individual component mispositioning would still, however, be present.

5.2.2 Solder Joint Experiments

Experiments were then conducted to determine if the degeneration of a solder joint on a PCB could be detected at the failure site itself.

The physical manipulation of a number of joints, including some that actually had no solder connection at all, resulted in measured resistance changes from a few milliohms to several ohms, prior to becoming a complete open circuit.

A printed circuit trace on one of the PCBs was intentionally cut and bridged by a bus wire. Figures 45a and 45b show the reference and delta images obtained when the board was operated under the same conditions with the jumper wire well soldered. The resistance across the jumpered cut was determined to be approximately 0.479 Ohms (including the lead length resistance). The wire was then manipulated to produce several different values of contact resistance, which was electrically observed to change between 1.0 and 3.0 Ohms (again including lead resistance) during delta runs under the same electrical conditions. Figures 45c through 45e illustrates the delta signatures showing a discernible difference at the location of the bad contact (location 1), which represents the heat due to the voltage drop across the poor contact. The cooling effect of this voltage drop on the load resistor of the Q1 circuit can be seen at location 2. It should be noted that the current flowing through this contact resistance was on the order of 125 mA. Subsequent experiments with the same type of poor contact within a lower current line produced undiscernible thermal differences.

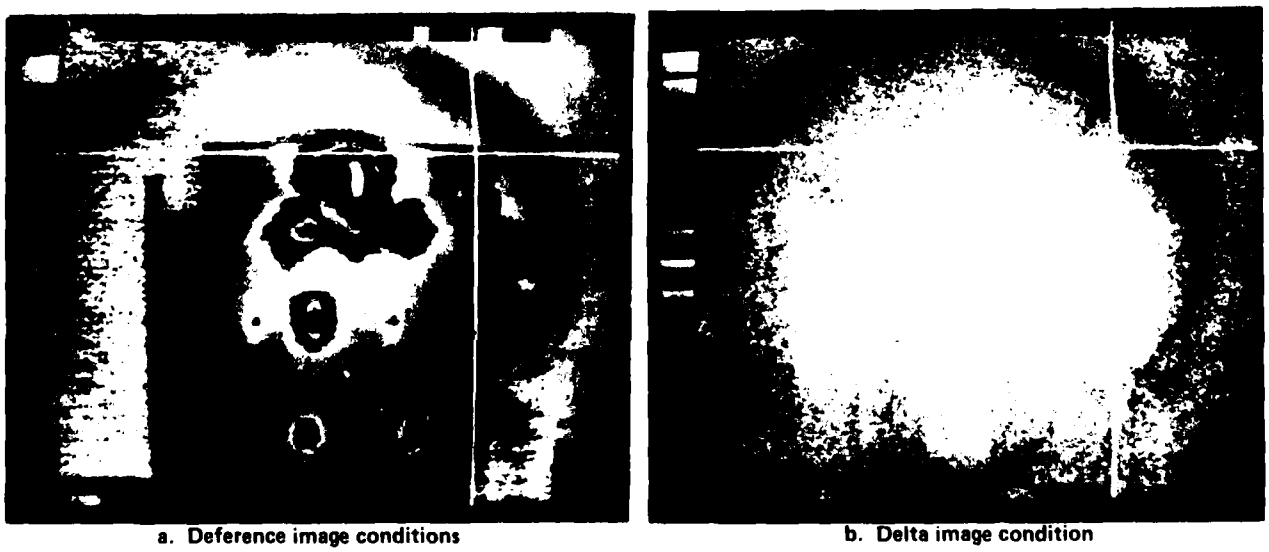

a. Deference image conditions b. Delta image condition

Figure 45 Solder joint experiment - PC trace cut and bridged with bus wire (sheet 1 of 2)

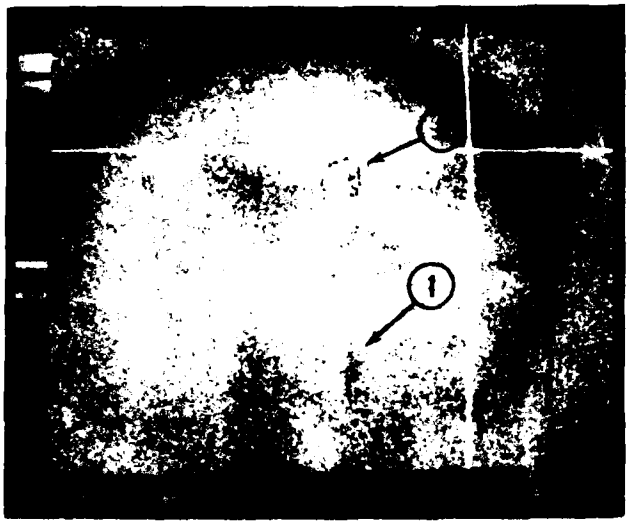

c. Resistance +1.0 Ohm

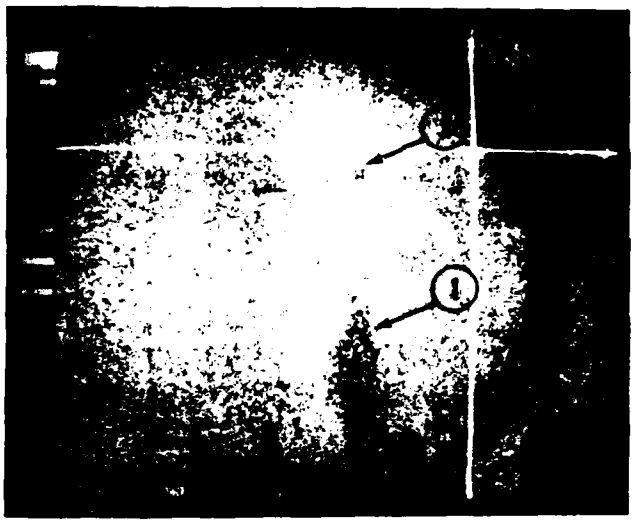

d. Resistance +2.0 Ohm

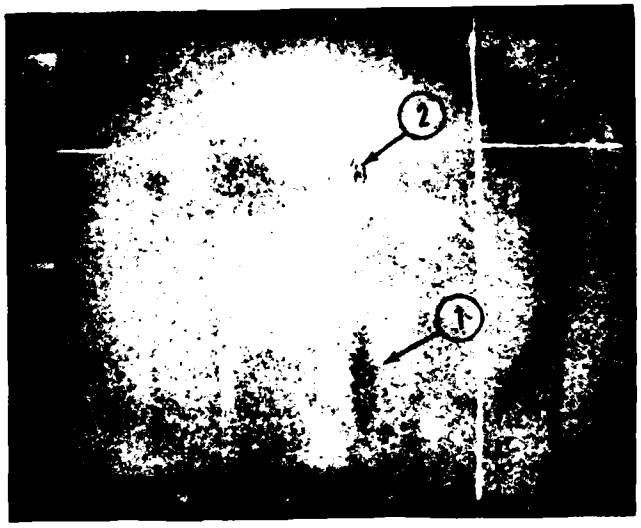

e. Resistance +3.0 Ohm

Figure 45 Solder joint experiment - PC trace cut and bridged with bus wire (sheet 2 of 2)

Experiments conducted with a very small "chip" resistor of 10 Ohms produced similar results as shown by Figure 46. Figure 46 shows a delta run of the same circuit of Figure 45 with a 10 Ohm chip resistor inserted at the site of the cut trace. Under the operating conditions used for the reference run (125 mA), the 10 Ohm resistance is readily discernible (Figure 46a). Other operating states of the circuit which drove lesser currents through the "failure" site were also evaluated, the 10 Ohm resistance was not as readily discernible. The obvious cool down at other board locations is due to circuit reconfigurations, which were necessary to drive lesser currents through the "failure" site.

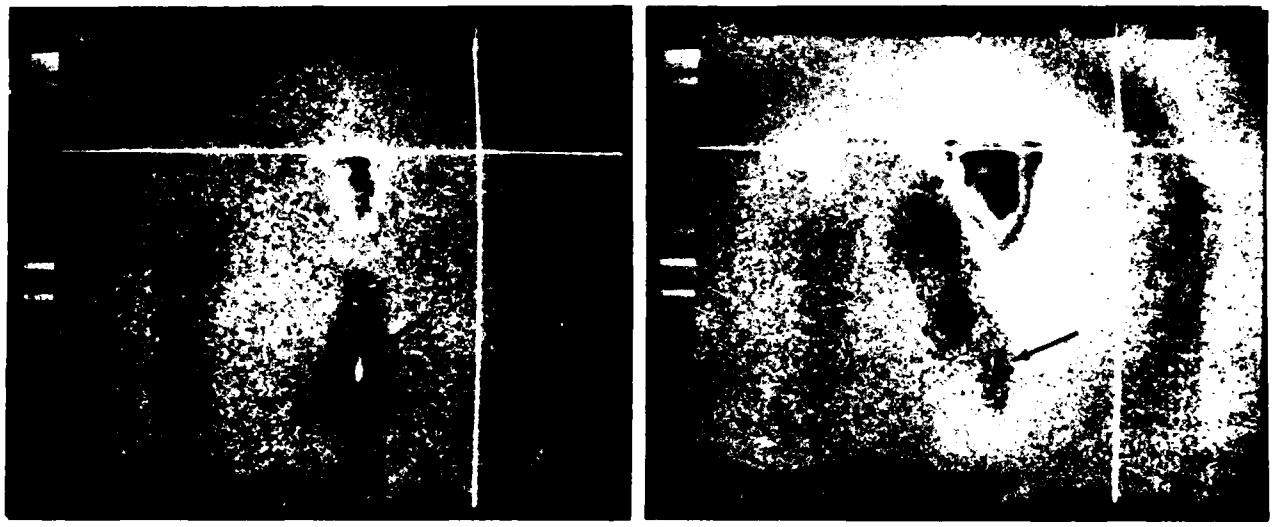

a. Delta image @ 1250 mW

b. Delta image < 1250 mW

Figure 46 PCB level solder joint experiments (clip resistant)

5.2.3 PCB Trace Defect Experiments

The system's ability to detect defects within PCB traces was then explored. A trace carrying approximately 150 mA had a wedge-shaped cut made in it (Figure 22) which progressively reduced its cross-sectional area (at the point of cut). Figure 47a shows the delta image where the area had been reduced by approximately 50%. No thermal indication was discernible at the known "failure site" (location 1). The difference at location 2 was attributed to a positional difference due to removal and re-insertion of the board when effecting the cut (the trace current was determined to have remained the same and therefore the cut did not alter the circuit operation). Figure 47b still shows no discernible delta mode difference at the failure site when the area was reduced to over 90%. Cutting the trace completely naturally produced an open circuit and a clear indication of the non-operation of the circuit.

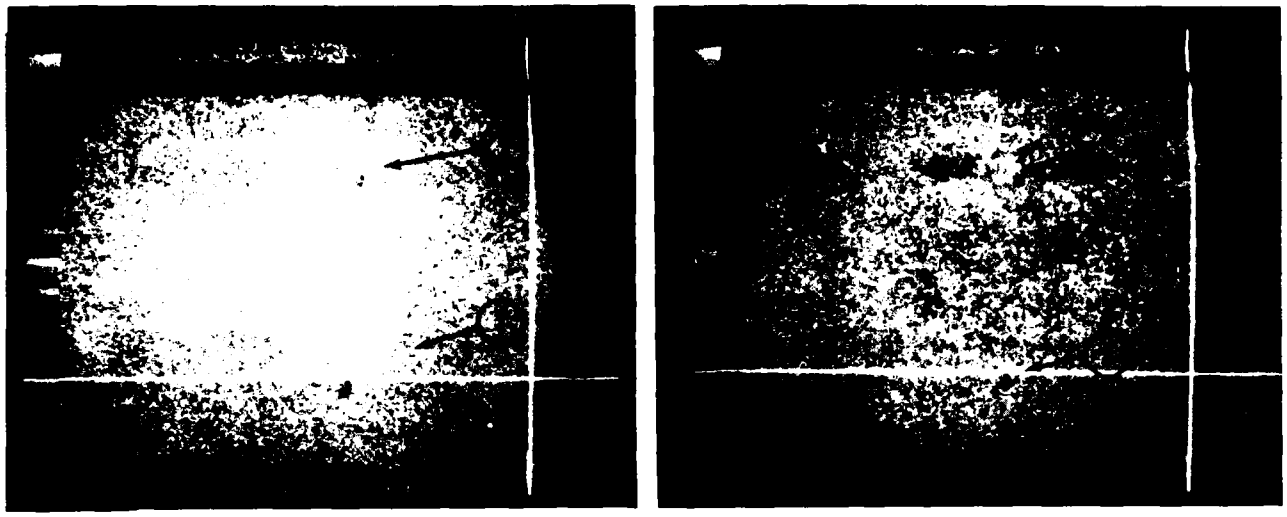

a. Delta image - trace area reduced ≈ 50%

b. Delta image - trace area reduced > 90%

Fig. 47 PCB Level circuit trace experiments

Currents in excess of 1.0 amp through the same type of cuts did produce visual indications, but they were considered unrealistic for most normally operating PCB circuits. It does, however, indicate that thermographic testing of traces of unpopulated boards has potential for detecting significant flaws. A controlled experiment utilizing this technique on a large production run of PCBs would be required to determine if the thermographic technique represents an improvement over currently employed visual and electrical test techniques.

5.3 PHASE III - PCB DYNAMIC ENVIRONMENTAL TESTS

Phase III of the study program was designed to develop practical methods of utilizing the data acquired during the previous two phases, in an environmental stress screening application. The test articles were the same as those used in Phase II, except that actual examples of environmentally-sensitive workmanship defects replaced the failure analogs during the latter part of this phase. It was originally intended to thermographically examine the test articles only under static conditions. A delta thermograph was to be obtained both prior and subsequent to each of the environmental exposures. Additional static delta thermographs were to be obtained at discrete intervals during random vibration and rapid thermal cycling. During the initial experiments, it became apparent that static thermographic examinations at discrete intervals would disclose only permanent failures. Recognizing the importance of detecting intermittent anomalies as well as permanent failures, and the fact that intermittents occur only during the application of environmental stimuli, it was concluded that a procedure to facilitate dynamic thermographic examinations must be developed. To achieve this objective, the experimental program was redesigned

to investigate the feasibility of and develop an appropriate method for continuous thermographic examinations during the application of random vibration and rapid thermal cycling.

The Phase III experimental program and its derived results are discussed in the following subsections.

5.3.1 Random Vibration Experiments

The following describes a sequence of experimental activities which began with some of the assumptions considered in our proposal and which eventually settled on a more practical direction/methodology. Many techniques were tried which might have adequately served a specific experimental purpose but were later abandoned as the investigation evolved. The ultimate objective was to devise a methodology that would allow both static and dynamic thermographic measurements. The latter would provide a powerful tool for the detection of intermittents as they occurred.

5.3.1.1 Test Set-Up Verification - A vibration test fixture was mounted to the MB-50 shaker head. This fixture held one PCB in a horizontal plane and contained the necessary connector to electrically power and monitor the Test Article (TA). The imager was mounted on its tripod and the front surface mirror was installed to facilitate viewing the TA.

A number of nonvibrating (static) delta runs of a board referenced to itself were made for the purpose of determining the practicality of operation outside of the thermal shroud. The tests were conducted when the room temperature had stabilized sufficiently to allow the TA ambient to remain within ±0.5 C, and when traffic in the immediate area was limited. The tests yielded repeatable "no failure" cancellations and the same TOD as was observed during Phase II tests. Figure 48 shows the complete cancellation obtained during one of these experiments.

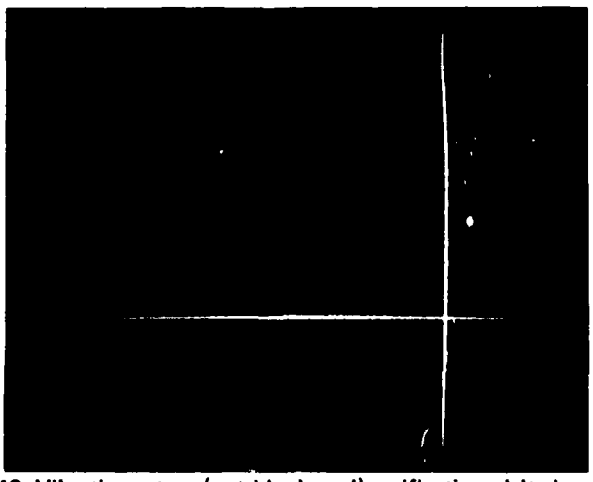

Figure 48 Vibration set-up (outside shroud) verification, delta image - no failure

An experiment was then conducted to determine if operation of the shaker head would have an adverse effect upon the repeatability and/or threshold of detection due to additional heating. A three minute static reference image was made. The same PCB was then exposed to five minutes of random vibration with power applied for the last three minutes only. Figure 49 depicts the resulting delta image, which shows an apparent failure of one of the transistor circuits (location 1). The monitoring panel and circuit board electrical measurements indicated no evidence of failure. A subsequent static thermograph confirmed this (Figure 50). The vibration run was repeated with the same results (Figure 51). Movement of the relatively large mass and long lead length resistors (due to the vibration) was considered to be the cause, but was subsequently disproven in experiments with short-leaded resistors.

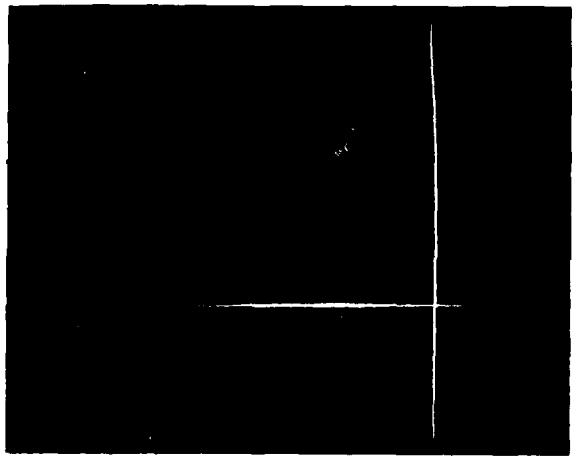

Figure 49 Vibration delta thermograph showing "cool down"

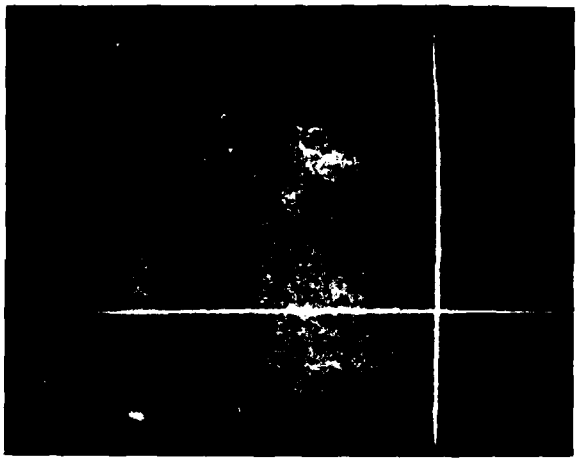

Figure 50 Static delta thermograph verifying no failure

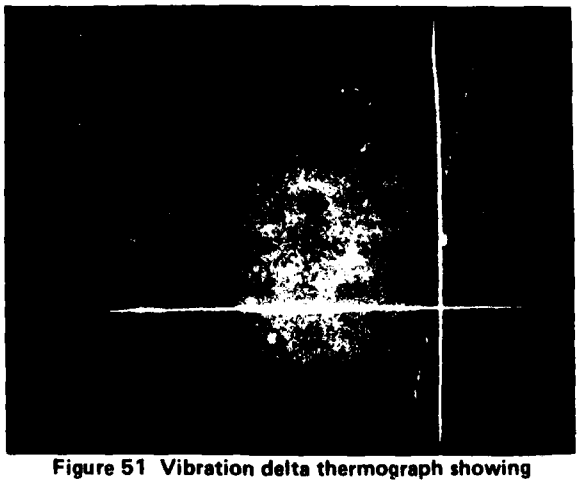

Figure 51 Vibration delta thermograph showing "cool down" - repeat

Eventually the cause of this apparent failure was concluded to be the result of the fanning effect of the vibratory motion, which caused increased convection cooling, especially apparent in the higher power areas.

Observation of this cool-down effect during periods of powered vibration showed it to be repeatable. The ability to observe a dynamically changing condition indicated that it might be possible to detect defects as they occurred. At this point this idea was proven by the insertion and removal of short term failure analogs (turn-off of various components). In addition, these short term failure simulations had no significant long term effect on the post-test static thermographic runs. It was obvious that the direction of the test plan (Ref 3) which called for a static delta run between periods of vibration, required modification.

5.3.1.2 Random Vibration Thermography Methodology - The observations made during the preceding set-up phase clearly indicated that other than a static reference was required to properly interpret thermographic data associated with random vibration. The following describes a sequence of experiments conducted to define a more valid reference.

A reference image was made after one minute of vibration with the test article powered throughout the vibration period. Since this reference contained the effects of the vibration induced cool-down, it was termed a "No fail - Dynamic Reference". A number of no failure delta mode runs were made against this reference and resulted in virtually complete cancellation, observed at the conclusion of the vibration period. While some ambiguities were observed, the concept of a 'dynamic' time, since the rapid rate of temperature rise during the initial turn-on period was already known to be a factor.

The temperature/time history of the TA within the vibration fixture was obtained and is shown graphically in Figure 52. It was determined that stabilization of all components had been achieved at ten minutes of power-on time. This thermally stable condition was used to provide a uniform starting point for all vibration runs. Dynamic reference runs could then be made for any desired vibration test time following thermal stability.

Using PCB no. 5 as the "golden board", both a thermally stabilized (ten minute power-on) static reference and a dynamic reference representing an additional five minutes of power-on time with vibration (a total of 15 minutes of power-on time, the last five minutes includes vibration) were made and recorded on discs. The series of delta runs, noted in Table 1 were then made by recalling this data and using it as a reference. In each case the PCB under test was initially examined against the PCB no. 5 static reference, thereby establishing its pre-vibration operational status. It was then continuously examined (in the delta mode against the dynamic

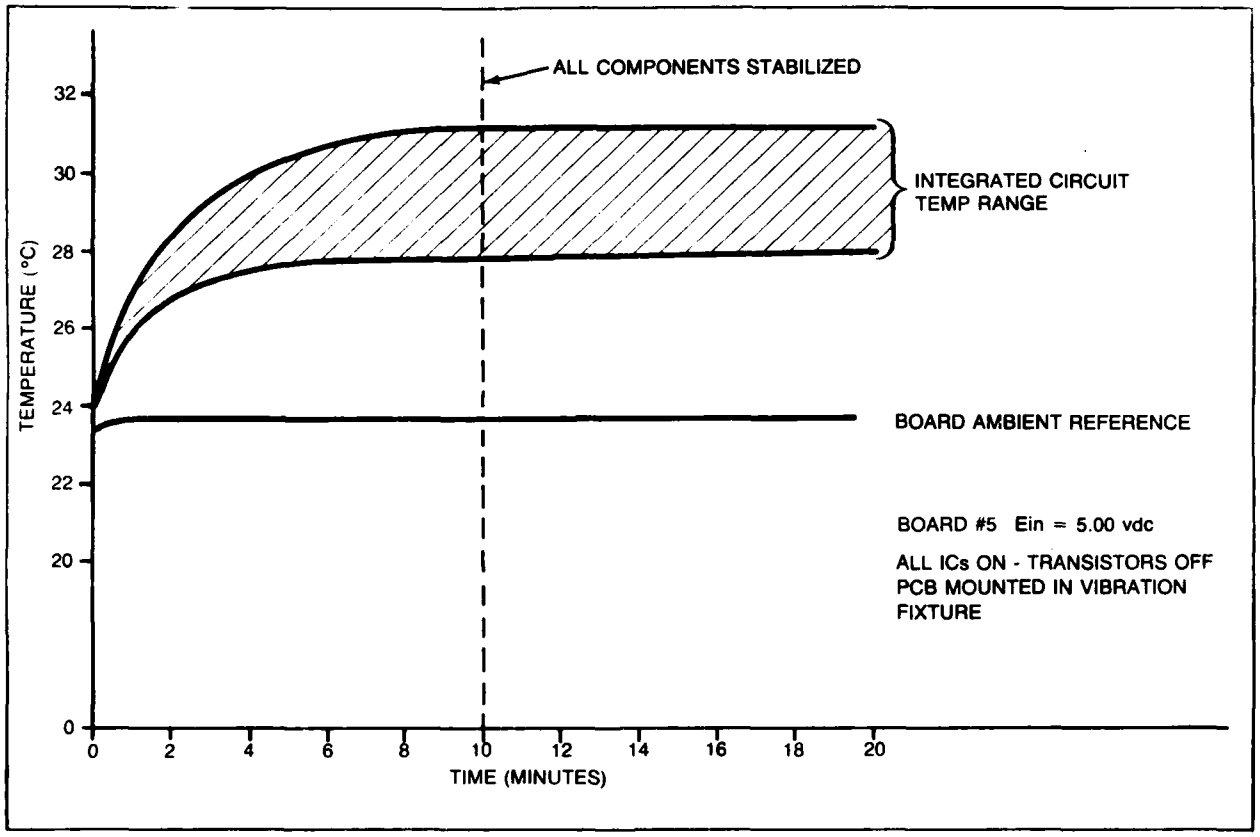

Figure 52 PCB temperature/time history

Table 1 PCB vs golden board reference data

Run Number	Reference Board	Test Article Board Number		Figure Number	Remarks
		Static	Dynamic		
1	5	-	-	-	STATIC REF IMAGE
2	5	-	-	-	DYNAMIC REF IMAGE
3	5	5	-	53a	
4	5	-	5	53b	
5	5	2	-	54a	
6	5	-	2	54b	
7	5	3	-	55a	
8	5	-	3	55b	
9	5	4	-	56a	
10	5	-	4	56b	
11	5	5	-	57a	
12	5	-	5	57b	
13	5	6	-	58a	
14	5	-	6	58b	
15	5	6	-	59a	RERUN OF RUNS
16	5	-	6	59b	13 & 14 FOLLOWING SHUTDOWN FOR WEEKEND
17	5	1	-	60a	
18	5	-	1	60b	FAILURE
19	5	1	-	61	FAILURE
20	5	1	-	62a	FAILURE MANIPULATED
21	5	-	1	62b	FAILURE MANIPULATED
22	5	1	-	63a	PARTIAL REPAIR
23	5	-	1	63b	REPAIR FAILED
24	5	1	-	64a	FAILURE RESOLDERED
25	5	-	1	64b	FAILURE RESOLDERED
26	5	-	-	-	NEW STATIC REF
27	5	-	-	-	NEW DYNAMIC REF
28	5	1	-	65a	OBVIOUS MISPOSITION
29	5	-	1	65b	OBVIOUS MISPOSITION
R85-0750-083					

reference) during the imposition of the vibration. Figure 53a shows the delta image of the static (pre-vibration) condition of board no. 5 against itself and Figure 53b shows the dynamic delta image of board no. 5 against itself. Figures 54a through 65b show static delta images of the other five boards referenced to no. 5. The differences observed were attributed to positional displacements.

Figures 54a through 65b show the no fail delta images obtained after ten minutes of static power and of power vibration of boards no. 2 through no. 6 compared to the dynamic reference of board no. 5.

It should be noted that the initial period of dynamic viewing against the dynamic reference indicated the high power areas to have a positive delta (i.e., appeared hotter than the reference). This was due to the fact that the dynamic reference represented the thermal signature existing at the end of the vibration and included the previously mentioned cool-down effects. Given that no permanent failure is induced by the vibration, the delta image at the end of the vibration period is a complete cancellation.

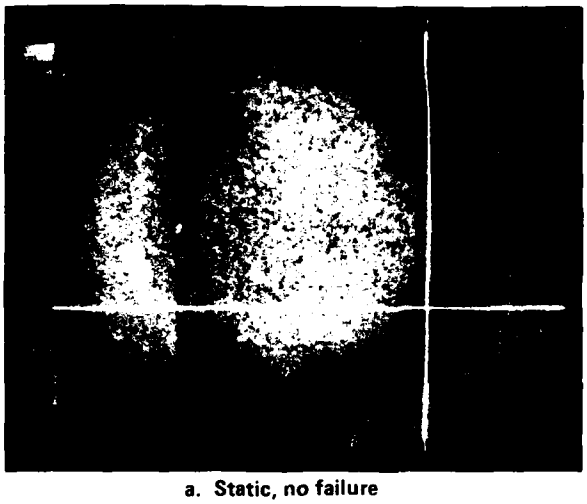

a. Static, no failure

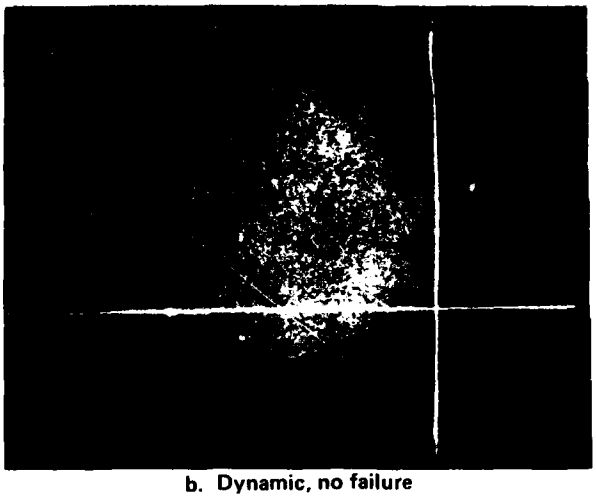

b. Dynamic, no failure

Figure 53 Delta image comparison - PCB no. 5 vs PCB no. 5 (base runs)

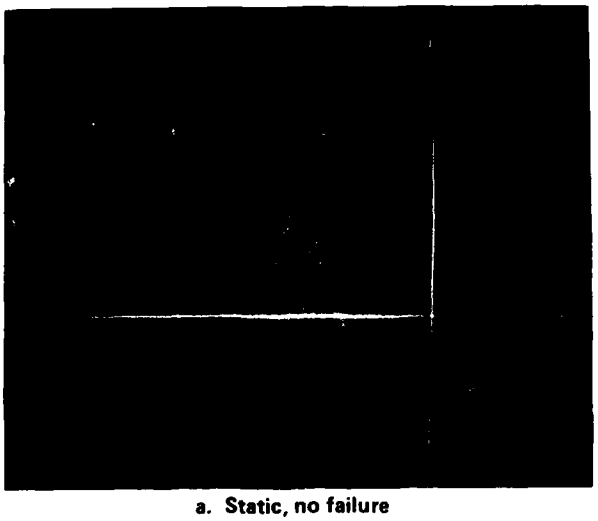

a. Static, no failure

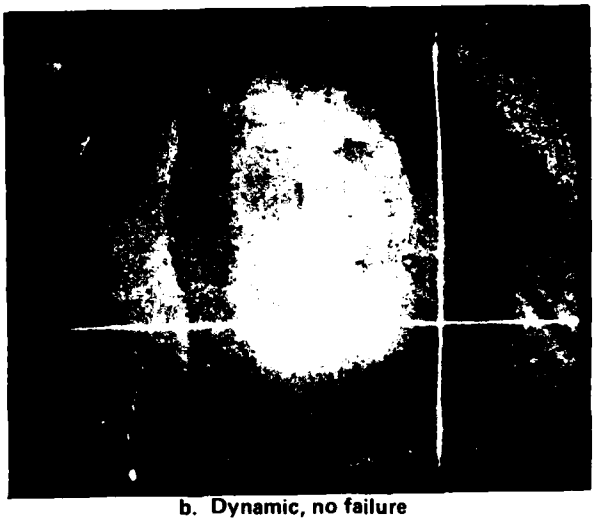

b. Dynamic, no failure

Figure 54 Delta image comparison - PCB no. 2 vs PCB no. 5

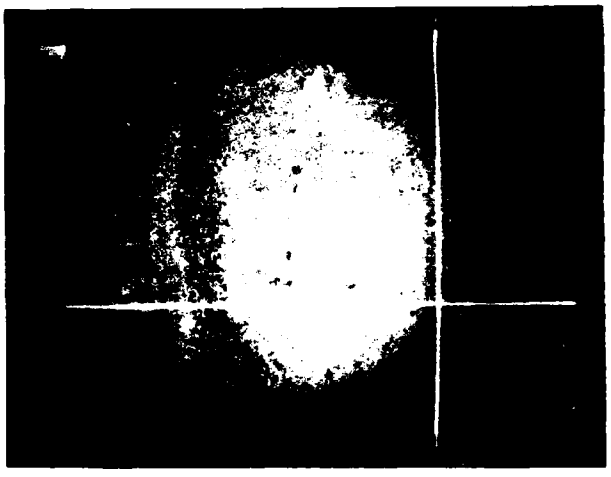

a. Static, no failure

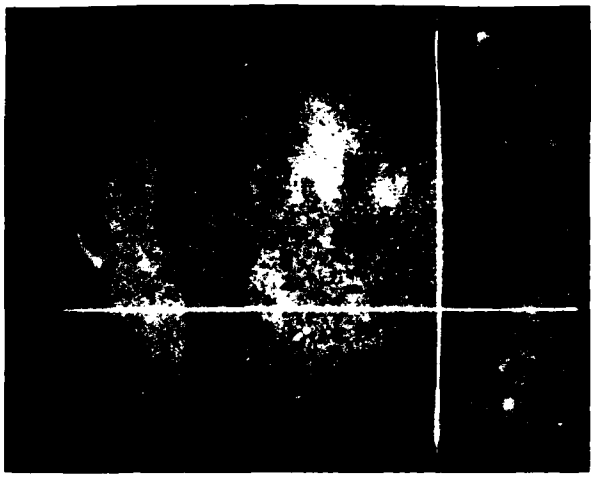

b. Dynamic, no failure

Figure 55 Delta image comparison - PCB no. 3 vs PCB no. 5

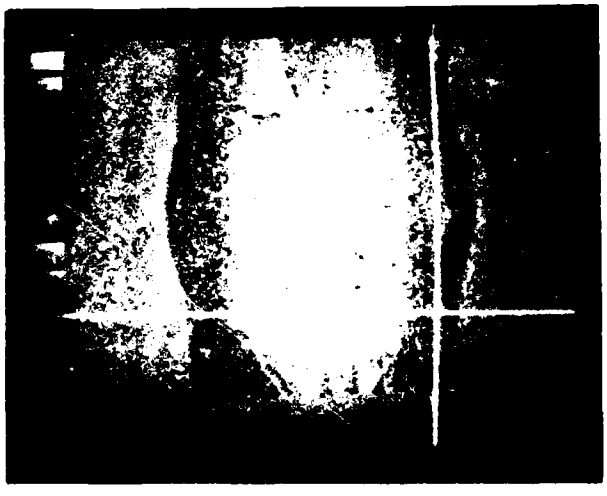

a. Static, no failure

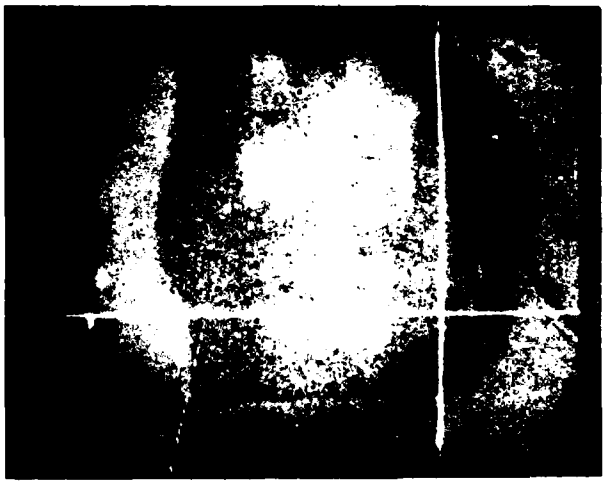

b. Dynamic, no failure

Figure 56 Delta image comparison - PCB no. 4 vs PCB no. 5

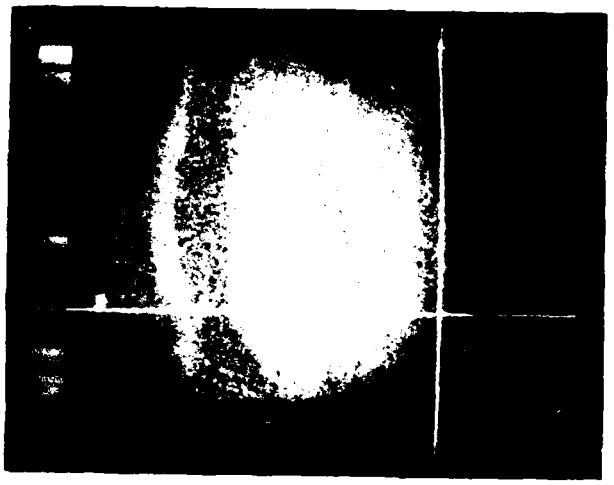

a. Static, no failure

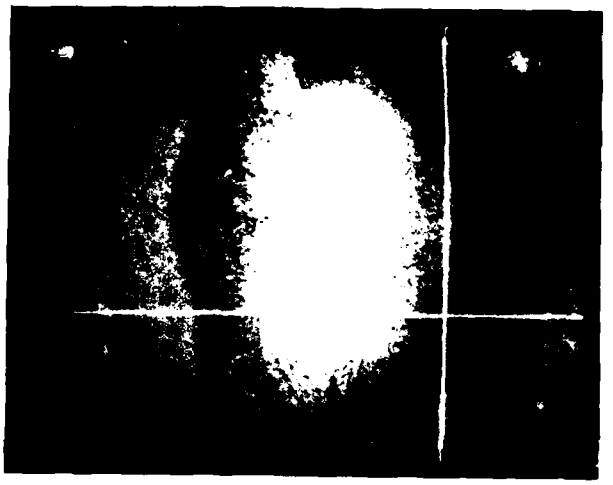

b. Dynamic, no failure

Figure 57 Delta image comparison - PCB no. 5 vs PCB no. 5

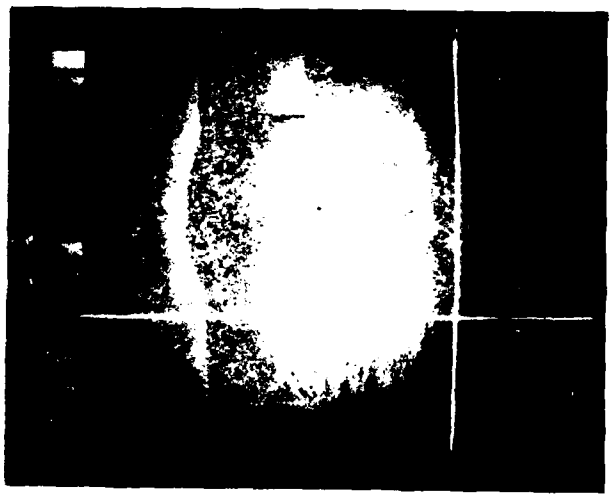

a. Static, no failure

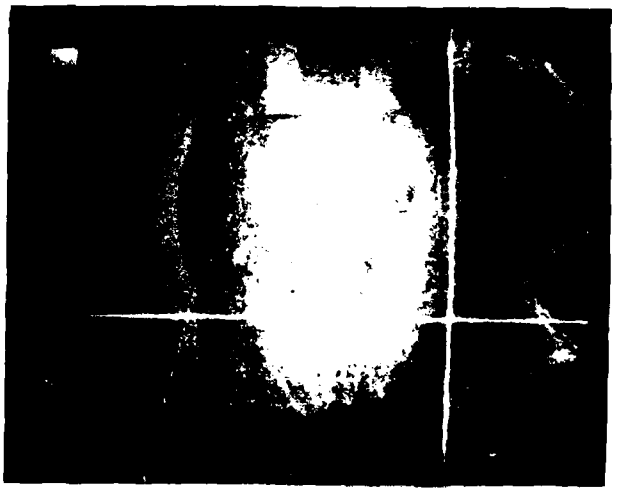

b. Dynamic, no failure

Figure 58 Delta image comparison - PCB no. 6 vs PCB no. 5

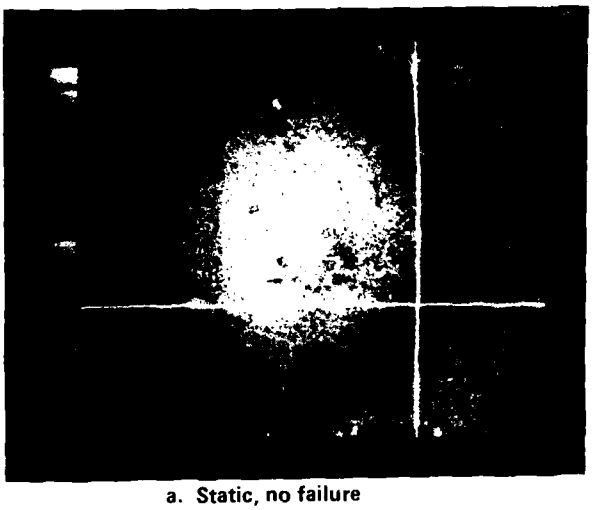

a. Static, no failure

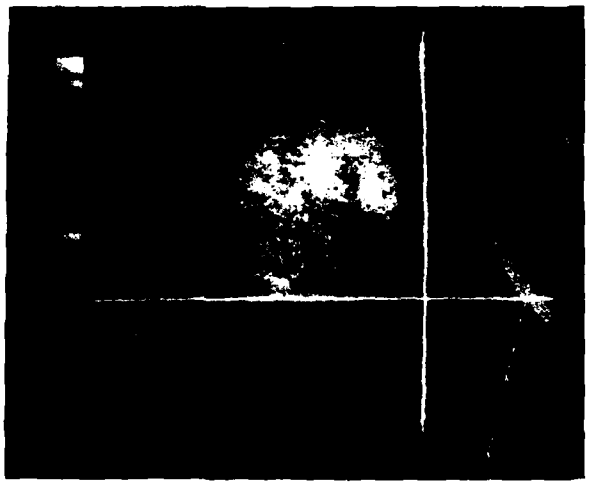

b. Dynamic, no failure

Figure 59 Delta image comparison - PCB no. 6 vs PCB no. 5 (check run following weekend shutdown)

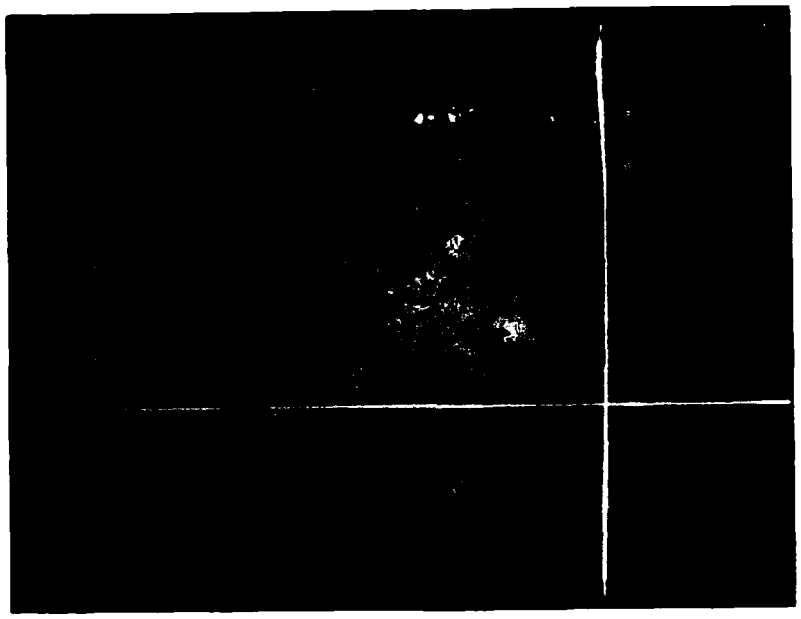

a. Static, no failure

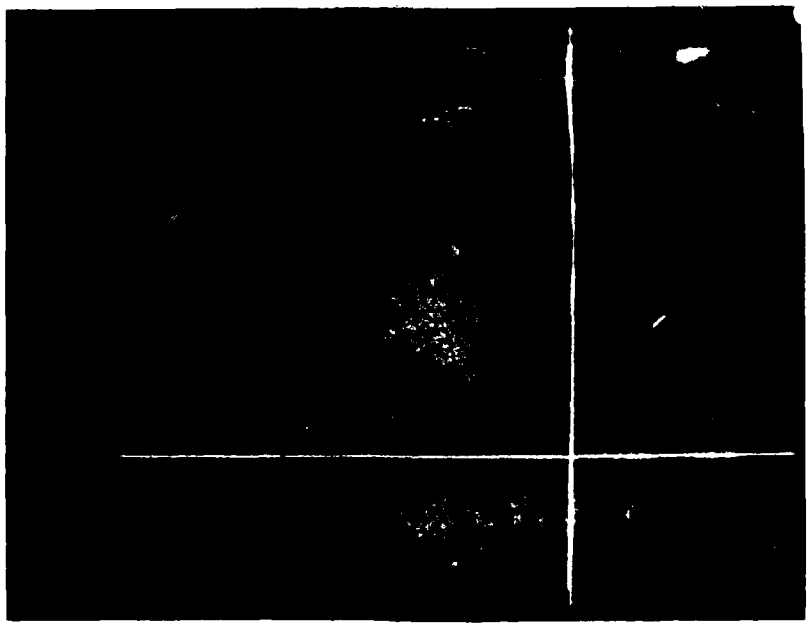

b. Dynamic ,failure

Figure 60 Delta image comparison - PCB no. 1 vs PCB no. 5

Figure 61 Delta image - PCB no. 1 vs PCB no. 5 - static ,failure

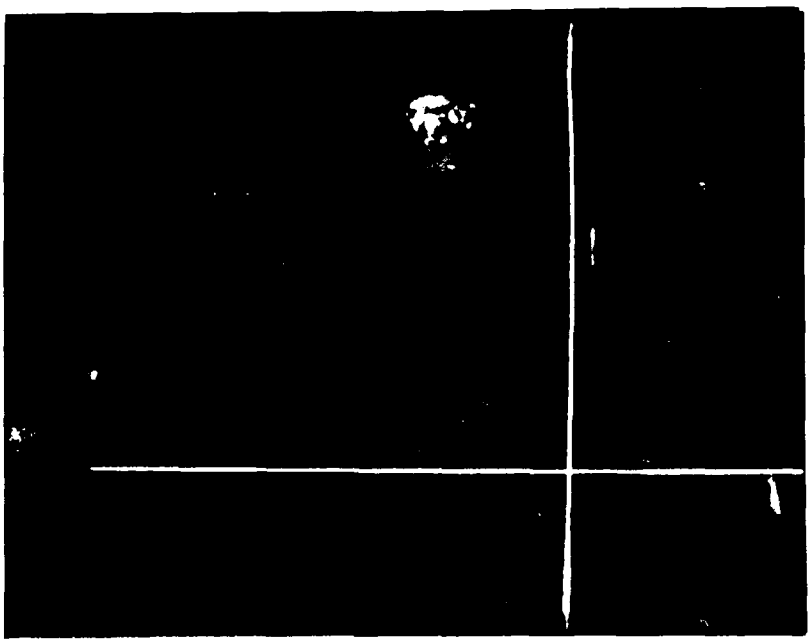

a. Static, failure manipulated

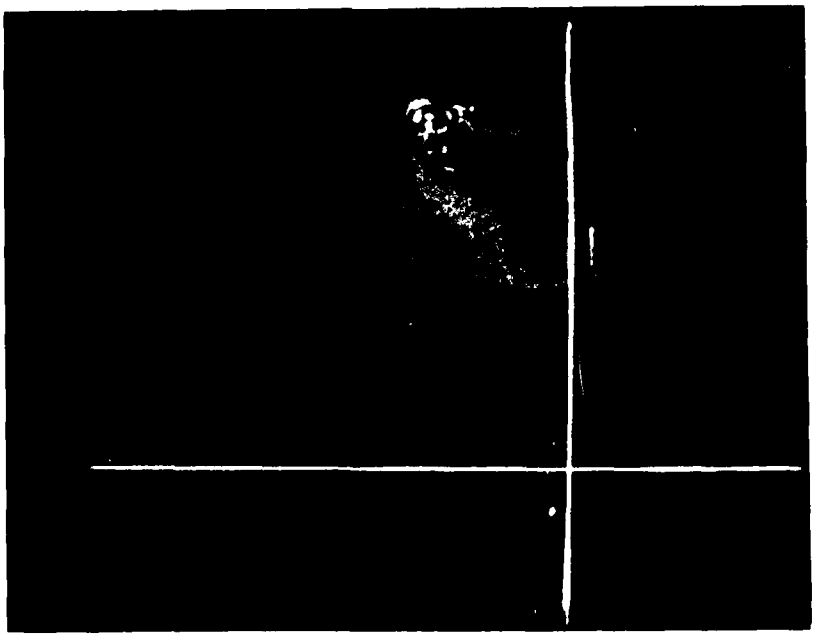

b. Dynamic, failure manipulated

Figure 62 Delta image - PCB no. 1 vs PCB no. 5

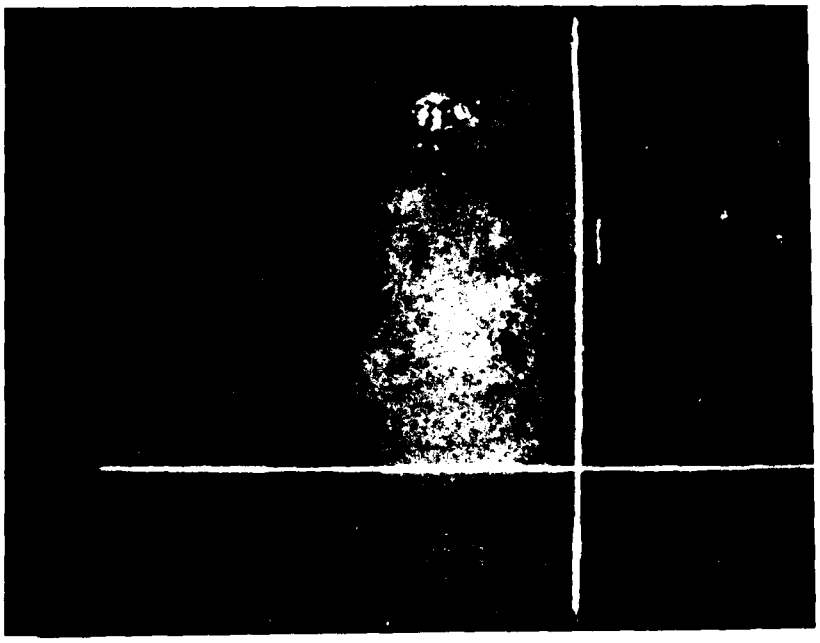

a. Static, partial repair

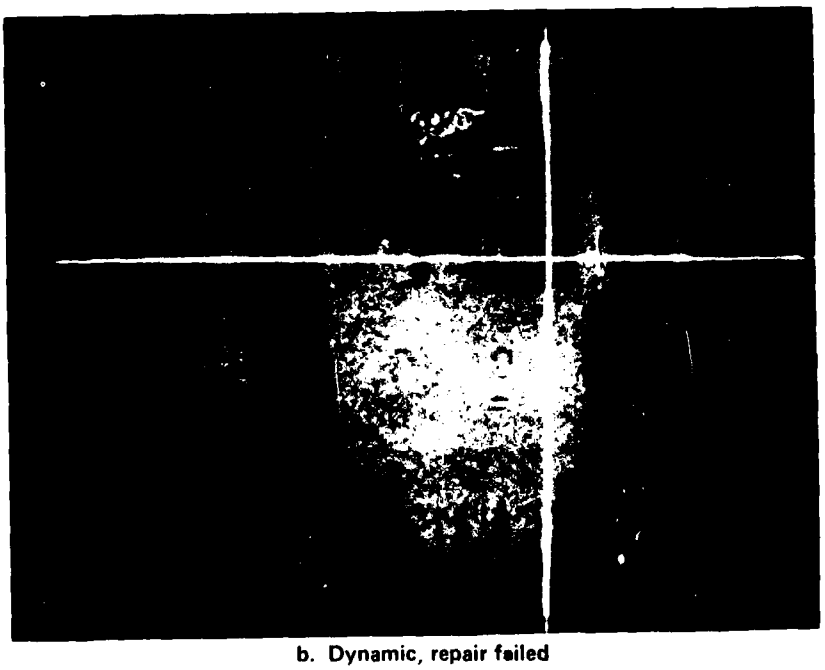

b. Dynamic, repair failed

Figure 63 Delta image - PCB no. 1 vs PCB no. 5

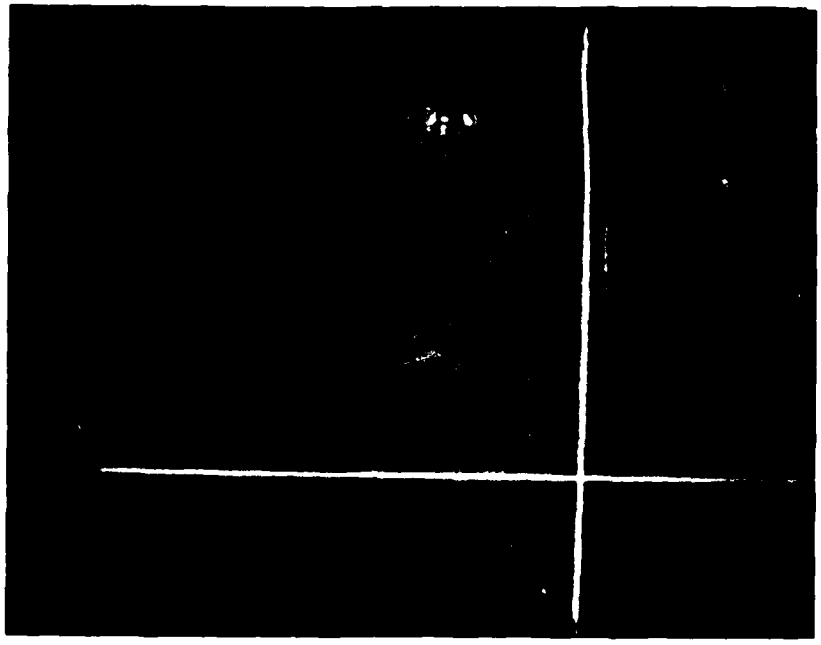

a. Static, failure resoldered

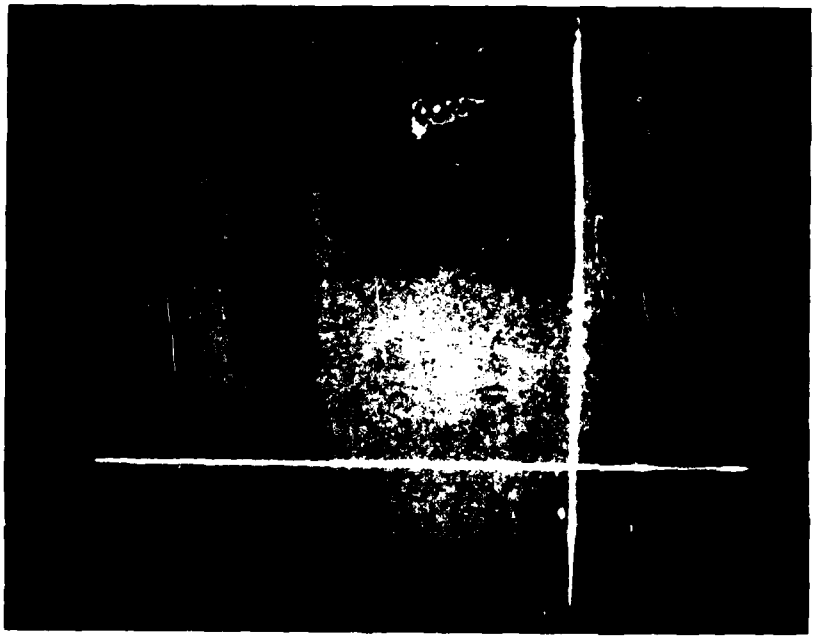

b. Dynamic, failure resoldered

Figure 64 Delta image - PCB no. 1 vs PCB no. 5

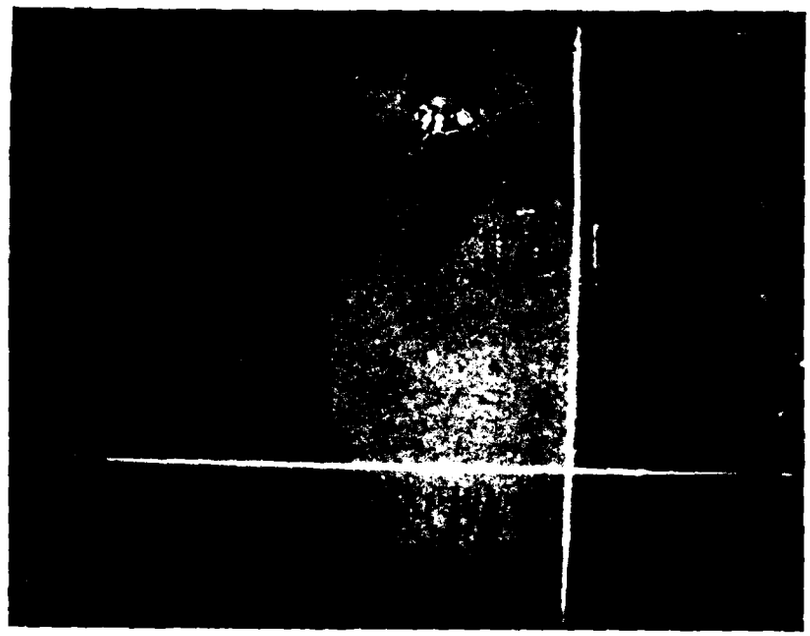

a. Static, no failure

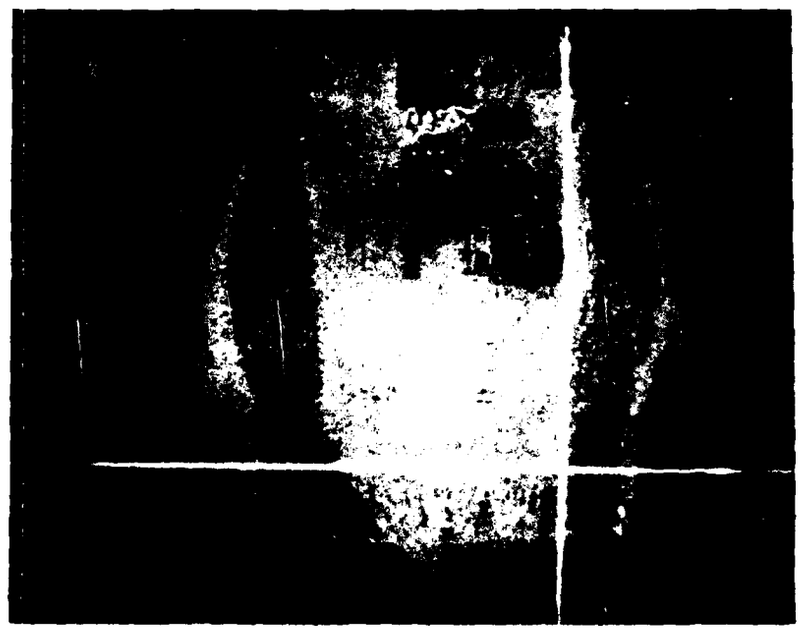

b. Dynamic, no failure

Figure 65 Delta image - PCB no. 1 vs PCB no. 5

Board no. 1 exhibited indications of an anomaly occuring with one of the integrated circuits (U1). A slight cooling of the integrated circuit was observed to occur intermittently during vibration. Vibration was started and stopped several times with power remaining on, and the condition was observed to appear and disappear (Figures 60b through 64b). The monitoring panel did not show any discernible indication of an electrical malfunction. Microscopic examinations of the board revealed no obvious problems, but the condition was thermographically found to reoccur during vibration. The possibility of intermittencies in the electrical connector was explored and disproved through hard-wiring to the board itself, with the condition still observed. Instrumentation of the board at several points produced no positive identification of an intermittency when the voltage across the device was monitored with an oscilloscope.

Subsequent examinations of the board revealed the solder connection at pin 7 of U1 to be bad. This unplanned, truly random real failure created havoc with the test operation and consumed many hours of troubleshooting time. It did, however, dramatically prove that the thermographic technique does work during random vibration. It picked up the existence of the failure when the electrical failure monitor did not. At least ten additional minutes of random vibration were accrued by the PCB until the intermittent became a permanent open failure. A routine application of a total of ten minutes of random vibration during a standard Environmental Stress Screening test alone would probably not have created this permanent failure condition.

5.3.1.3 Random Vibration Testing with Failures - After our encounter with the true random failure experienced by PCB no. 1, our subsequent testing with known failures (both analogs and inserted) was somewhat anticlimactic.

The simulation of failures during periods of vibration was first accomplished through the insertion of various failure analogs, and with the TA continuously examined as before. Positive identification of permanent failures (above the threshold of detection) was demonstrated by the delta image at the conclusion of the vibration period. The occurrence of intermittent failures was accomplished by insertion of a given failure analog for short periods of time, and then returning the affected circuit to its original status of operation (reference image condition). It should be noted that the failure analog could be made to represent an increase in the power dissipation of a component as well as a decrease. The occurrence of either condition was observable as a dynamic thermal condition when the power change was ±15 mW for a period of ten seconds or greater. Power changes greater than this were discernible at less times after their occurrence. The return to the normal operating temperature after the removal of the failure analog was also

dynamically observable and the delta image at the conclusion of vibration again showed a no-failure condition to exist. These tests provided data which showed that the derived methodology could, in fact, enable the detection of intermittent occurring during random vibration of a given test article. This data, in the form of video tapes, is available for review. Excerpts of this data have been submitted to the funding/sponsoring organization in an edited video tape format.

Similar data was obtained when the following actual defects were inserted: jumper wire on board no. 2 opened and gently laid upon its contact point; board no. 5 emitter lead on Q2 was unsoldered; board no. 1 base resistor on Q2 was cut. All failures showed up during random vibration live dynamic scans. In view of the results obtained with the above defects and those with both analogs and the true random failure of board no. 1, further defect insertion was deemed unnecessary, since the validity of the thermographic technique developed was clearly proven.

5.3.2 Rapid Thermal Cycling Experiments

The objective of this series of experiments was to assess the feasibility of thermographically detecting workmanship defects prior to, at discrete points during, and subsequent to rapid thermal cycling. Our initial attempts to follow the Ref 3 test plan were not fruitful. Further investigations led to the incorporation of an IR transmissible window (Ref 5 and 6) in the door of the thermal chamber. This allowed the implementation of the original test procedures, which were followed in order to verify the validity of this new test set-up. Based upon the experience gained during the random vibration experiments, a concentrated effort was expended toward developing a method of continuous thermographic monitoring during exposure to the prescribed rapid thermal cycle. As was the case during vibration testing, it was postulated that this continuous monitoring would provide the most effective method of detecting short term intermittent anomalies as well as permanent failures.

The problems associated with the unexpected random failure of a solder joint on one of the TAs during random vibration testing (see Subsection 5.3.1.3) suggested the advisability of using a simpler circuit for assessing the feasibility of thermography during rapid thermal cycling tests.

The primary test article for these tests was a PCB having 21 resistors mounted to it (Figures 66 and 67). Verification of the revised test set-up was accomplished with this test article. Subsequent tests utilized this same test article with the ability to insert failure analogs at twelve discrete locations. As these experiments progressed, it was postulated that a modified form of continuous thermographic monitoring could be accomplished during the dynamic periods of the thermal cycle above 0.0 C. This theory was proven by the insertion of both permanent and short term intermittent failure analogs.

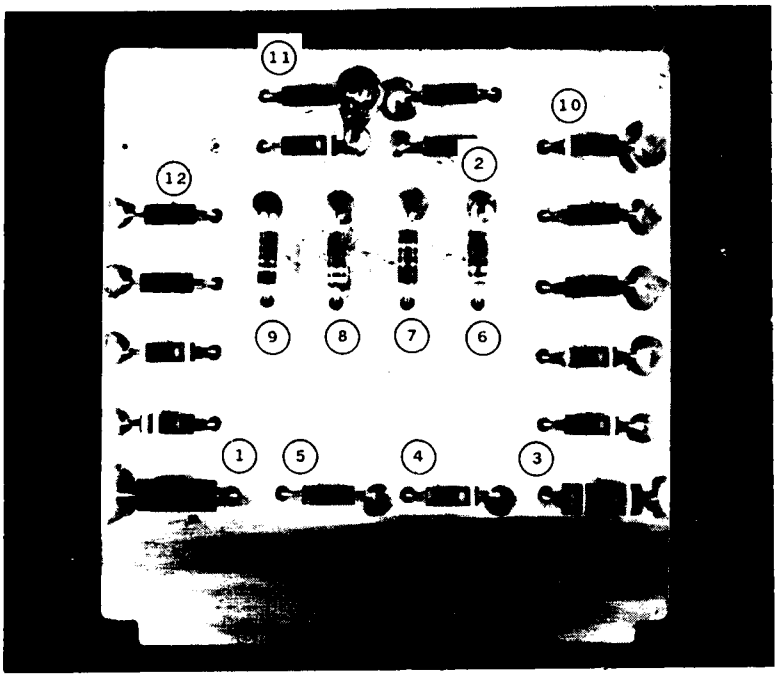

Figure 66 Temperature cycling test resistor board - component side view

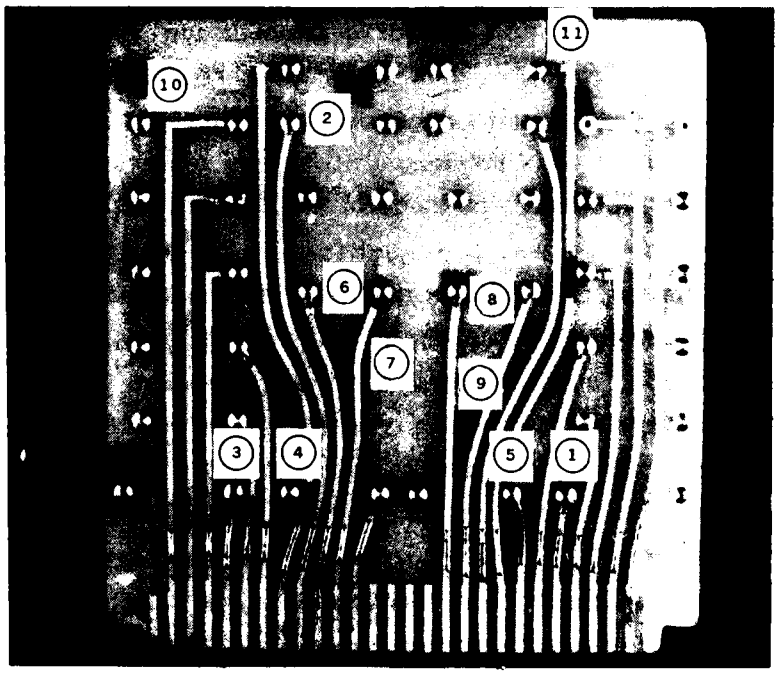

Figure 67 Temperature cycling test resistor board - wiring side view

Having accomplished the above, the program was revised and rapid thermal cycling test was conducted with a TA modified to include examples of actual defects. Workmanship defects which would affect the operation of twelve of the resistors were incorporated on the TA. Provision was made to periodically monitor the currents through these resistors while they were subjected to the thermal environment. This TA was then subjected to a series of thermal cycles, during which both periodic electrical measurements and a modified form of continuous thermographic monitoring as described below were accomplished.

5.3.2.1 Initial No Failure Thermal Experiments - Employing the modified thermal chamber with an IR transmissible window, a series of baseline experiments were conducted utilizing a resistor board. The purpose of these experiments was to verify the validity of using the IR window; to determine the effect of the attenuation associated with the window; and to evaluate the feasibility of obtaining repeated delta thermographs of a test article at room ambient temperature using a single room ambient reference image.

Having established that it was possible to view the test article through the window, the test article was energized and remained energized throughout this series of tests. The thermal chamber was set to +23 C and allowed to stabilize. Following chamber stabilization and with the test article powered for a period in excess of ten minutes, a reference thermographic image was obtained and recorded on disk. The system was placed in delta therm and complete cancellation was obtained. The reference image was recalled from the disk and another successful delta therm cancellation was obtained. The chamber control was then set to +71 C and the chamber was allowed to stabilize at that temperature for a period of ten minutes. Upon completion of the dwell period, the control was set to +23 C and again a ten minute dwell to stabilization period was provided. Upon the completion of the dwell period a cancelled delta thermograph was obtained. The chamber control was set to -54 C and after the dwell period, the chamber was returned to +23 C and another successful delta thermograph was obtained. This procedure was successfully repeated for a total of five cycles, providing verification of the validity of the use of this window and the feasibility of obtaining repeated delta thermographs of a test article at room ambient temperature using a single room ambient reference image.

The effect of the window's attenuation upon a delta thermograph was empirically determined by a set of room ambient experiments. With the test article powered and stabilized, a room ambient reference thermograph was obtained while viewing the test article through the window. A delta thermograph of the still powered test article,

viewed directly (not through the window), produced complete cancellation thereby verifying that the window had no adverse effect. Repeats of this experiment produced the same results.

Having verified the feasibility of using an IR transmissible window to obtain repeated valid delta thermographs at room ambient, a set of experiments still using the powered resistor board were performed to evaluate the feasibility of obtaining valid delta thermographs at temperatures other than room ambient. The test article was exposed to the same thermal cycle as previously outlined and a reference image was produced at +23 C and at +71 C. Since the thermograph will not function for temperatures below 0.0 C, the low temperature reference was produced at +5.0 C. Subsequent delta thermographs against these reference images verified the feasibility of this technique.

5.3.2.2 Thermal Cycling Tests (Analog) - The current through each of the twelve selected resistors was measured with the input voltage set to 5.00 Vdc and the test article within the thermal chamber. Electrical measurements were made at temperatures of +25 C, +71 C and -54 C. This served to establish the deviations which could be expected throughout the extremes of the thermal cycling.

The insertion of failure analogs representing permanent failures during any part of the thermal cycle was determined to be thermographically detectable when Delta runs were made against references accomplished at discrete temperature points, e.g., +25 C, +71 C, and +5.0 C. Intermittents inserted during the excursion to the reference temperature were not detectable. This further corroborated the requirement for a method of continuous thermographic monitoring.

It was considered that local reference Delta runs made continuously during the higher than 0.0 C portions of the cycle might enable detection of intermittents. The approach was to make a reference at a given temperature (above 0.0 C) enter into the Delta mode and view the resulting image for a period of time. When the difference in temperature (WT) between the reference image and that in the FOV exceeded 2.0 C, the Delta mode was exited and then re-entered. This produced a new "local" reference which again allowed viewing the Delta image until the ambient WT of 2.0 C was exceeded.

The available viewing time is a function of the instantaneous rate of change of the thermal chamber. Since a minimum of 20 seconds was necessary to allow a defect at the TOD to be visually detectable, and since changes in ambient temperature in excess of 2.0 C confounded the interpretation of the display, chamber rates of change greater 6.0 C/minute precluded the use of this technique (Figure 68).

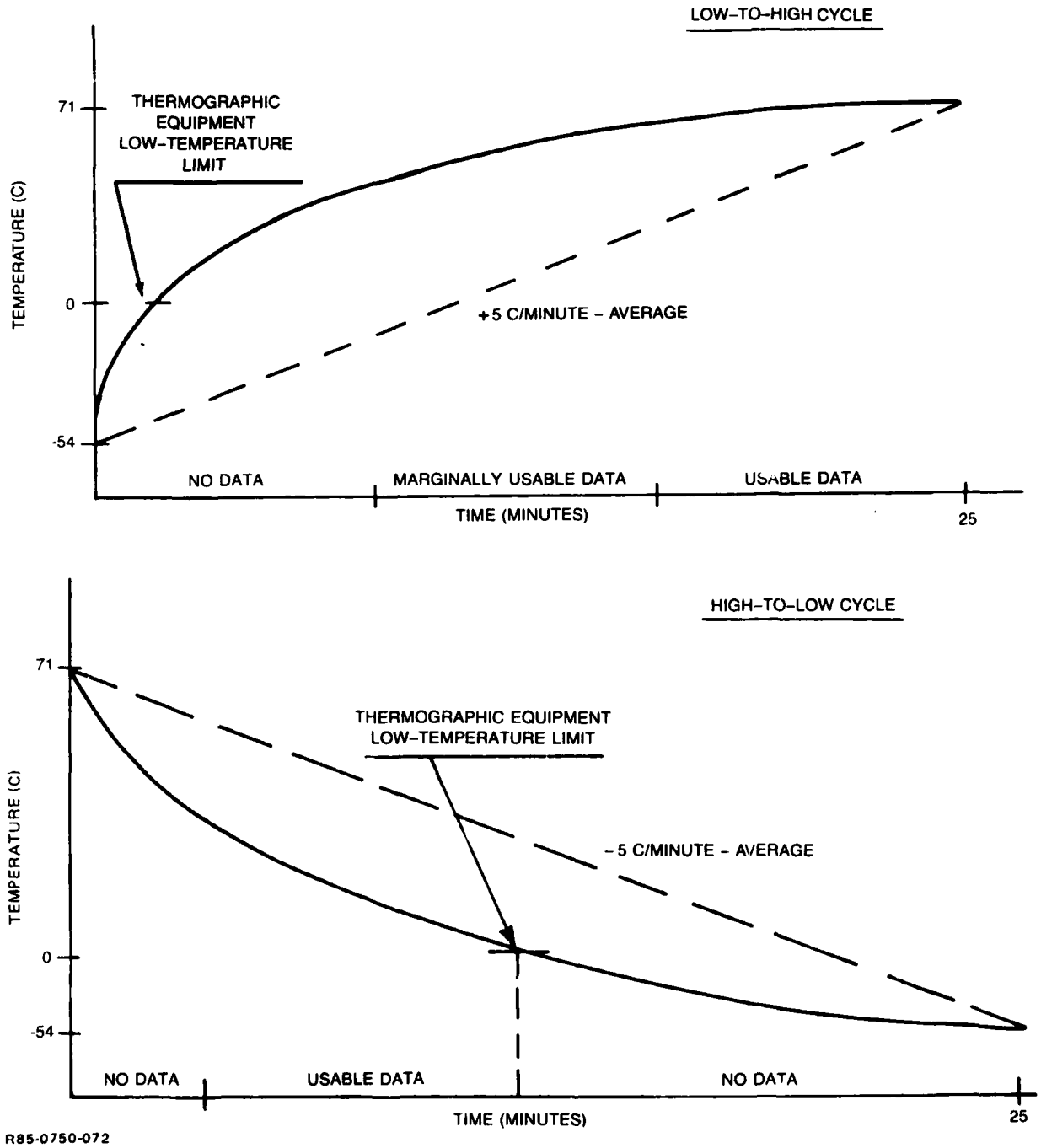

Figure 68 Typical chamber cycle

It should be noted that the capability provided by this technique is strongly dependent upon the visual accuity and experience of the operator. While it was possible to observe and point out to others the presence of failures that were at known locations, the ability to similarly observe random failures on the fly may not be obtainable in a practical application of the technique.

5.3.2.3 Defect Insertion - Examples of thermally sensitive workmanship defects were then inserted into the test article at the locations described below:

Solder joint problems were considered to be the most typical defect and a total of six of them were incorporated at locations 1 through 5 and 12 (Figures 66 and 67). These defects were effected by removing the original solder and resoldering, with movement of the leads and heat sinking to prevent proper solder flow. Most of the resulting joints became worst-case conditions of a no-solder joint, i.e., mechanical contact only. The circuit traces at locations 6 through 9 were cut and bridged by examples of defective ball and wedge bonds made on the substrate of a "dummy hybrid" circuit added to the PCB (not shown in photo). One of the leads of the resistor at location 10 was completely cut through; continuity was re-established through mechanical contact only. The circuit trace at location 11 was cut through, with continuity re-established through manipulation of the board.

The TA was then returned to the electrical test fixture within the temperature chamber and the currents through each of the 'defect' components were again measured. Several of the 'defects' were determined to have opened due to handling during insertion into the connector and had to be manipulated until all current measurements yielded normal no-fail conditions.

5.3.2.4 Rapid Thermal Cycling Tests (Actual Defects) - The chamber door with its IR transmissible window was then put in place and the thermal cycling tests were initiated.

Thermographic monitoring was continuous during the greater than 0.0°C portion of each cycle and the individual currents were monitored periodically throughout the entire cycle. Whenever either a thermographic or electrical anomaly was observed, the current at that position was monitored continuously for indications of changes that could be related to the thermal image.

A total of 35 thermal cycles was accomplished in the thermal chamber. The solder joint examples at locations 1 through 3 exhibited electrical intermittencies throughout most of the testing while the ones at locations 4, 5 and 12 showed little or no activity. The intermittent conditions were observed both thermographically and electrically.

The broken component lead wire was electrically observed to have failed (completely open) only once during the -55 C portion of one of the last cycles. This was not observed thermographically since it is below the lower limit of the thermographic equipment, i.e., 0.0 C.

The examples of defective wire bonds were never observed to fail either electrically or thermographically.

6 - CONCLUSIONS

The results of this study program show that it is technically feasible to use infrared thermographic techniques to detect environmentally-sensitive workmanship defects in electronic printed circuit board assemblies. Furthermore, this technique provides sufficiently sensitive and accurate defect growth tracking capability to enable the acquisition of data for use in subsequent studies leading to the development of techniques for failure prediction.

The thermographic system used for this study was the CCT-9000 manufactured by UTI Instruments Corporation. This system was chosen because it contains unique features especially well suited to accomplishing the study objectives. In addition, a computer interface is provided to supplement the system's capability. However, due to program limitations, this option was not utilized.

This study resulted in the following specific conclusions:

- The delta therm mode of operation is optimum for both failure detection and growth tracking
- The system's offset capability, which was designed to correct the visual image for ambient temperature changes, is effective only for small changes (±2.0 C) in ambient temperature. This feature does not provide thermodynamic correction
- A system sensitivity setting of 0.1 C, a zero dead band, and the interlace mode with 256 color levels provide the best results
- At normal laboratory temperatures, failures in populated PCBs, resulting in power deviations as low as 15 mW and existing for a minimum of 15 seconds, are positively identifiable. This defines the minimum Threshold Of Detectability (TOD)
- The unit-unit variations between like components within a production lot have no significant adverse effect upon the threshold of detectability
- The minimum TOD is not raised as a result of heat spreading from adjacent high-power components
- The TOD is a function of ambient temperature stability and magnitude
- Both permanent and intermittent failures at the minimum TOD are detectable during random vibration at laboratory ambient temperatures

- The visual detection of permanent and intermittent failures during rapid thermal cycling is possible at temperatures above 0.0 C, and only at points in the thermal profile where the chamber temperature is changing at a rate low enough to allow a 20 second viewing period between reference images. This limits the usefulness of the technique, since intermittent failures are most likely to occur during periods of rapid temperature change
- The comparison of multiple assemblies of a given production lot to a single reference ("golden board") is feasible due to the following principal observations:
  - unit-unit component power variations within a given lot are not materially significant
  - given an experienced viewer, positional disparities between the reference image and the image in the field of view are readily differentiated from actual failures
- The system is especially suitable for applications in which a given assembly, monitored for changes in operational status resulting from external stimuli, is referenced against itself.

AD-A172 737 ENVIRONMENTAL STRESS SCREENING TECHNOLOGY(U) GRUMMAN AEROSPACE CORP BETHPAGE NY H QUARTIN ET AL. OCT 85 RSM-85-R-03 AFWAL-TR-85-3073 F33615-83-C-3406 2/2

UNCLASSIFIED F/G 9/3 NL

END
DATE FILMED
11-86
DTIC

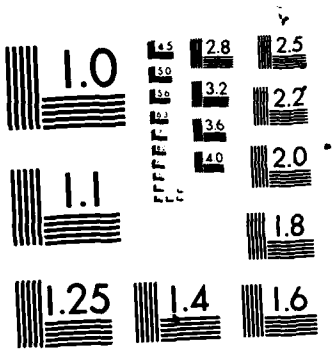

MICROCOPY RESOLUTION TEST CHART
NATIONAL BUREAU OF STANDARDS-1963-A

7 - RECOMMENDATIONS

1. The use of IR thermography as a defect screen during random vibration is felt to have been sufficiently well defined during the study to warrant consideration of a production PCB pilot screening program. Since thermography requires that the boards be vibrated under power as individuals, it is acknowledged that some additional expense in terms of fixturization and repeated test time will be incurred. The purpose of a suitable pilot program would be to measure the screening effectiveness of IR thermography in sufficient depth to determine whether the benefits gained in terms of additional workmanship defects captured and reduced troubleshooting times would offset the additional costs.

2. The use of IR thermography during thermal cycling was shown to be of limited usefulness primarily due to the fact that the rapidly changing visual display requires continuously-variable reference data. A computer-aided analytical mode could be developed and integrated directly into the existing hardware. This capability could be used to provide the following:

- A thermodynamic math model, which can be continuously updated and provide corrections for variations in ambient temperature
- A pixel-by-pixel delta therm in conjunction with a thermodynamic math model
- Pattern recognition enabling automatic corrections for positional displacements, e.g., a shift in PCB location
- End-to-end self-test capability of the thermograph system
- Continuous identification of system mode configuration.

3. Since the results of our defect growth tracking feasibility experiments were positive, it would be beneficial to further pursue the subject of failure predicability. The pilot program noted under Recommendation 1 could be augmented to provide a database for failure prediction. Anomalies in reference runs or pre-vibration exposure delta therms against a "golden board" would not be removed until they resulted in a non-functional PCB state. Given a large enough production PCB sample, this would provide data concerning the growth of defects in a non-laboratory setting.

REFERENCES

1. Kube, F. O. and Hirschberger, G., An Investigation to Determine Effective Equipment Environmental Acceptance Test Methods (Phase I - Vibration), Report No. ADR14-04-73.2, Grumman Aerospace Corporation, Bethpage, NY, April 1973.
2. Hirschberger, G. and Quartin, H., An Investigation to Determine Effective Equipment Environmental Acceptance Test Methods (Phase II - Thermal Environment), Report No. ADR14-02-77.4, Grumman Aerospace Corporation, Bethpage, NY, October 1977.
3. Environmental Stress Screening Technology Study Test Plan, Grumman Aerospace Corporation, Bethpage, NY, May 1984.
4. Navy Manufacturing Screening Program, Report No. NAVMAT P-9492, Department of the Navy, Naval Material Command, May 1979.
5. Kodak Irtran Infrared Optical Materials, Kodak publication No. U-72, Eastman Kodak Co., Rochester, NY.
6. Special Filters from Kodak for Technical Applications, Kodak Pamphlet No. U-73, Eastman Kodak Co., Rochester, NY.

APPENDIX A
EQUIPMENT DESCRIPTION

This system provides a high-resolution, full-color display of the infrared (IR) energy of objects between 0 C and 200 C within its field of view. Its ability to display difference images in increments representing temperatures as low as 0.1 C was considered of primary importance in observing the inception and tracking of a failure resulting from a workmanship defect. All thermal images are displayed on a 13 in. RGB (red, green, blue) color monitor with a digital temperature readout from any cursor-selected point.

The system is microprocessor-based with a 640 by 512 RAM storage capable of holding more than 300,000 picture elements. This allows the user to store the entire thermal range of the image in memory for post-processing. Floppy disc storage is provided, and computer interfacing is available through the IEEE 488 module.

The CCT-9000 System makes use of a low-noise, fast-response IR detector which operates in the 8-14 micron-infrared spectral region. A dual-function range feature provides 0.1 C thermal resolution in the 0-100 C range and 0.2 C thermal resolution in the 0-200 C range. A real-time numeric thermal readout can be displayed for any picture element.

Images are displayed on the color monitor with a 20 MHz bandwidth. A user-selectable, 16 color gradience is displayed on the left-hand edge of the viewing screen for identifying corresponding temperature bands. A closer examination of any selected portion of the screen is possible when the magnifier modes are used.

A.1 SYSTEM ELEMENTS

The major assemblies of the system are shown in Figures 69 through 75 and are briefly described below:

A.1.1 Scan Head Assembly

This assembly (Figure 69) scans the test article through a system of moving mirrors. These mirrors reflect the IR energy radiated by an object through a focusing lens and onto a solid state mercury cadmium-telluride (HgCdTe) sensor. This sensor converts the energy into electrical signals which are subsequently processed into a visual display. The assembly contains a refillable liquid nitrogen dewar which is used to cool the sensor and mounting provisions for external optics and also can be mounted onto a movable tripod.

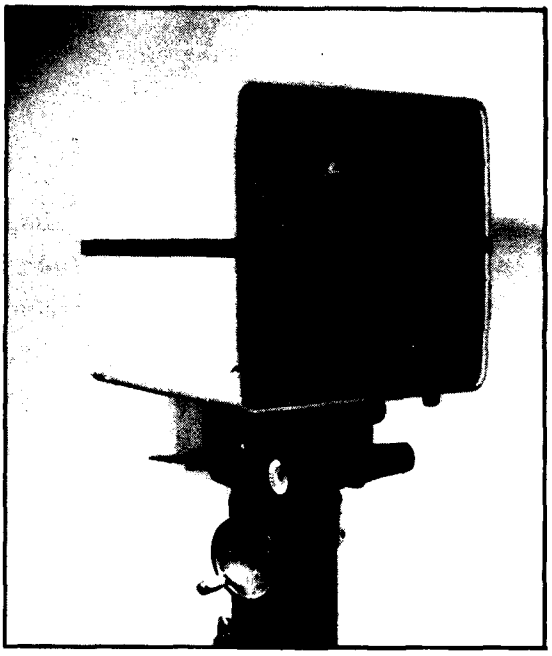

Figure 69 Scan head assembly

A.1.2 Display Monitor

The display monitor (Figure 70) is a 13 in. diagonal RGB type with a 20 MHz (-3 dB) video bandwidth having a frame rate of 45 frames per second. User-accessible controls provide for adjustment of brightness and contrast and for degaussing.

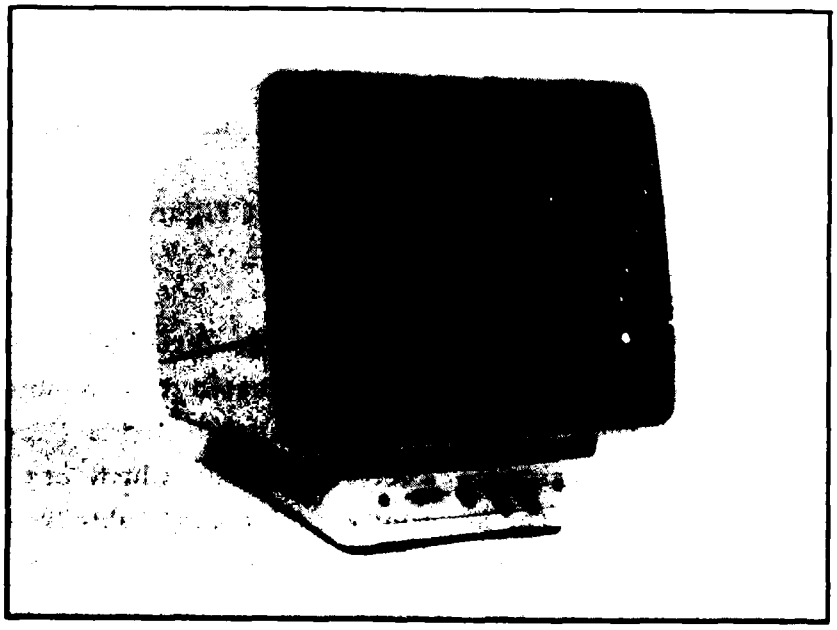

Figure 70 Display monitor

A.1.3 Central Processing Unit

The Central Processing Unit (Figure 71) is a Z80A microprocessor control system that includes image memory of 640 x 512 x 16 bits; real-time video calculator; audible alarm (input error conditions); and the following firmware:

- Color level temperature reference
- Automation temperature readout at cross-hair location
- Temperature range selection
- 4:1 interlacing
- Hold (freeze frame)
- Component swap
- 16X image enlargement
- Label and text writing (up to three pages)
- Simple and weighted averaging
- "Delta therm" comparison mode, image subtraction
- Electronic focusing aid
- Emittance correction factor
- Real-time calendar clock.

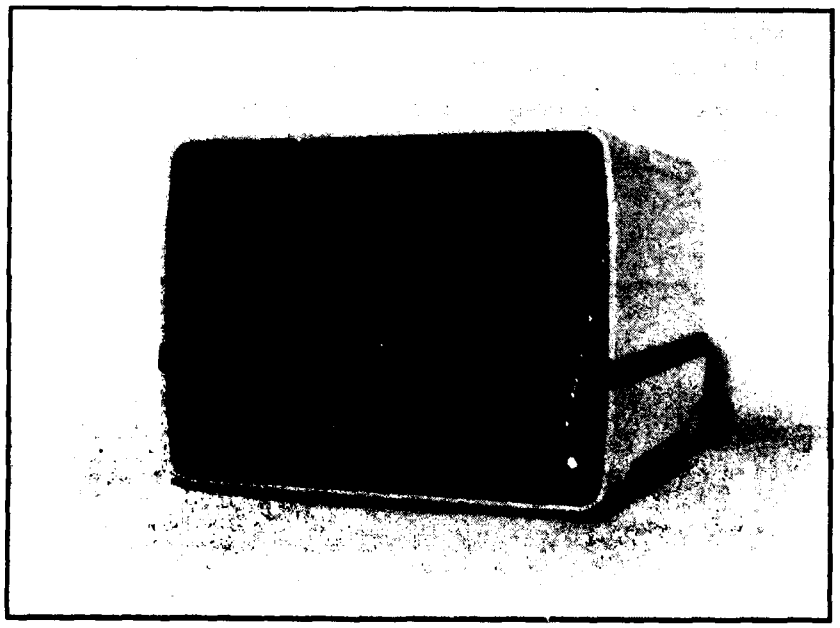

Figure 71 Central processing unit

A.1.4 Keyboard Entry System

The Keyboard Entry System (Figure 72) consists of an ASCII standard-key layout for user convenience. A 16-key, special function keypad is situated on the right-hand side for easy command.

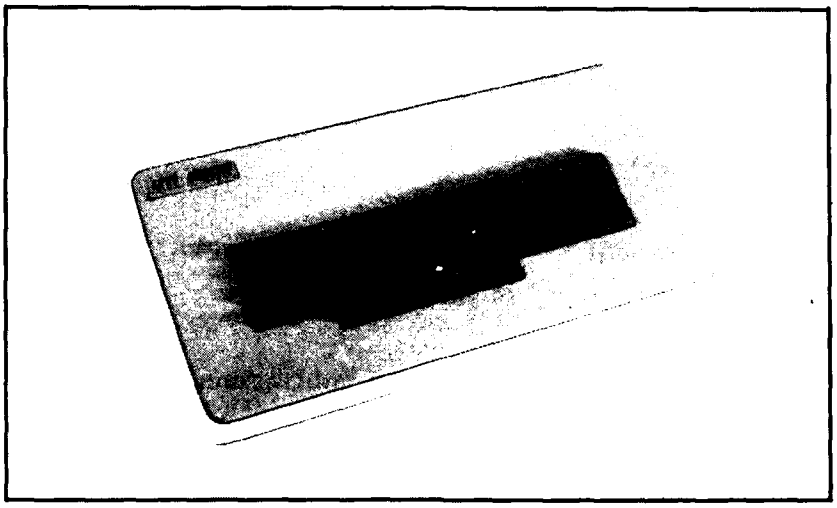

Figure 72 Keyboard entry system

A.1.5 Disk Storage Unit

An 8 in., double-sided, double-density floppy disc for image storage and recall is provided and capable of storing a 1.0 Mbyte image (Figure 73). The system features automatic disc formatting, date and time stamping, prompting, and operator error detection.

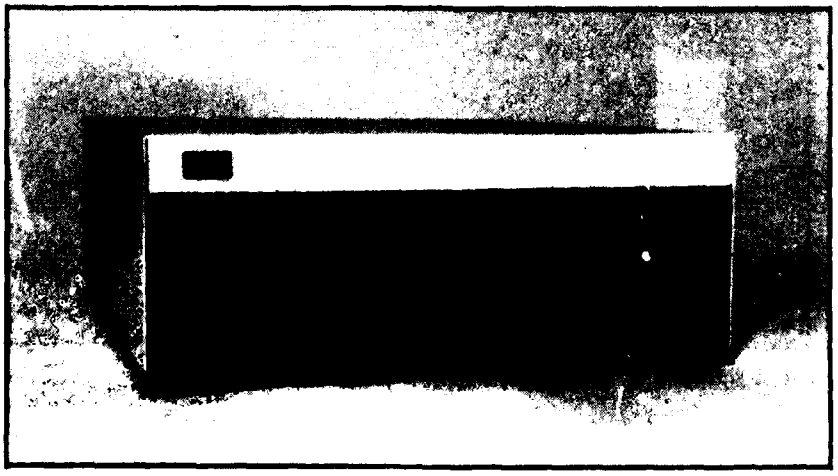

Figure 73 Disc storage unit

A.1.6 Front Surface Mirror

The Front Surface Mirror (Figure 74) fastens to the scanning head and permits the viewing of horizontally configured test specimens without rotating the scanning head 90°.

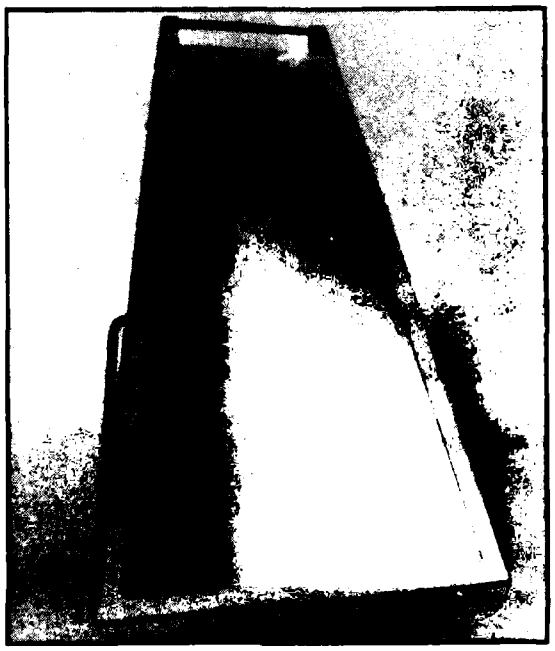

Figure 74 Front surface mirror

A.1.7 Close-up Lens Assembly

The Close-up Lens Assembly (Figure 75) creates 2.5X optical magnification of the thermal images. In addition, this assembly includes an X-Y-Z sample positioning stage.

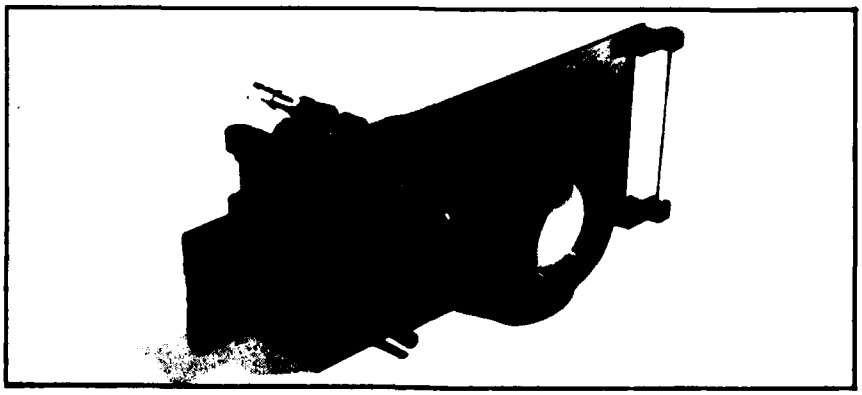

Figure 75 Close-up lens assembly

A.2 SYSTEM SPECIFICATIONS

The thermographic system specifications are shown in Table A-1.

TABLE A-1. Thermographic system specifications.

IMAGE SCANNER	
DETECTOR ANGULAR SUBTENSE	1.2 MILLI RADIANS
FIELD OF VIEW	30 x 19 DEGREES
SPATIAL RESOLUTION:	
LIMITING 2%	600 LINES
50% RESPONSE	250 LINES
RANGE OF FOCUS	10 CM TO INFINITY
FRAME CYCLE TIME:	
1:1 INTERLACE	1.5 SECONDS
4:1 INTERLACE	0.4 SECONDS
DEWAR HOLD TIME	6 HOURS (TYPICAL)
DETECTOR MATERIAL	HgCdTe
DETECTOR MDTD	<0.1 C @ <30 C
SPECTRAL RESPONSE	6 TO 14 MICRONS
DISPLAY FORMAT	
IMAGE SIZE	13 INCH DIAGONAL
ASPECT RATIO	4 HORIZONTAL x 3 VERTICAL
VIDEO OUTPUT	RS-170
FRAME RATE	45 FRAMES/SECOND
LINE RATE	23.5 kHz
IMAGE PROCESSING FUNCTIONS	
PIXEL FIELD	640 HORIZONTAL x 512 VERTICAL
DYNAMIC RANGE	12 BITS
EMITTANCE AND REFLECTANCE CORRECTIONS	DISCRETE OR UNIFORM CORRECTIONS AT CURSOR LOCATION
DRIFT COMPENSATION	AUTOMATIC
IMAGE SUBCONTRACTION (DELTA THERM)	CONTINUOUS
IMAGE AVERAGING:	
MULTI-FRAME WITH HOLD	UP TO 16 FRAMES
CONTINUOUS	1/4 & 1/2 WEIGHT
IMAGE DISPLAY MODES:	
IMAGE CURRENTLY IN FIELD OF VIEW (FOV)	
IMAGE STORED IN RAM	
THE DIFFERENCE BETWEEN FOV AND STORED IMAGE	
ALPHANUMERIC DISPLAY:	
TEXT CAPTIONS ON IMAGE	
IMAGE PARAMETERS CONTINUOUSLY UPDATED	
FULL SCREEN TEXT, 64 CHARACTERS BY 32 LINES	
TEXT EDITOR FOR TEXT ENTRY AND CORRECTION	
IMAGE ENLARGEMENT	2, 3, 4, 6, 8, 12, OR 16 PIXEL
CURSOR CONTROL	X, Y, AND DIAGONAL CONTROL KEYS
IMAGE PARAMETER CONTROL	ONE KEY COMMAND
TEMPERATURE READOUT	3 DIGITS PLUS 1 DECIMAL PLACE
TEMPERATURE RANGES	
RANGE 1	0 TO 100 C
RANGE 2	0 TO 200 C
TEMPERATURE RESOLUTION (MDTD)	
RANGE 1	0.1 C @ 35 C
RANGE 2	0.2 C @ 35 C
DISPLAY SENSITIVITY INCREMENTS (PER COLOR)	
RANGE 1	0.1 TO 6.4 C
RANGE 2	0.2 TO 12.8 C
DISPLAY BASE LEVEL RANGE	
THE MID-COLOR TEMPERATURE CAN BE ADJUSTED IN MINIMUM-SENSITIVITY INCREMENTS (0.1 C RANGE 1; 0.2 C RANGE 2) TO PROVIDE OPTIMUM COLOR DISPLAY	
STABILITY AND ACCURACY	
REPEATABILITY	±0.2 C STD OF 30 READINGS/HR
STABILITY	±0.5 C STD OF 30 READINGS/8 HR
ACCURACY	±1.0 C BOTH RANGES FOR BLACK BODY TEMPERATURE

APPENDIX B
TRANSIENT PCB THERMAL ANALYSIS

Consider a pixel (i) on a PCB with input power $\dot{g}_i$, heat capacity $(mCp)_i$, and coupling to the ambient environment $(hA)_i$, where the h includes both convective and linearized radiative heat transfer. Then a heat balance (neglecting conductive couplings to surrounding pixels on the PCB) can be written.

$$(mCp)_i \frac{dT_i}{dt} = \dot{g}_i - (hA)_i (T_i - T_a) \tag{1}$$

which can be rewritten

$$\frac{d\theta_i}{dt} = -\phi_i \theta_i + \psi_i \tag{2}$$

where $\theta_i = T_i - T_a$ (with T_a constant), $\phi_i = +(hA/mCp)_i$ and $\psi_i = (\dot{g}_i/mCp)_i$, yielding the solution:

$$\theta_i = \theta_{i,m} (1 - e^{-\phi_i t}) \tag{3}$$

which satisfies the initial condition, $\theta = 0$ @ $t = 0$ and the steady state condition, $\theta = \theta_m$ @ $t \rightarrow \infty$ (with $\theta_m = \psi_i/\phi_i$).

If pixel data is taken during the transient rise at $t = t_1$ and at steady state, then ϕ_i can be determined by rearranging equation (3) into the form

$$-\phi_i = \frac{1}{t_1} \ln \left[1 - \frac{\theta_i (t = t_1)}{\theta_{i,m}} \right]$$

While highly simplified, equation (3) should provide a fairly good description of the transient heating curve for the pixel, given constant heat input and constant ambient environmental temperature.

To apply this analysis, assume that an addressable clock is provided and that a good determination of the set of ϕ_i values for the PCB "golden board" is made. The clock also permits a precise time to be associated with pixel measurements of the test article during the early portion of the heating transient. Equation (3) can then be used to provide a reference value for the pixel, at the same time as the test article reference.

The advantage of this approach is that steady state measurements need only be made for the "golden board". Test articles can be measured early in the heating cycle, permitting shorter test cycles.

☆U.S.Government Printing Office: 1986 — 646-067/40983

ATE

LMED

8